

SOLUTIONS UNLIMITED

G-LAY:grapheneLayer(gL):

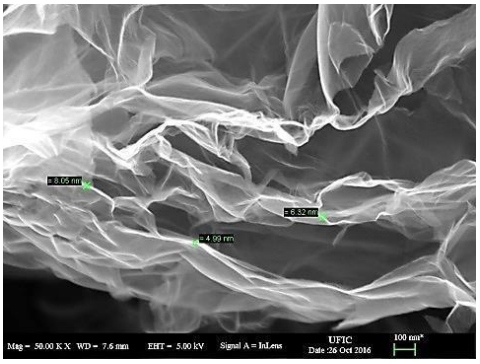
Premium quality Graphene based lubricant oil additive
Graphene layer coating technology
Enhance properties of conventional & synthetic oil :
Improve lubricity by reducing friction between moving parts
Excellent increasing wear resistance of engine components
Boost fuel efficiency
For easy & self engine restoration without disassembling
Great reduction of friction & wear

Graphene called wonder material of dream is substance that is treated as a innovative material of next generation: strongest material in the world: strength of 200 times stronger than steel, thinnest, lightest most conductive and excellent stretch ability with many extraordinary characteristics.

We manufacture premium quality rGO(reduced graphene oxide) by our manufacturing system of chemical exfoliation in our own laboratory.

The final size of rGO as key ingredient of G-LAY:grapheneLayer(GL) is 0.25nm thickness & diameter 50nm.

Above size is world uniquely developed by our proprietary nano technology so that best optimized particle acts improvement of maximizing lubrication ability without clogging oil filter.



Miracle effective with G-LAY

For all types of engine

Restore friction surface of engine & protect by graphene Laying
Stable & strong coating of wear crevices
max 42% engine power improvement
max 80% reduction of friction coefficient
5% - 17% increase fuel efficiency
5 times lower noise and vibration levels
Max 78% emission reduction in CO and CH
Long life time of engine by outstanding ability of anti-wear
Much smoother, quieter, powerful driving

Extend Life time of engine oil, till 30,000km run due to excellent effect of thermal conductivity, dispensability,, abrasion resistance, heat resistance & oxidation resistance. Life time of conventional oil needs to change every 5,000 – 9,000km run.

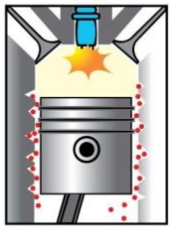
For small Engine & all metallic mechanism

Restoration & protection of worn-out metallic surface
Outstanding extension of life time for Chain, Bearing, Pivot, etc
Great reduction of friction and abrasion, Mechanical failure at Lubrication system & noisy on operating part.
reduction of Mechanical failure at Lubrication system &
reduction of noisy on operating part, temperature on friction part
More suitable for high speed bearing and machine
Enhance properties of conventional & synthetic oil :
Improve lubricity by reducing friction between moving parts
Extend life time of lubricant oil max 3 times

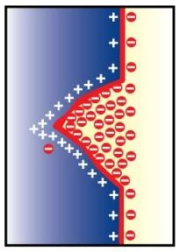


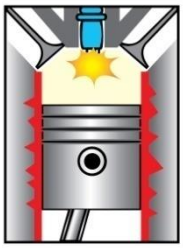
Miracle Graphene layer Coating Technology on metallic surface

nano graphene mixed with engine oil
Self-restoring coating & graphene Layer process
on metallic surface
cracked parts have high electric potential,
charged graphene is moved selectively
on metallic surface, and cohesion is conducted
by heat and pressure.

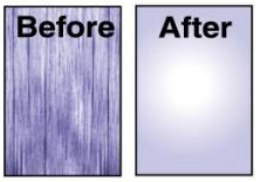


After restoring abrasion parties and
coating on surface with graphene,
enhance lubricant properties,
improve engine performance
with wear resistance, fuel efficiency,
engine power, extend engine life time,
reduce emission and reduce friction.





before & after
graphene coating & Laying treatment



After inject grapheneLayer, graphene layer coating will be proceeded from 30km run, and feel big differences of effect: more smoother, quieter, powerful driving

Upon graphene layer coating on metallic surface completed after 1,000km run, you could change motor oil, and the effect of G-LAYwill be continued till 25,000km – 30,000km run.

GRAPHENE LAYER
G-LAY
NANO COAT
PREMIUM

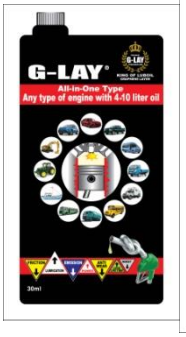


grapheneLayer AIO(all-in-one) type

any type of engine: petrol, diesel & CNG available
Inject one 30ml pouches AIO into oil tank for 4 – 10 liter oil capacity

Inject two 30ml pouches AIO into oil tank for any type of big engine upon 25 liter oil capacity

Restore friction surface of engine & protect by graphene Laying
max 67% engine power improvement
max 80% reduction of friction coefficient
8% – 12% increase fuel efficiency
5 times lower noise and vibration levels
3 –5 times emission reduction in CO and CH
Long life time of engine by outstanding ability of anti-wear
More smoother, quieter, powerful driving





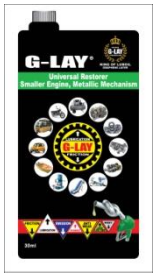


grapheneLayer Smaller(Universal Restorer)

Smaller engine: Less than any types of 600CC engine
Motorcycle, 3 wheeler
Any types of metallic mechanism
Compressor, bearing, gear box,
transmission case, differential, power steering
various kinds of machine tool
convey belt, etc

Restoration & protection of worn-out metallic surface
Outstanding extension of life time for Chain, Bearing, Pivot, etc
Great reduction of friction and abrasion
Great reduction of Mechanical failure at Lubrication system
Great reduction of noisy on operating part
Temperature down on friction part
More suitable for high speed bearing and machine

Inject 30ml pouches smaller





G-LAY(graphene Layer):

King of luboil

Incomparable & essential additive to maximize the effectiveness of all luboils

Incomparable characteristic of G-LAY against used material of all additives: MoS2(very harmpful to environmental), Teflon, many different types of ceramic & carbon: silica & boron, graphite, metalizing particle: Nickel alloy, WS2, titanium etc.

Improve lubricating ability of G-LAY:

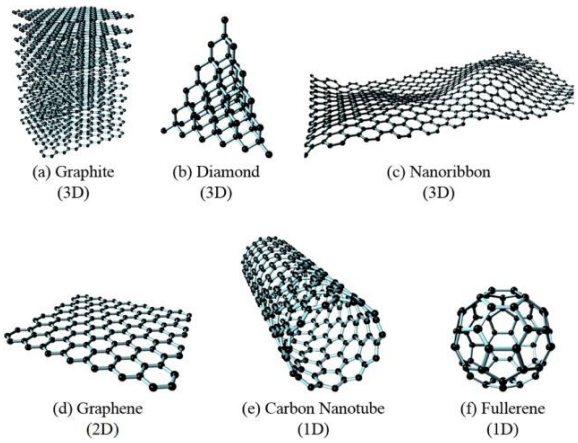
nano based graphene oil additive restore worn out metallic surface and laying lubrication membrane on friction party and maximize lubrication ability

strong oil adhesion to metallic surface

minimize friction

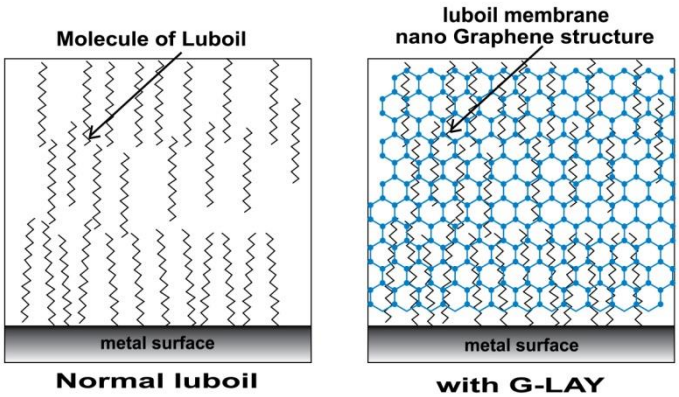
improve cooling ability

high heat conduction(2,500W/mk): excellent characteristic of nano graphene. Rapid transferring high temperature by friction and explosion to reduce temperature of lubricant oil and engine



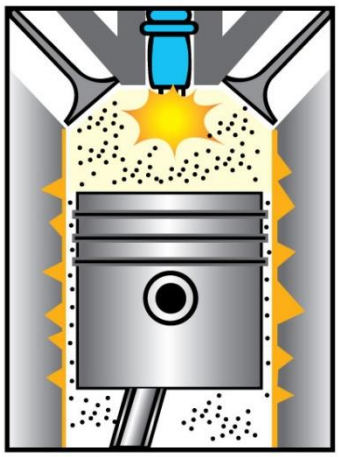
Strong reinforce of luboil membrane on metallic surface

forming coat and laying graphene membrane: nano graphene constructs honeycomb structure to each lubrication molecule to make strong lube membrane.



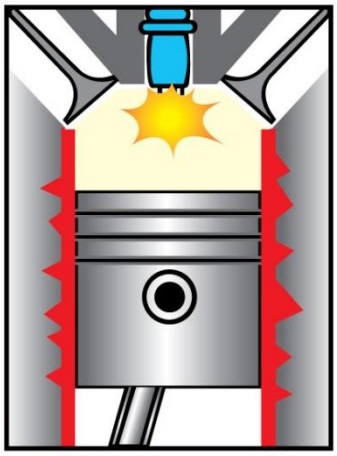
Sealing function in engine chamber

(solve leakage problem of non combusted emission)
through worn out metallic surface occurred by reciprocation motion of piston



Emission leakage

Normal oil

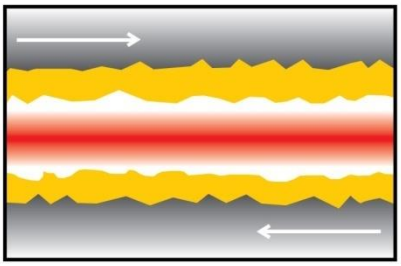


block leakage
increased pressure
adding G-LAY

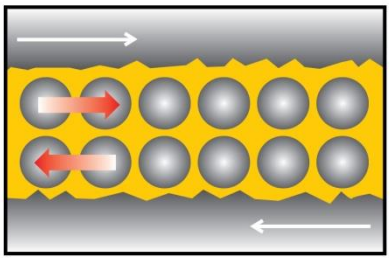
Emission max 83% reduced
Output Max 20% and fuel efficiency max 14% improved
Extend life time of engine oil to 2 – 3 times
Reduce noise and vibration
Power increased

Excellent abrasion resistance, high heat conduction

nano graphene particle acts to ball bearing function on friction between metallic parties, minimize friction space(space friction > dot friction), dramatically increase lubricating ability and reduce abrasion loss to average 65%.



Normal oil



with G-LAY

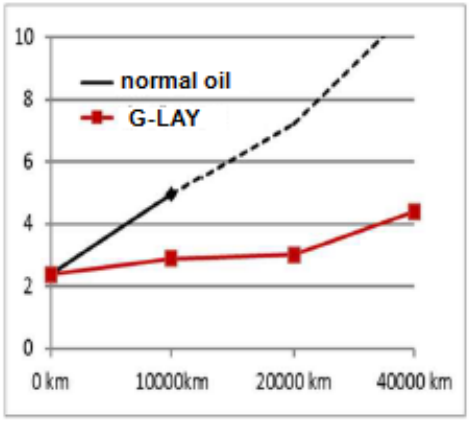
nanoTec International

Testing of total Acid Value
numerical value of Acidity contained in lubricant oil

Dated Jan 5 - May 23, 2019
Vehicle; Hyundai Delivery truck. Running record 359,391km
Tested by Korean Institute of machinery & materials(KIMM)
Testing before and after G-LAY injection

Testing of total Acid Value:
numerical value of Acidity contained in lubricant oil
Oxidation of lubricant oil occurred according to long time exposure of oxygen and high temperature of long distance running.

G-LAY has wonder character:
excellent effect of thermal conductivity, dispensability,, abrasion resistance, oxidation resistance.



Acid Value(mg KOH/g)

Compared with normal oil, Acid value of G-LAY reduce to max 88%

Therefore, G-LAY extends life time of conventional engine oils till 30,000km run. Life time of conventional oil needs to change every 5,000 – 9,000km run.

G-LAY extend life time of industrial oil 2 time & maximum 3 times longer.

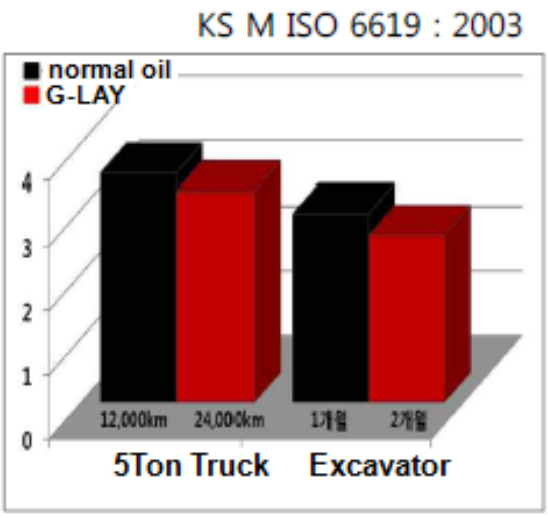
nanoTec International

Testing of Engine Oil Life Time
total Acid Value & viscosity
numerical value of Acidity contained in lubricant oil

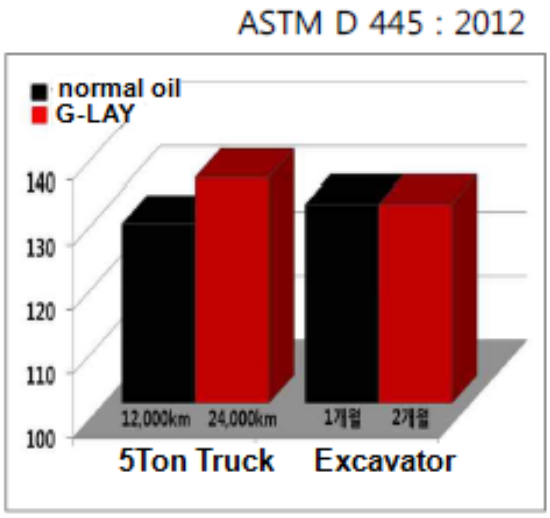
Dated Jan 5 - May 23, 2019
Tested by Korean Institute of machinery & materials(KIMM)
Testing before and after G-LAY injection

Testing of total Acid Value:
numerical value of Acidity contained in lubricant oil
Oxidation of lubricant oil occurred according to long time exposure of oxygen and high temperature of long distance running.

G-LAY has wonder character:
excellent effect of thermal conductivity, dispensability,, abrasion resistance, oxidation resistance.



Acid Value(mg KOH/g)



viscosity Index

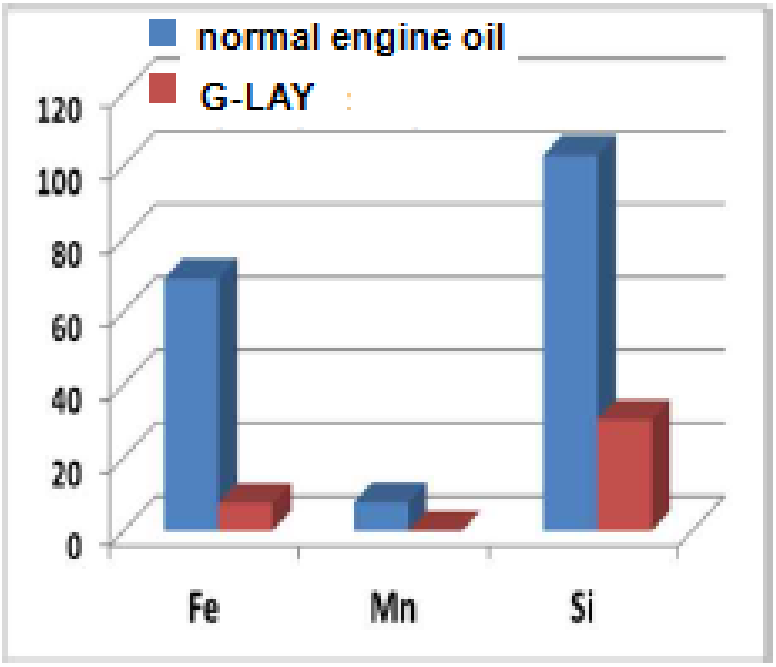
After injection G-LAY, Acid Value decreased & viscosity index increased
Therefore, Life time of engine oil extended to 2 - 3 times

nanoTec International

Testing of Abrasion Loss on metallic surface of engine metallic particle: Fe, Si, Mn etc testing occurred by abrasion in engine oil

KING OF LUBOIL
GRAPHENE LAYER

Dated Jan 5 - May 23, 2019
Tested by Korean Institute of machinery & materials(KIMM)
Vehicle; Hyundai Delivery truck. Running record 359,391km
Testing before and after G-LAY injection



metal particle mg/kg

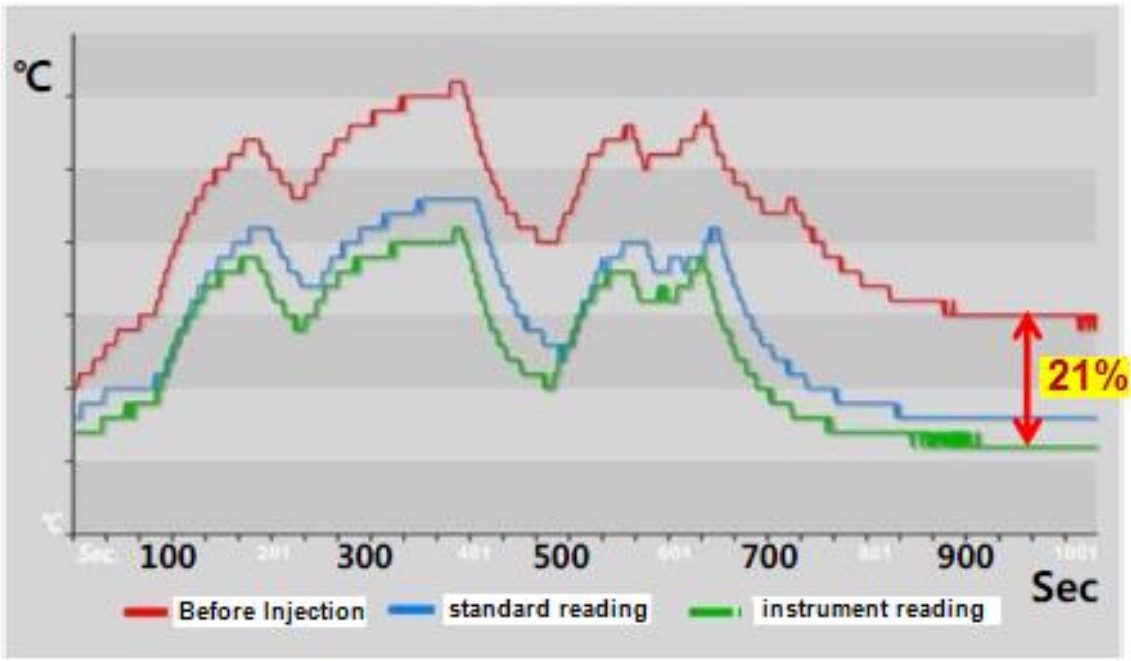
Detectable Amount of measured value

Compared with normal engine oil, G-LAY added oil dramatically shows reduction of Abrasive Loss

nanoTec International

Testing for Temperature of engine oil
By Increased Lubricant membrane & effect of thermal conduction

Dated: April 18, 2019
Tested by Korean Institute of machinery & materials(KIMM)
Vehicle: Kia Delivery Ban
Diesel engine
year 1995
Running record 440,355km
Testing Method: After injection G-LAY, test changed temperature of engine every second



nanoTec International

Emission Testing Report

The Effectiveness of emission reduction

Dated Feb, 2019
Tested by Korea Automotive Technical institute
Testing Method: Normal engine oil and after inject grapheneLayer(G-LAY)
Test with Emission Tester in each condition, 30minutes engine idling



Before inject

After inject

Vehicle name	Year of production	Running record(Km)	Passed Standard(%)	Before Injection (%)	After Injection(%)	Reduction rate(%)
Tusan	2018	187,443	20	64	18	71.9

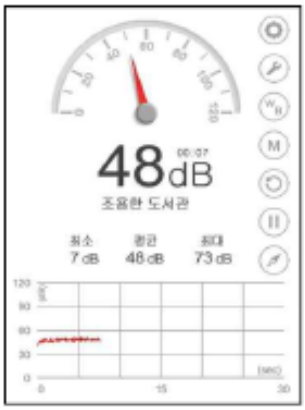
Reduction of Emission 71.9%

nanoTec International

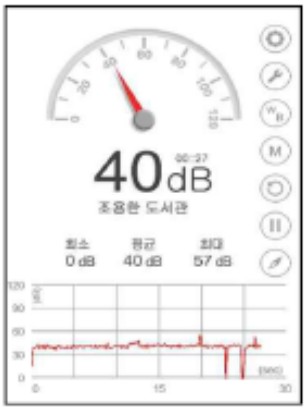
KING OF LUBOIL
GRAPHENE LAYER

Test for noise reduction

Dated: March 21, 2019
Tested by Dong Yang Car Maintenance Service Center
Vehicle name: Eccus year 2010
Running Record: 223,971km
Testing Method: Normal engine oil and after inject grapheneLayer(G-LAY)
Test with dB Tester in each condition, 60 minutes engine idling



Before Inject G-LAY



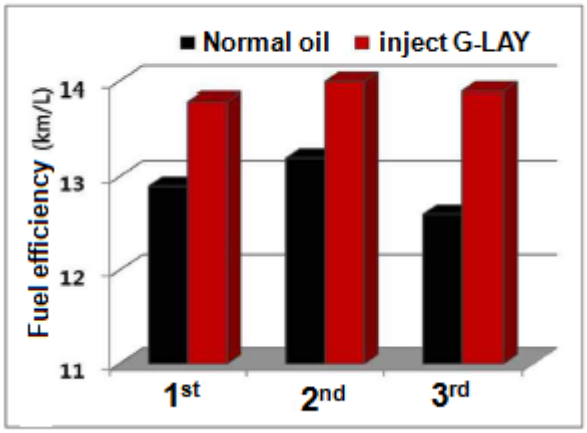
After Inject G-LAY

nanoTec International

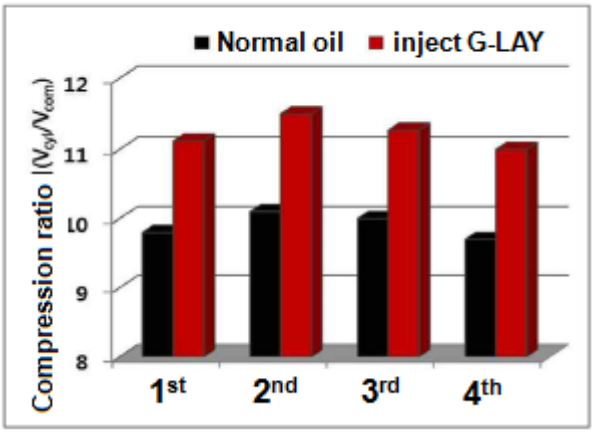
Test of fuel efficiency

Dated March 25, 2019
Tested by Korean Automobile Technical institute
Vehicle name: Eccus year 2010 2,999cc
Running Record: 224,992km
Testing Method: Normal engine oil and after inject grapheneLayer(G-LAY)
Average testing speed: 80km/h run

Test of Fuel consumption



Test of Compression ratio



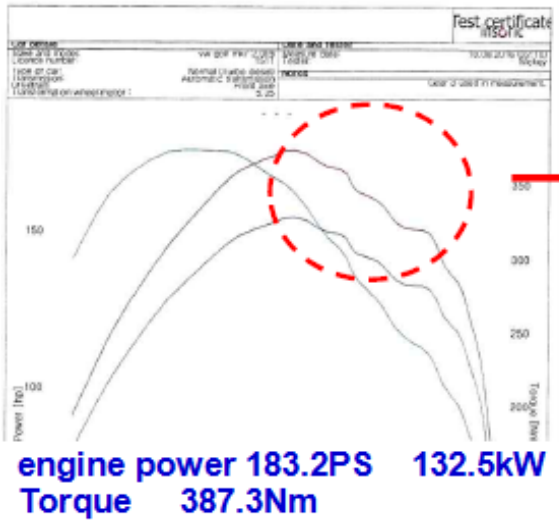
Output and fuel efficiency
Compression ratio approx 17% increased
Output approx 8 – 9% increased

nanoTec International

Test of engine output

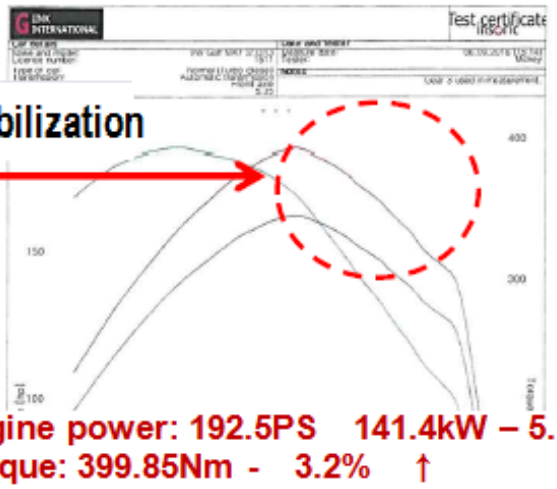
Dated March 12, 2019
Tested by Korean Automobile Technical institute
Vehicle name: Hundai Tucsan year 2011
Running Record: 165,996km

Testing Method: 300km run with Normal engine oil
and 300km run after inject grapheneLayer(G-LAY)



Normal engine oil

output stabilization



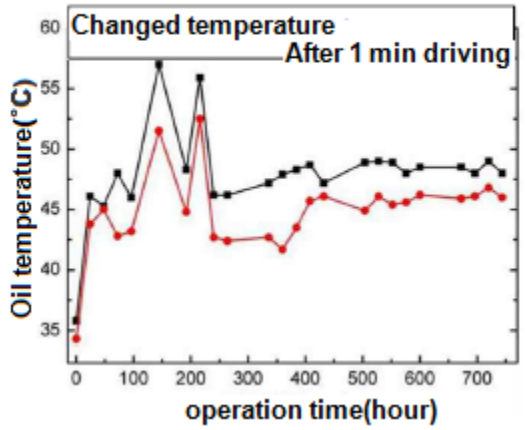
Add G-LAY

nanoTec International

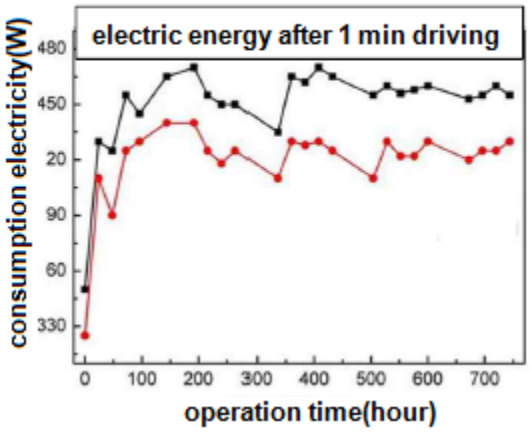
Compressor Test

Dated March 14, 2019
Tested by Korean Institute of machinery & materials(KIMM)
Compressor Cylinder 5hp
Testing before and after G-LAY injection
Testing Period: 0hr – 200hr

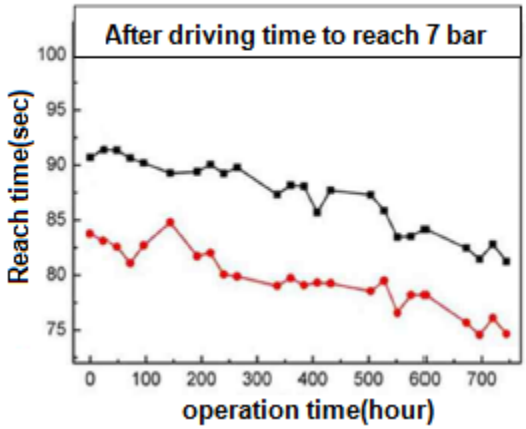
Engine heat value reduce(7 – 11%)



driving energy reduce(9 – 13%)



Pressure increased time(6 – 8%)

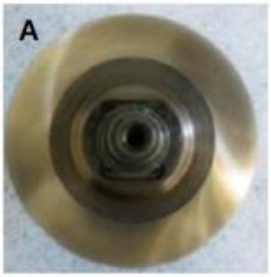


Normal oil
G-LAY adding

nanoTec International

Abrasion Testing Report

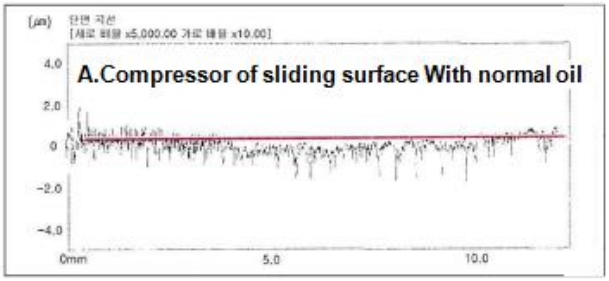
Dated Feb 23, 2019
Tested by Korean Institute of machinery & materials(KIMM)
Durability of Abrasion for Car air-conditioned Compressor Cylinder 5hp
Testing before and after G-LAY injection

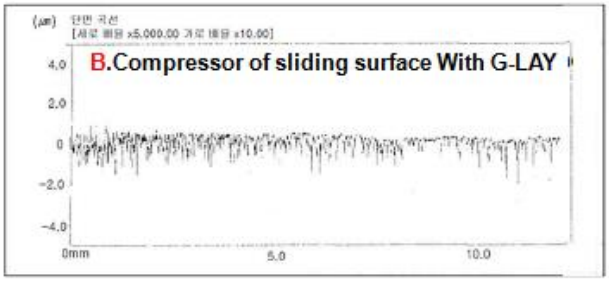


Evaluation of anti-wear(Avg 1kg/cm2)

Result:
normal oil: ani-wear 1μm
with G-LAY: no anti wear







nanoTec International

Testing for Temperature of engine oil
By Increased Lubricant membrane & effect of thermal conduction

Dated: April 14, 2019
Tested by Korean Institute of machinery & materials(KIMM)
Vehicle: Hundai Grandeur:
gasoline engine
year 1998
Running record 329,012km
Testing Method: Before 7 after injection of grapheneLayer(G-Lay)
After 2 hours engine idling, test temperature on oil fan party
Using thermal image camera

G-LAY		Temperature of Engine Oil ($°C$)			
	Q'ty	Before Injection	After Injection	Temperature Differences	Temperature(%) Reduction Rate
G-Lay AIO	1 pouch	94.3	84.2	10.1	13.4

Atmospheric Temperature: 29$°C$
Normal Temperature of Engine idling: 85$°C$ - 90$°C$

Dated: April 15, 2019
Tested by Korean Institute of machinery & materials(KIMM)
Vehicle: Kia Sorento:
Diesel engine
year 2001
Running record 270,355km
Testing Method: Before 7 after injection of grapheneLayer(G-Lay)
After 2 hours engine running on road, test temperature on oil fan party
Average running speed 80km/hr
Using thermal image camera

G-LAY		Temperature of Engine Oil ($°C$)			
	Q'ty	Before Injection	After Injection	Temperature Differences	Temperature(%) Reduction Rate
G-Lay AIO	1 pouch	130.3	109,5	20.8	16.0

Atmospheric Temperature: 25$°C$
Normal Temperature of Engine on 30km run: 105$°C$ - 130$°C$

nanoTec International

Emission Testing Report

Dated Feb, 2019
Tested by Korea Automotive Technical institute
Testing Method: Normal engine oil and after inject grapheneLayer(G-LAY)
Test with Emission Tester in each condition, 30minutes engine idling

Testing Date: Feb 1st week, 2019

Vehicle name	Year of production	Running record(Km)	Passed Standard(%)	Before Injection (%)	After Injection(%)	Reduction rate(%)	Remark
Sorento	2003	205,338	20	49	15	69.4	
Santafe	2005	187,237	20	52	16	69.3	
Carnival	2011	143,095	20	43	12	72.9	

Testing Date: Feb 3rd week, 2019

Vehicle name	Year of production	Running record(Km)	Passed Standard(%)	Before Injection (%)	After Injection(%)	Reduction rate(%)	Remark
Trasse	2009	212,499	20	67	16	76.2	
Rivero	2007	307,350	20	48	11	77.9	
Tusan	2014	122,549	20	41	13	68.3	

Average reducing rate of emission after inject grapheneLayer(G-LAY): 72%

Q & A

Why is G -LAY is King of Lubricant oils ?

Graphene called wonder material of dream is substance that is treated as a innovative material of next generation: world strongest material in the world: strength of 200 times stronger than steel, thinnest, lightest and excellent stretch ability with many extraordinary characteristics with excellent effect of thermal conductivity, dispensability,, abrasion resistance, heat resistance & oxidation resistance

Why is G-LAY is essential additive of all Lubricant oils ?

Miracle & outstanding effectiveness of G-LAY:grapheneLayer(GL) on vehicle engine and metallic mechanism is scientifically proven, compared with existing lubricant oil additives and all conventional types of lubricant oil: automotive & industrial oil using with MoS2, many different types of ceramic: silica & boron, synthetic chemical, metalizing particle: Nickel alloy, WS2, titanium etc.

Therefore, G-LAY is alternative solution to maximize and supplement function of engine and all metallic mechanism adding to conventional type of Lube oils.

G-LAY extend life time of conventional engine oils till 30,000km run due to excellent effect of thermal conductivity, dispensability,, abrasion resistance, heat resistance & oxidation resistance. Life time of conventional oil needs to change every 5,000 – 9,000km run.
G-LAY extend life time of engine & all industrial oil maximum 3 times longer.

How is differences between G-LAY and other lube oils and their additives ?

Researchers at the US Department of Energy's Argonne National Laboratory have published a new study that effectively exploits graphene as a new abrasion resistant material that can be used extensively in a variety of exposure situations.

The single layer of graphene was found to withstand 6,500 wear cycles. These values are dramatically improved compared to conventional graphite or molybdenum disulfide, all of metallic: Nickel alloy, WS2, titanium etc and ceramic materials: silica & boron etc.

Conventional lubricants required about 1,000 membranes to withstand 1,000 wear cycles. This shows that graphene lubricants can greatly improve wear resistance of mechanical systems and reduce their costs.

G-LAY is outstanding functional effect compared with additives using above materials.

What kinds of graphene do you use ?

Our produced rGO in our laboratory in quality and size is totally different compared with lower grade micron based GO or imitation graphene(nano graphite) manufactured in China, Taiwan and India.

The final size is 0.25nm thickness & diameter 50nm.
Above size is world uniquely developed by our proprietary nano technology so that best optimized particle acts improvement of maximizing lubrication ability.



Re: Comparison between key particles of G-LAY & other additives: Micron based ceramic, nano metallic, carbon, Boronlite, etc

1. Micron based silica(xado: 5 micron)
Silica based xado is not suitable for quality coating on metallic surface.
Over 5 Micron based ceramic is also negative to be pass completely through standard oil filtering diameter.

Dispersion problem into lubricant oil & uneasy coating in short term due to big particle size Short time effect finished within less than 10,000km.

2. nano Metallic particle & other metallic particles likely Titanium, WS2, Cu & Ni (Resus)
Restoration on worn-out surface could be achieved initially by metallization process. But smaller nano metal alloy particle is not so stable in high temperature of engine explosion, as individual nano metal particle is melted and burn out in short term.

Dispersion problem into lubricant oil was found on many research papers.
Generally, improved effect is disappeared within 5,000km run.

3. Micron based Boronlite, Carbon, etc
According to testing report, no outstanding effect except slight improvement on just initial treatment and cannot get long lasting effect.

Micron based ceramic is also negative to be pass completely through standard oil filtering diameter.

4. MoS2(LiquMoli)Teflon, etc
Not environmental friendly product.
Very serious problem for our environmental.

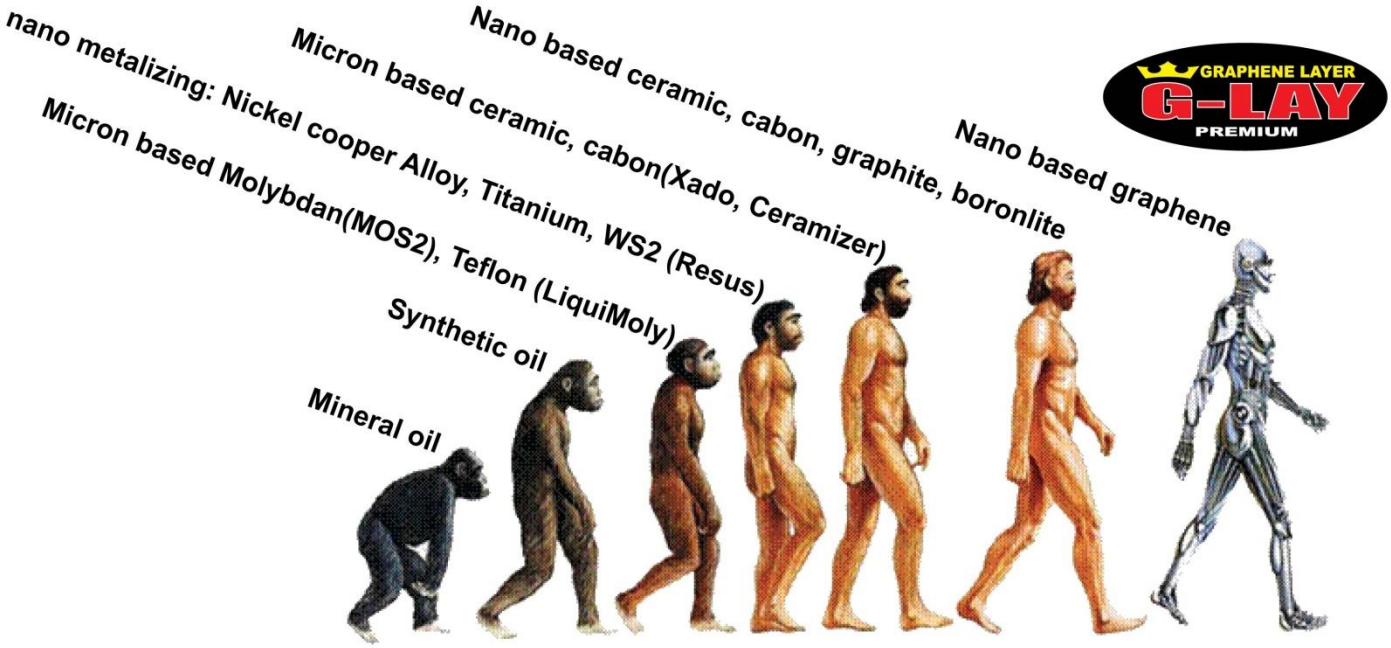
5. imitation graphene
Grinted grapite using less than 1000nm partile is marketed under name of graphene.
These are totally different compared with nano graphene in characteristic.

The advantage of G-LAY
against above mentioned oil additives :
King of all lubricant oil
Incomperable & essential additives
to maximize effect for all conventional type of lub oils

Using nano graphene: wonder material of dream for next generation.
Incomperable effectiveness against all existing additives in market.

Environmental friendly, No side effect

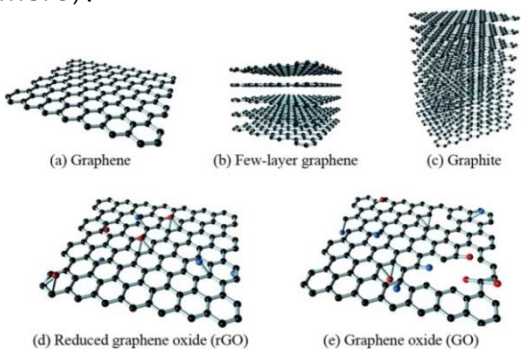
Grapahene is power to change the world and dream of future generation. Graphene is the strongest known material, harder than diamond yet more elestic than rubber; tougher than steel yet lighter than aluminium, heat 2x better than diamond, electrical conductivity is 13x better than copper with amazing characteristics.



Our manufacturing of reduced Graphine Oxide (rGO)

Today's graphene is normally produced using mechanical or thermal exfoliation, chemical exfoliation, chemical vapour deposition (CVD), and epitaxial growth.

Graphene is a material made of carbon atoms that are bonded together in a repeating pattern of hexagons. Graphene is so thin that it is considered two dimensional. Graphene's flat honeycomb pattern gives it **many extraordinary characteristics, such as being the strongest material in the world, as well as one of the lightest, most conductive and transparent. Graphene has endless potential applications**, in almost every industry (like electronics, medicine, aviation and much more).



The single layers of carbon atoms provide the basis for many other materials. Graphite, like the substance found in pencil lead, is formed by stacked graphene. Carbon nanotubes are made of rolled graphene and are used in many emerging applications from sports gear to biomedicine.

Graphene may be promising for a next generation channel material that is useful for LSI (large-scale integration). In addition, t**he physical strength of graphene is 100 times greater than that of iron.** The current density tolerance is much better than that of copper, thus it is expected to be an electrical wire transporting large currents.

Graphene oxide is an oxidized form of graphene, laced with oxygen-containing groups.

Graphene oxide (GO), the functionalized graphene recently attracted much interest thanks to its outstanding properties such as large surface area, lubricant field to reduce friction on metal surfaces, mechanical stability, tunable electrical and optical properties.

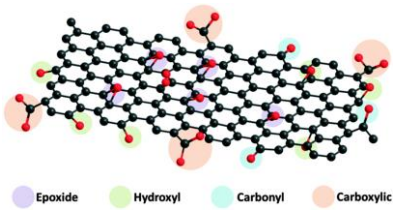
We manufacture premium quality rGO(reduced graphene oxide) by our manufacturing system of chemical exfoliation in our own laboratory.

Graphene produced by all of graphene manufacturers in China & India could not be used for lubricant oil additive due to micron sized diameter:
lateral length which could clog filters of oil system.

Our produced rGO in our laboratory in quality and size is totally different compared with lower grade of GO manufactured in China, Taiwan and

India.

The final size is 0.25nm thickness & diameter 50nm.
Above size is world uniquely developed by our proprietary nano technology so that best optimized particle acts improvement of maximizing lubrication ability.



Graphene:

Graphene called new material of dream is substance that is treated as a Miracle material of next generation especially in lubricant oil industry.

Graphene's flat honeycomb pattern: two-dimensional structure in which carbon molecules are bonded by SP2 is world thinnest material and many extraordinary characteristics.

Scientists are constantly looking for new ways to overcome friction problems, wear resistance, maximizing efficiency without side effect against all conventional lubricant and their additives: , MoS2, many different types of ceramic, synthetic chemical, metalizing particle: Nickel alloy, WS2, titanium etc.

Graphene has physical and chemical stability as high as nanometer and world strongest material in the world: strength of 200 times stronger than steel, lightest & most conductive and excellent stretch ability, so it is directly attached to the surface of a mechanical part or steel ball.
This surface adhesion is very excellent and when it is coated on the inner wall of the cylinder, the friction of piston is dramatically reduced, and the abrasion resistance of the automobile engine can be remarkably improved.

Graphene based engine oil nanofluids of **frictional characteristics** (FC), **anti-wear** (AW), and **extreme pressure** (EP) properties have been highly evaluated. The improvement in FC, AW, and EP properties of nanofluids is respectively by 80, 33, and 40% compared with conventional types of base oil.

Comparison between grapheneLayer and all oil additive & lube oil

Miracle & outstanding effectiveness of grapheneLayer(GL) on vehicle engine and metallic mechanism is scientifically proven, compared with existing lubricant oil additives and all conventional types of lubricant

oil: automotive & industrial oil: MoS2, many different types of ceramic: silica & boron, synthetic chemical, metalizing particle: Nickel alloy, WS2, titanium etc.

Researchers at the US Department of Energy's Argonne National Laboratory have published a new study that effectively exploits graphene as a new abrasion resistant material that can be used extensively in a variety of exposure situations.

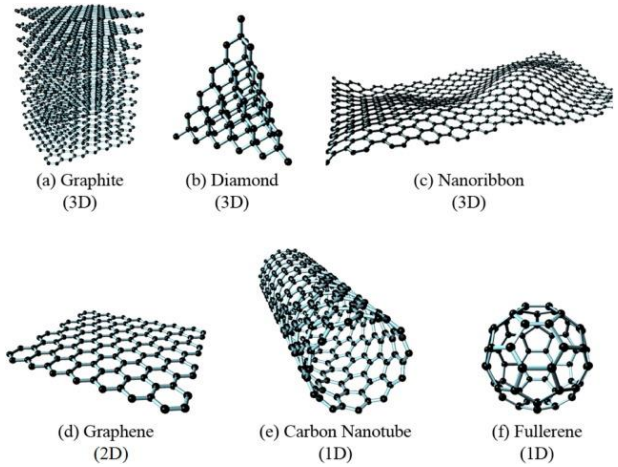
The single layer of graphene was found to withstand 6,500 wear cycles. These values are dramatically improved compared to conventional graphite or molybdenum disulfide, all of metallic and ceramic materials.

Conventional lubricants required about 1,000 membranes to withstand 1,000 wear cycles. This shows that graphene lubricants can greatly improve wear resistance of mechanical systems and reduce their costs.

Graphene has been reported to be an excellent lubricant additive that reduces friction and wear when coated on the surface of various materials or when dispersed in lubricants as an atomic thin material with the low surface energy.

The synthesized graphene oxide (GO) were dispersed at 0.02 wt% in PAO–0W40 oil and its tribological characteristics were investigated using a high frequency friction/wear tester. The friction coefficient and the wear track width of poly alpha olefin (PAO) oil added with graphene oxide (GO) were tested by a ball–on–disk method, and the measured results were reduced by ~5.88 and ~3.8%, respectively compared with those of the conventional PAO oil.

Thus, it was found that the wear resistance of PAO oil was improved. In this study, we demonstrated the successful functionalization of GO as well as the improvement of dispersion stability and tribological characteristics of GO.



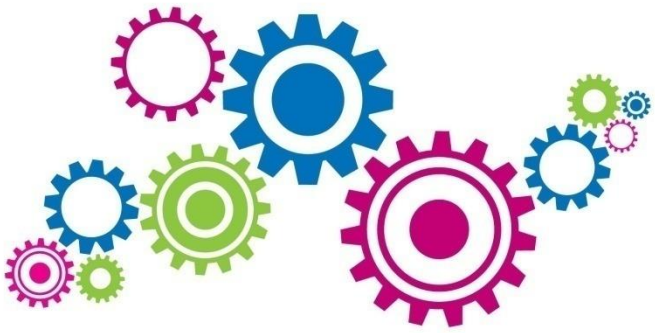


our real nano based grapahene dispersed into oil: G-LAY particle



imitation Graphene: graphite micron based

maybe clog oil filter





nanoTec International
117-3 Chimsan Daegu, Korea Tel: 82 53 354 5502 www.nanozr.com nanotec7777@naver.com

TECHNICAL DATA SHEET

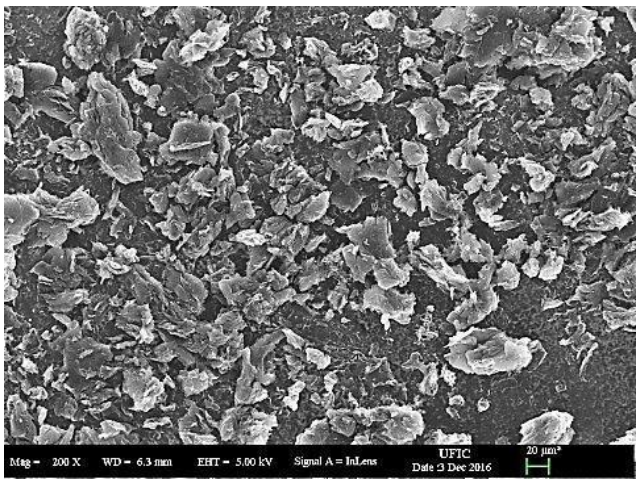
General Characteristics : Chemically Synthesized grapheneLayer

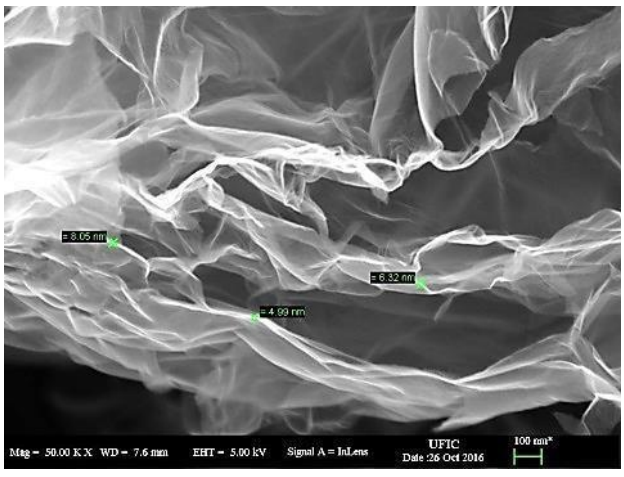
PRAMETER	SPECIFICATIONS
VISUAL:	Light Powder in oil
COLOR:	Match Standard, Black
SPECIFIC SURFACE AREA:	500 m_2/g – 700 m_2/g
Electrical Conductivity:	Ave. 5 S/cm (as powder resistance)
CARBON BY WT%:	78% – 82%
OXYGEN BY WT%:	10% – 15%
SULFUR BY WT%:	< 0~0.5%
ASH BY WT%:	≤ 4.0%

PHYSICAL SIZES:

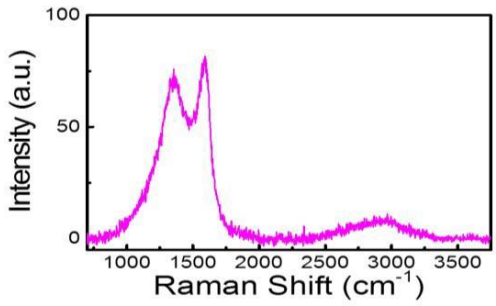
AVERAGE LATERAL DIMENSION (x & y) ≥ 50nm
AVERAGE THROUGH-PLANE DIMENSION (z) ~ 0.18 – 0.30 nm (as estimated by BET)

SEM Images



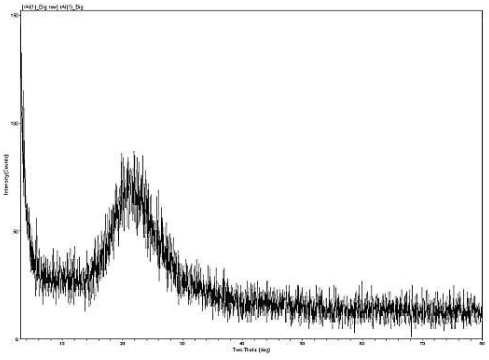


Raman Results

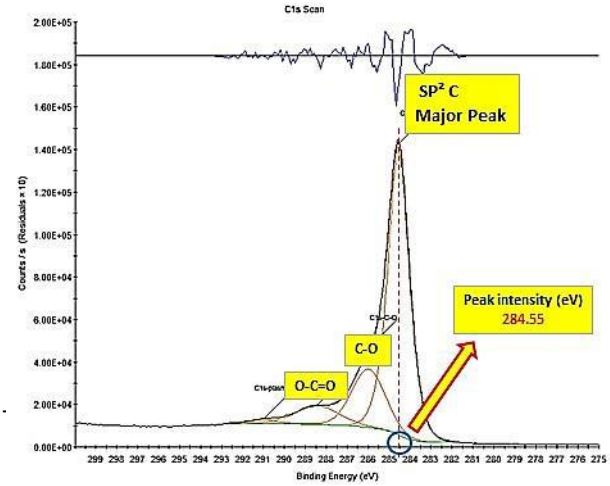


D/G Intensity Ratio: 0.89

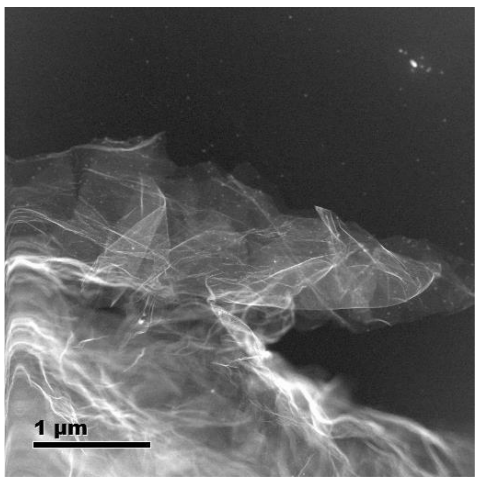
XRD Data

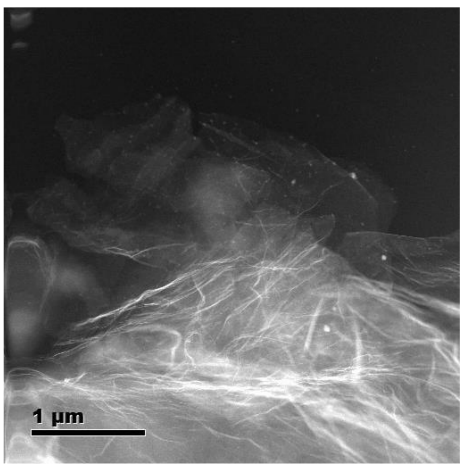


XPS Data



Performed by an accredited Outside Test Facility
Data Written 05/01/2019





nanoTec International
117-3 Chimsan Daegu, Korea Tel.: 82 53 354 5502, Fax: 82 53 354 5503 www.nanozr.com

Quality Certificate

Item : grapheneLayer - graphene based oil additive for engine & all metallic mechanism

March 24, 2019

Name of Article	grapheneLayer	Remarks
Appearance	Black Color	Solution type
Flash Point(℃)	245	ASTM D92
Density	0.01g/cm3	
Thickness (nm)	0.25nm ± 0.07 nano meter	Final treated size
Diameter (nm)	50nm ± 12 nano meter	Final treated size
Water Content(%)	None	Final treated size

Issued by P. J. Lee

Chief Production Engineer

NANOTEC INTERNATIONAL
Jaxon Park
JAXON PARK
MANAGING DIRECTOR

	MSDS	Original Date	2019. 3. 15
		Revised Date	
	grapheneLayer	Revise No.	0
		Total Pages	1

Material Safety Data Sheet

Product	COMPOSITION & INGREDIENTS	CAS No.	UN No.	EN No.
grapheneLayer (Graphene based oil additives)	Graphene(rGO) Mineral oil	1034343-98-0 64742-54-7	- -	- 265-157-1

No	Item	Description
1	CHEMICAL PRODUCT & CCOMPANY IDENTIFICATION	a. Product name : grapheneLayer (Auto engine &Industrial oil additive with graphene based) b. Name of Company: NanoTec International Address: 117-3 Chimsan, Daegu, Korea Telephone: (+82) 53 354 5502, Fax: (+82) 53 354 5503 Web Site: www.nanozr.com
2	COMPOSITION & INGREDIENTS	Ingredient / Composite Proportion (%) / CAS No. Graphene(rGO) / 0.83% / 1034343-98-0 Mineral Oil / 92.47% / 64742-54-7 OTHER ADDITIVES: dispersion Additive, anti Aging, Platinum & etc / 6.70% / -
3	HAZARDS IDENTIFICATION	a. Physical state: Nonvolatile Liquid b. Name of Classification : Not on name of classification c. Potential health effects • Inhalation : Acute exposure : Slight irritation Chronic exposure : May cause irritation, lung trouble and heart trouble • Skin : Acute exposure : Slight irritation. Immediately flush skin with plenty of soap & water Chronic exposure : May cause Irritation • Eye : Acute exposure : immediately flush eyes with plenty of water. Slight irritation Chronic exposure : May cause Irritation and eye damage • Ingestion : Rinse mouth with water, slightly hazardous in case of ingestion • Carcinogenic : No.
4	FIRST AID TREATMENT	• Inhalation exposure: Move person to fresh air. If breathing stop, apply artificial respiration and seek medical attention. • Skin exposure: Remove contaminated clothing and shoes immediately. Wash affected area with mild soap and water and get medical attention if necessary. Use contaminated clothing and shoes after washing. • Eye exposure: Immediately wash eyes with clean water and get medical attention. • Oral exposure: If swallowed lots of chemicals, vomiting and contact a physician immediately.
5	MEASURES AGAINST EXPLOSION OR FIRE	• Fire/Explosion Hazards: Not Available • Fire Fighting Instructions: Use proper extinguishing media and remove the chemical vessel to non-fire area. Be careful not to inhale chemicals and gases from chemicals. Keep away from under area with wind.
6	MEASURES FOR ACCIDENTAL RELEASE	• Collect the released substance in a safety container. Move to and store in safe place. Soak the rest by sand or non-flammable material. • Even though there is no environmental pollution hazard, isolate and keep chemicals from water supply and drainage because chemicals can affect aquatic creatures.
7	HANDLING AND STORAGE	• Handling: To handle with proper container under no heat and sufficient ventilating atmosphere. • Storage: Keep away from direct sun-heat and store in a cool and well ventilating storage.
8	EXPOSURE CONTROLS & PROTECTION	a. Ventilation: Keep ventilated equipping with ventilation fan and keeps it away from direct sun when storage. b. Personal protective equipment: To wear compatible chemical-resistant/safety clothes, gloves, mask and goggles.
9	PHYSICAL AND CHEMICAL PROPERTIES	a. Physical state: black, nonvolatile odorless liquid b. PH: No information. c. Pour Point : -19°C d. Boiling Point : Not available e. Freezing Point : -21°C f. Flash Point : and method : 245°C, ASTM D92 d. P- Particle size : thickness:0.25nano meter , Diameter :50 nano meter e. Water content, %(by mass) : none f. Vapor pressure, vapor density, solubility: No information. g. No other information is available.
10	STABILITY AND REACTIVITY	a. Stability & Reactivity: Stable at/under Normal Handling Conditions (normal temperature and pressure). b. Conditions to avoid: To keep free from Heat, Flame, Electric Spark & other Ignition Sources. c. Incompatibility with other materials: Peroxides, acids, oxidizing agent, flammable materials.
11	TOXICOLOGICAL INFORMATION	a. Skin causticity, Irritating(Skin, Eye), mutagenicity: May cause slight irritation in skin and eye, but hazards are little. No other specific information found. b. Cancer Exposure, Acute Toxicity, Chronic Toxicity, Genital Toxicity, Teratogenicity: Not classified as a carcinogenic substance and no relevant information found.
12	ECOLOGICAL INFORMATION	• Environmental Influence information: Be careful for handling, storage and disposal because chemicals can affect aquatic creatures if released. • Resolvability and accumulation: No information found.
13	DISPOSAL CONSIDERATION	• Direct Disposal or Assigned Disposal according to Waste Disposal Law and related Regulations is required.
14	TRANSPORT INFORMATION	a. DOT CLASSIFICATION : Not a Dot controlled material (United States) b. Identification : Not available c. Special Provision for transport : Not DOT
15	REGULATORY INFORMATION	a. Korean Regulations • Industrial Safety & Public Health Law, Toxic Chemical Handling Regulation, Dangerous Safety Handling Regulations: Not regulated. b. USA Regulations • Generally not a restricted or control item under CERCLA, SARA and OSHA. • SARA hazard classification (29CFR1910.1200): "No" in acute, chronic, fire, reactivity, sudden exhaust.
16	REFERENCE & PRECAUTION	• Reference Material: Material Suppliers' MSDS and General information from the Data Base of the Chemical Substances are quoted or referenced. • Precaution: Appropriate precaution has to be paid under the responsibility of the user. - All Chemical Products may cause unexpected dangerous accident subject to the storage conditions and other cause. - In application and handling of this product, keen consideration of the above information has to be paid under safety application conditions.

Responsibility for use, storage, handling and disposal of the products described herein, ether alone or in combination with other substance, is that of the purchaser and/or end user.

This is the end of MSDS for grapheneLayer. HS Code:3811.29.0000

KNU 경북대학교 Kyungpook National University

Date: May 26, 2019

Test Report

Test Sample: grapheneLayer Submitted by NanoTec International
Test Cell: Automobile Test Lab
Engine Type: RV 1.6 Gasoline, 4 Cylinder, 1500cc
Test Machine: Engine Dynamometer Tester
Engineer: JK Jang Ph.D.

Before Injection of grapheneLayer

speed	power	Torque	FCR	BSFC	Exhausted Gas	
rpm	ps	Kgfm	g/s	g/psh	P(mmHg)	
3521	59.4	12.19	5.20	321.2	121.0	
2507	43.3	12.98	3.48	285.8	66.8	
1521	22.9	10.86	1.92	292.8	30.21	

After running 50Km with injected grapheneLayer

speed	power	Torque	FCR	BSFC	Exhausted Gas	
rpm	ps	Kgfm	g/s	g/psh	P(mmHg)	
3526	67.6	15.10	4.22	230.7	94.6	
2510	52.7	17.20	2.67	214.8	43.2	
1523	31.30	14.20	1.39	191.45	20.23	

After running 200Km with injected grapheneLayer

speed	power	Torque	FCR	BSFC	Exhausted Gas	
rpm	ps	Kgfm	g/s	g/psh	P(mmHg)	
3491	73.2	16.20	4.17	198.80	86.43	
2493	56.20	19.10	2.08	192.50	41.90	
1517	32.10	14.91	1.25	181.49	18.56	

nanoTec International

PISTON COMPRESSOR TEST REPORT

March 18, 2019

On measuring the parameters of piston compressor M110Y Ser. 2003122 treated by grapheneLayer

Parameter	Prior to treatment	After treatment	Remark
Current consumption [A]	30.06	24.20	24.0% reduced
Temperature at outside [℃]	38.50	29.91	29.0% reduced
Pumping time [sec]	72	46	From 1 to 5.9atm 35.2% reduced
Noise level [dB]	83.2	61.3	35% reduced

**After treatment, power consumption was reduced by 24.0%
and vibration and noise levels were improved.
Compressor capacity increased positively in part of energy coefficient.**

**J. N. Song
Chief Manager
KATech**

nanoTec International

Emission Testing Report

March 20, 2019

Testnig Date: March 11 – March 20, 2019
Emission testing: grapheneLayer
by DongYang Car Maintenance Service, Daegu Korea

Year	Name of Vehicle	Running Record(KM)	Emission before inject gL(%)	Emission after inject gL(%)	Emission reduction rate(%)	Remark: Running Km after injection
2013	Carnival	204,290	57	21	64	625km
2014	Sorento	240,673	69	16	77	370km
2014	Sonata	158,442	64	14	78	762km
2016	Musso	142,074	48	19	61	430km
2017	Tusan	125,976	42	23	46	302km

Tested by DongYang Car Maintenance Service
Before Inject rapheneLayer to above t vehicles, emission tested and.
After Inject rapheneLayer to above vehicles and
Emission tested after one week run around 300km – 800km run.

Engine Emission Tester indicates positive from 46% - to 78%.

NANOTEC INTERNATIONAL
Jaxon Park
JAXON PARK
MANAGING DIRECTOR

Hansung Motor Co Ltd/Official Dealer of Mercedes Benz
Hansung Motor Tower, 935-41 Bangbaedong Seochoku, Seoul, Korea Tel: 02-533-3420

The Certificate for grapheneLayer Engine Oil additive

Supplier: **nanoTec International**
117-3 Chimsan, Bukgu, Daegu, Korea
Tel: 053-354-5502 Fax: 053-354-5503

Dear sirs,
grapheneLayer All-In-One Type was tested strictly on the base of international standard Testing procedure & regulation of Mercedes Benz specification, and Testing was focused on standard operating of engine oil in Mercedes Benz vehicles, side effect of nano graphene particles on metallic surface of cylinder and effect of power & noisy on running in our laboratory & testing department.

We are pleased to inform you that using of grapheneLayer All-In-One Type has been approved, and the engine performance & positive restoring effect of of grapheneLayer All-In-One Type was testified by Official Authorized Mercedes Benz Maintenance Center

Sincerely yours,

Feb 23, 2019

K.G. Lee

K.G. Lee
Engineering Manager
Hansung Motor Co Ltd
Official Dealer of Mercedes Benz

HONDA
The Power of Dreams

HONDA KOREA LIMITED
DAECHI TOWER 6TH FLOOR 891 DAECHIDONG KANGNAM SEOUL, KOREA TEL 02-3416 3330 FAX 02-3416-3449

Feb 12, 2019
Ref: HD-KR-2019-325433UG
Subject: Quality Certificate & Approval

Supplier: NanoTec International
Hwasung Bldg 117-3 Chimsandong
Daegu
Korea

Quality Certificate of graphenelayer(gL)

Upon international standard testing results of grapheneLayer all-in-one type by our Laboratory of HONDA Korea,

grapheneLayer(gL) all-in-one type based on graphene(rGO) complies with HONDA standard specification of engine oil: gasoline & diesel, and is approved to be used for HONDA vehicles.

Yours Sincerely,

J. M Kim

Jae Moon Kim
General Manager

TOYOTA
moving forward

TOYOTA Korea Limited
Official Service Center
Kongduck 232-2 Seoul
Tel: 02)3420-4221/9
Telefax: 0203420-4231/2

To:
nanoTec International
117-3 Chimsan, Bukgu
Daegu, Korea

Dated: March 15, 2019
Our Doc ref: EMJ SEV 19-00391

Title: The Certificate of Quality Approval

Item number: grapheneLayer Oil Additives for engine restoration
grapheneLayer All-in-one Type

Dear nanoTec International,
grapheneLayer All-in-one Type accords with standard requirement of Toyoda to be used for Toyoda internal combustion engines

Therefore, grapheneLayer All-in-one Type is approved for using in all series of Toyota vehicles and their assemblies.

Truly yours,

Park Youn Ki
Senior Engineering manager
Toyota Korea Limited

TOYOTA
moving forward

TOYOTA Korea Limited
Official Service Center
Kongduck 232-2 Seoul
Tel: 02)3420-4221/9
Telefax: 0203420-4231/2

To:
nanoTec International
117-3 Chimsan, Bukgu
Daegu, Korea

Dated: March 15, 2019
Our Doc ref: EMJ SEV 19-00392

Title: The restorative effect of POWER STEERING SYSTEM related with grapheneLayer Smaller(Universal Restorer)

grapheneLayer Smaller(Universal Restorer) was injected into power steering fluid, as several old Toyota vehicles including gasoline & diesel engines are in noisy and heavier wheel handling problem which need replace whole power steering system.

Most of vehicles which were injected with grapheneLayer Smaller(Universal Restorer) had positive effect to achieve smooth steering wheel handling and perfect reduction of noisy in very short term average within 30 minutes running.

In this connection, grapheneLayer Smaller(Universal Restorer) is positively recommended to use for restore the condition of power steering system for all series of Toyota vehicles.

Truly yours,

박 연 기

Park Youn Ki
Senior Engineering manager
Toyota Korea Limited

HYUNDAI MOTOR GROUP

Supplier: nanoTech International
117-3 Chimsan, Daegu, Korea

Re: The Certificate of official Supplier

Product: grapheneLayer(gL) All-In-One Type
Engine Oil Additive

It is certified that Hyundai Kia Motor Group approves grapheneLayer Engine Oil Additives to be used at Hyundai-Kia Maintenance Service Network, and Graphel Engine Oil Additives is nano based graphene layer coating additive for all Hyundai & Kia vehicles which need to improve engine performance.

April 22, 2019

Nam sang jin
CEO/Vice President
Manufacturing Management Div
Hyundai-Kia Motor Group

Meister Motors limited
Volkswagen Official Dealer. Korea

CERTIFICATE OF APPROVED SUPPLIER

Name of Supplier : nanoTech International
117-3 Chimsan, Daegu, Korea

Supplied Product: grapheneLayer AIO(All-In-One Type)
(Automotive Oil Additive for improving engine performance)

Herewith, it is certified that grapheneLayer manufactured by NanoTec International is approved as Automotive Oil Additives to Volkswagen Auto Maintenance Network in Korea, and Meister Motors Ltd allows Volkswagen vehicles to use grapheneLayer motor oil additive at Volkswagen Maintenance shops.

March 25, 2019

Jun Sung Sohn

Jun Sung Sohn
Engineering Manager

Meister Motors Limited 683-73 Hannamdong Youngsangu Seoul Korea TEL:02.747 4200 FAX:02.24726722/
1194-2 Guwhundong Nandonggu Inchon Korea 1194-2 TEL:032.472 6200 FAX:032.463 0066

nanoTec International

Automobile Field Test Report

Testing date : Match 1st week - April 2nd week, 2019 April 21, 2019
Dynamo Testing: grapheneLayer testing by KATech
Engineer: J.O. Jung, Chief Manager/KATech

Model	SORENTO (2199 CC, 2009)	Total mileage	167.432 km
Manufacture	KIA Motors	Normal Mileage	13.8 km/ℓ
Company	KNTech	Phone	053-936-7176
Parameters	Prior to treatment	50Km after treatment	200km after treatment
Noise of engine (IDLE state)	92.4 dB	82 dB	58 dB
Noise of inside (IDLE state)	65.8 dB	57 dB	38 dB
Temperature of engine (IDLE state)	82 ℃	80 ℃	67 ℃
Testing distance	50 km	50 km	201.0 km
Noise of inside (under driving)	81~82 dB	73~77 dB	53~54 dB
Mileage (fuel coefficient)	15.20 km/l	17.30 km/l	17.40 km/l

The testing of grapheneLayer showed that fuel coefficient improved by 17% and noise reduced 47%

NANOTEC INTERNATIONAL
Jaxon Park
JAXON PARK
MANAGING DIRECTOR

KIMM 한국기계연구원
KOREA INSTITUTE OF MACHINERY & MATERIALS

KOREA INSTITUTE OF MACHINERY & MATERIALS
104 SHINSUNGRO 104 YOUSUNGKU DAEJUN TEL: 042 860 7401 FAX: 042 860 7402

02- 07-2019

Subject:
Testing Report of GrapheneLayer (Universal Restorer) for Gear Box, Generator, Transmission & Bearing

Testing Purpose: The effect of graphene based lubricant oil additive on metallic surface & evaluate restoration condition of worn out surface.

Submitted Samples:(collected from Junk Shops)
Gear Box,
Bearings
Transmission case

Before injection of grapheneLayer(gL), the surface of abrasive metallic parties was inspected by microscope. High resolution microscope indicates that most of equipments were in seriously crevasse and estimated out of normal operation condition due to serious vibration, excessive noisy and etc.

grapheneLayer(gL) was applied to each submitted old samples:
Upon operation of each equipments I day - 10 days continuously, we evaluated abrasive surface & restoration of surface upon macrograph & noisy test.

Graphene layer coating which were applied on above mentioned equipments was tested with injecting grapheneLayer(gL).

Testing Report:
Upon macrograph & noisy test, coating was not proceeded within half hour.
On 1 hour operation, graphene coating was proceeded, upon macrograph abrasive surface was repaired with graphene and realize reduction of noisy and vibration, and after 1 hour operation, general condition was much improved and after 2hours operation, condition was same as initial testing 1 hour. We estimate Graphene coating was proceeded on abrasive metallic parties on 1 hour operation and coating will be long last.

It is proven that proprietary Graphene layer coating which is applied by NanoTec is stable & strong coating material especially for abrasive metallic surface, their material character is high heat resisting property, high abrasion resistance by our testing lab.

It is certified that above report is proceeded upon macrograph & noisy test and based in fact.

Sang Hoo Youn
Senior Researcher KIMM

KIMM 한국기계연구원
KOREA INSTITUTE OF MACHINERY & MATERIALS

KOREA INSTITUTE OF MACHINERY & MATERIALS
104 SHINSUNGRO 104 YOUSUNGKU DAEJUN TEL: 042 860 7401 FAX: 042 860 7402

02- 17-2019

Subject: Friction Testing Report of grapheneLayer(gL) Smaller On Friction Machine SMC-2

Test of grapheneLayer was proceeded on Friction Machine SMC-2 with method of comparison of normal engine oil and grapahenelayer.

Detailed Test condition:

disk material steel 46
Tempered to hardness 60-62 HRC
Loading P = 650 N
Operating mode n = 380 rpm

Friction was measured before and after by weighting on electronic weight instrument in 0.0003 tolerance.

Testing Results: During period of testing, oil temperature of normal oil from 116 – 124 'C.

Sample wearing when gL was applied was decreased to 46% - 51%, compared with injected normal oil.

Composition of gL shows high efficiency of friction decrease to maximum 51% in experimental result of Friction Machine SMC-2, and real friction testing in actual condition of machinery mechanism is also recommended.

It is certified that above report was carried on Testing of Friction Machine SMC-2 with method of comparison of normal engine oil and grapheneLayer and based in fact.

Oh Hyung

Jae Hyung Oh
Researcher KIMM

Union Chemical Institute
1370 Sankyuckdong, Bukgu, Daegu, Korea UCI Laboratory Science based
High-Tech Development Complex Tel:053 950 5112 Fax: 053 950 5117

Re:Testing Report of grapheneLayer Smaller for 2 & 4 Stroke MotorBike

These testing was requested by NanoTec International

Application sample: 10 pouches samples(grapheneLayer Smaller) to be injected to each motorbike.

Testing Period of each Motorbike: running till 50km, 70km, 100km

Testing Motorbikes: 2 Stroke & 4 Stroke 10 Motorbikes Each which are actively operated by Short Delivery Transportation Service Company.

Testing Motorbikes Condition:

		Total Running Record	
5 2-stroke motorbikes:	2 Honda	228,432 km	62,587Km
	2. Hyosung	384.006	89,578
	1. Daerim	14,543	75,109
5 4-stroke motorbikes:	2. Honda	329,665	12.945
	1. Suzuki	78,403	
	1. Yamaha	76,009	
	1. Daerim	145,665	

The condition of each Motorbike: all of old bikes which are in running record over 50,000km are in bad condition with heavier emission & noise, serious power problem.

Testing Method:
Before injection of grapheneLayer, tested by dynamometer to monitor Power, fuel consumption, noisy and smoke.
Each Motorbikes are approx estimated average daily run 50 – 200km.
After injecting grapheneLayer, monitor engine condition in 50km, 70km & 100km run.

Union Chemical Institute
1370 Sankyuckdong, Bukgu, Daegu, Korea UCI Laboratory Science based
High-Tech Development Complex Tel:053 950 5112 Fax: 053 950 5117

Testing Result:

After injection and run just 50km, found Great change:
reduction of noisy(average 52%) and smoke(average 73%), Increase power(22%), Reduction of Fuel consumption(average 4.5%)

After injection and run just 70km & 100km run each
The tested data is almost same as that of 50km run test.

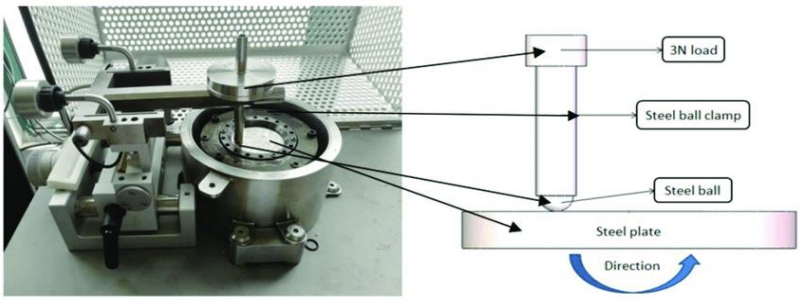
Conclusion: It is concluded that Graphel has great & rapid effect for motorbike engine restoration and engine performance as below: grapheneLayer coating is proceeded within 10km run from graphenelayer Smaller injection, so very positive restoration is completed within 50km run.

January 27. 2019

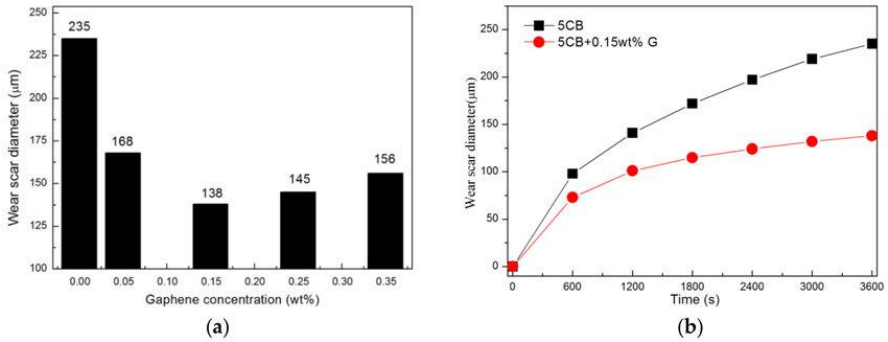
Hae dong Jung/ PhD
Material Engineering

Lubrication Performance of Graphene as Lubricant Additive in 4-n-pentyl-4′-cyanobiphyl Liquid Crystal (5CB) for Steel/Steel Contacts

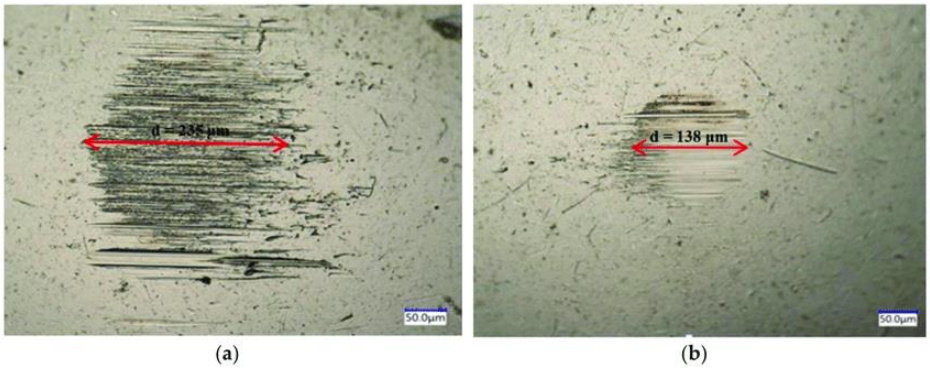
The lubrication performance of graphene used as additive in 4-n-pentyl-4′-cyanobiphyl liquid crystal (5CB) for steel/steel contacts was studied on a ball-on-plate tribotester. The friction test results show that when the graphene content in the 5CB was 0.15 wt.%, and the lubricant and friction pairs were heated to 44–46 °C before friction tests, the lubrication performance of the 5CB was most improved. Compared with pure 5CB, 5CB+0.15 wt.% graphene suspension reduced the friction coefficient and wear scar diameter by up to 70.6% and 41.3%, respectively. The lubrication mechanisms have been tentatively proposed according to the test results. We speculate that the excellent lubrication performance of graphene/5CB suspensions may be attributed to the low shear resistance adsorption layer formed by graphene and 5CB molecules on the sliding surfaces. As the protective layer, it not only prevents direct contact between the rough sliding surfaces but also is easy to slide.



The high temperature tribometer and schematic view of ball–on–plate assembly.



(a) The average wear scar diameter at various graphene concentrations after friction tests. (b) The average wear scar diameter of 5CB and 5CB+0.15 wt.% G lubricants at different times during friction tests.



optical micrographs of wear scars of the steel balls lubricated with (a) 5CB and (b) 5CB+0.15 wt.%

Graphene oxide Lubrication Tribology Additive

raphene has been reported to be an excellent lubricant additive that reduces friction and wear when coated on the surface of various materials or when dispersed in lubricants as an atomic thin material with the low surface energy. In this study, reduced graphene oxide (rGO) nanosheets for oil-based lubricant additives were prepared by using three types of alkyl chloride chemicals (butyl chloride, octyl chloride, and tetradecyl chloride). The chemical and structural properties of the synthesized rGOs were analyzed by Fourier transform infrared (FT-IR), X-ray photoelectron spectroscopy (XPS), X-ray diffraction (XRD), Raman spectroscopy, scanning electron microscope (SEM), and transmission electron microscope (TEM). The synthesized rGOs were dispersed at 0.02 wt% in PAO-0W40 oil and its tribological characteristics were investigated using a high frequency friction/wear tester. The friction coefficient and the wear track width of poly alpha olefin (PAO) oil added with rGO-14 were tested by a ball-on-disk method, and the measured results were reduced by ~5.88 and ~3.8%, respectively compared with those of the conventional PAO oil. Thus, it was found that the wear resistance of PAO oil was improved. In this study, we demonstrated the successful functionalization of rGO as well as the improvement of dispersion stability and tribological characteristics of rGOs based on various alkyl chain lengths.

quote research paper from UCI(KEPA)

SOLUTIONS UNLIMITED

lubricants

MDPI

Article

The Tribological Properties of Multi-Layered Graphene as Additives of PAO2 Oil in Steel–Steel Contacts

Yan-Bao Guo * and Si-Wei Zhang *

College of Mechanical and Transportation Engineering, China University of Petroleum, Beijing 102249, China
* Correspondence: gyb@cup.edu.cn (Y.-B.G.); swzhang99@sina.com (S.-W.Z.);
Tel.: +86-10-89733727 (Y.-B.G.); +86-10-62396260 (S.-W.Z.)

Academic Editor: Robert J. K. Wood
Received: 29 May 2016; Accepted: 29 August 2016; Published: 31 August 2016

Abstract: Multi-layered graphene was prepared by supercritical CO_2 exfoliation of graphite. As the additives of polyalphaolefin-2 (PAO2) oil, its tribological properties were investigated using four-ball test method. The friction reduction and anti-wear ability of pure lubricant was improved by the addition of graphene. With a favorable concentration, the graphene was dispersive. The PAO2 oil with 0.05 wt % graphene showed better tribological properties than that for the other concentration of graphene additives. It could be used as a good lubricant additive for its excellent tribological characteristics, and the multi-layered graphene can bear the load of the steel ball and prevent direct contact of the mating metal surfaces. However, a higher concentration would cause the agglomeration of graphene and weaken the improvement of tribological properties.

Keywords: graphene; additives; PAO2; lubrication; tribological properties

1. Introduction

Friction and wear remain the primary modes of mechanical energy dissipation in moving mechanical assemblies [1]. Sliding, rolling, and rotating contact interfaces in every artificial, natural, and biological system can generate friction. If friction is not controlled or reduced, it often causes greater wear losses and, hence, shorter life and poor reliability [2]. The most effective way to control friction is to use a lubricant in liquid or solid forms. Thus, the major demand for low-friction and long-life of mechanical assemblies is satisfied for purposes of energy saving, emission reduction, and environmental protection. Green tribology is emphasized in environmentally friendly energy and materials, as well as the enhancement of the environment and the quality of life [3–5].

As is well known, lubrication is an important measure to reduce friction and wear in many engineering fields. There are two kinds of liquid lubricants, namely water-based and oil-based. The oil-based lubricants are generally used in most areas due to its many advantages, such as its wide sources, high thermal conductivity, etc. [6]. In recent years, the anti-friction and wear additives are usually used to improve the tribological behaviors of lubricants at low concentrations, especially for the environmentally friendly lubricants [7]. Low-dimensional nanomaterials with self-lubricating capability (such as MoS_2, WS_2, graphite, carbon nanotubes, and so on) might be considered as potential low-friction and anti-wear additives for future engine oil application owing to their unique size, shape, chemistry, and structure morphology. Recently, Erdemir [8] reviewed the latest research trends in 0 to 3D self-lubricating nanomaterials as potential oil additives and their prospects for commercial applications. He concluded that self-lubricating nanomaterials with 0 to 3D structural architectures may hold great promise for further enhancing the friction reducing, anti-wear, and anti-scuffing performance of future lubricating oil.

Graphene, a promising material with 2D laminated structure, has attracted considerable attention since its discovery [9,10]. In recent years, graphene has played important roles in many fields due to its

SOLUTIONS UNLIMITED

amazing mechanical, optical, and electronic properties [11–13]. There are several methods to prepare graphene, such as redox process [14], micro-mechanical stripping method [9], SiC epitaxial growth method, and chemical vapor deposition (CVD) [15]. A potentially useful method of supercritical carbon dioxide ($SCCO_2$) exfoliation of graphite was used to provide less-damaged graphene sheets [16], and this technique offers a low-cost, simple approach to large-scale production of pure graphene sheets without the need for complicated processing steps or chemical treatment [17].

With the development of carbon nanomaterials, nanoplatelet-structural graphene as a lubricant additive has gained wide attention [18–20]. Song and coworkers have found that oxide graphene nanosheets show better tribological properties than oxide multiwall carbon nanotubes (CNTs–COOH) in aqueous medium [21]. The performance of graphene oxide dispersions in water contacting diamond-like carbon and stainless steel were studied, and the tribological mechanism of graphene oxide additives in water was presented [22]. In addition, the compound lubricants containing graphene as an additive is a promising measure in the lubrication domain. Min et al. [23] investigated the polyimide (PI)/graphene oxide (GO) nanocomposite films and their tribological behaviors under seawater lubrication, which could effectively transfer load between the contact surfaces. Some researchers have reported the tribological behavior of graphene oxide nanosheets in mineral oil for boundary and mixed lubrication, and showed the relationship between protective film and the frictional coefficient trend in the boundary regime [24]. Eswaraiah et al. [25] investigated the friction reduction behavior and anti-wear performance of ultrathin graphene (UG) prepared by exfoliation of graphite oxide by a novel technique based on focused solar radiation, and pointed out the importance of forming nanobearings in reducing the friction and wear. Furthermore, graphene nanoflakes as an addition to grease are usefulness for decreasing the coefficient of friction and wear of friction pairs [26,27]. In order to make graphene homogeneously dispersed, some measures were taken. Investigators reported a study on friction and wear performance when graphene sheets were modified by oleic acid as additives to lubricant oils [28]. More recently, a series of calcium borate/graphene oxide (CB/GO) and Cu/reduced graphene oxide composites were synthesized, which indicated that the formation of an interfacial boundary lubrication layer improved friction and wear properties [13,29].

Recent studies in the nano- and macroscale have shown graphene to have the potential to substantially lower friction and wear under specific conditions [1]. As lubrication additives, the graphene and graphene oxide are modified. However, mass production of graphene as lubrication additive at engineering scales has yet to be demonstrated for a better prospect of application. Therefore, the aim of this study is to investigate the tribological properties and to reveal the lubrication mechanism of multi-layered graphene (prepared by supercritical CO_2 exfoliation of graphite) as lubrication additives in polyalphaolefin-2 oil (PAO2) in order to assess the application prospect.

2. Experiments

2.1. Materials

The multi-layered graphene was supplied by the State Key Laboratory of Heavy Oil Processing at China University of Petroleum, Beijing. It was prepared by shear-assisted supercritical CO_2 exfoliation (SSCE) process [30], which can produce high-quality and large-quantity graphene nanosheets. Furthermore, the graphene synthesized by SSCE method consists of 90% exfoliated sheets with less than 10 layers and about 70% that have between 5 and 8 layers; this was clearly shown in Yi Liu's research [31]. The scanning electron microscope (SEM) image of graphene is shown in Figure 1. It can be seen that the diameter of the particle is about 10 μm.

SOLUTIONS UNLIMITED

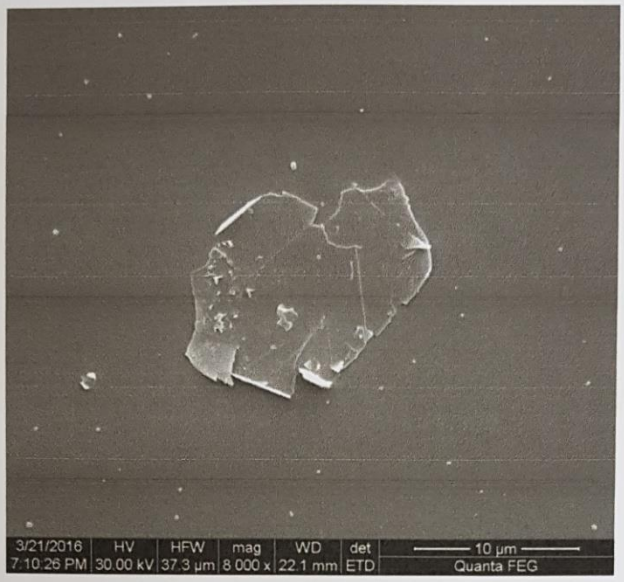


Figure 1. Scanning electron microscope (SEM) image of grapheme.

The lubricant oil, polyalphaolefin-2 (PAO2), with a viscosity of 2 mPa·s at 40 °C was supplied by Beijing Yanshan Petrochemical Co., Ltd. (Beijing, China). The graphene, without further treatment, was added into pure PAO2. The mixed solutions (three lubricant samples) containing several different concentrations of graphene were ultrasonicated for 30 min before each test. Hereinafter, the four samples in this study are expressed as: 0.0 wt % (pure PAO2), 0.05 wt %, 0.1 wt %, and 0.5 wt %. Graphene can be easily dispersed without any surface modification or surfactant in the oil-based lubricants after ultrasonication, as shown in Figure 2b–d. Furthermore, digital pictures taken 2 weeks after ultrasonication of the different concentration are shown in Figure 2e–g. For the samples just ultrasonicated, it can be noticed that the multi-layered graphene can be dispersed in PAO2. In can be seen that the multi-layered graphene can be easily dispersed without surface modification or surfactant in the oil-based lubricants, as shown in Figure 2b–d, after ultrasonication. At low concentration, the graphene particles are uniformly dispersed, and as time passes, the particles gradually aggregate and precipitate at a low speed. However, as shown in Figure 2f,g, with a higher graphene concentration, the graphene particles easily assemble and become high-weight particle groups which are easily precipitated for the gravity effect. The dispersions displayed only short-term stability and precipitated completely after a few weeks. Comparing the different concentrations, increasing graphene concentration increased the precipitation rate. This is due to the aggregation of particles at a higher concentration.

2.2. *Instruments and Experimental Parameters*

The frictional coefficient, wear scar tests of multi-layered graphene as additives of PAO2 were evaluated by a multispecimen test machine (FALEX tribology 1506, USA) with a four-ball configuration. The tester was operated with one steel ball under load rotating against three steel balls held stationary in the form of a cradle. Before operating the machine with the test balls, the components were cleaned with petroleum ether under ultrasonication, rinsed with alcohol, and finally dried with a stream of nitrogen. Steel balls—made of AISI-52100 steel with a diameter of 12.7 mm and a hardness of 64~66 HRC—were used in the four-ball test. Before and after each test, the steel balls were cleaned in petroleum ether and absolute ethyl alcohol with ultrasonication, respectively. Then, the samples

SOLUTIONS UNLIMITED

were dried with a stream of nitrogen. Three 12.7 mm diameter steel balls were clamped together and covered with pure PAO2 or graphene-added PAO2 lubricants to be evaluated. The experimental set up of the tribometer is shown in Figure 3 along with schematic view of the four-ball assembly.

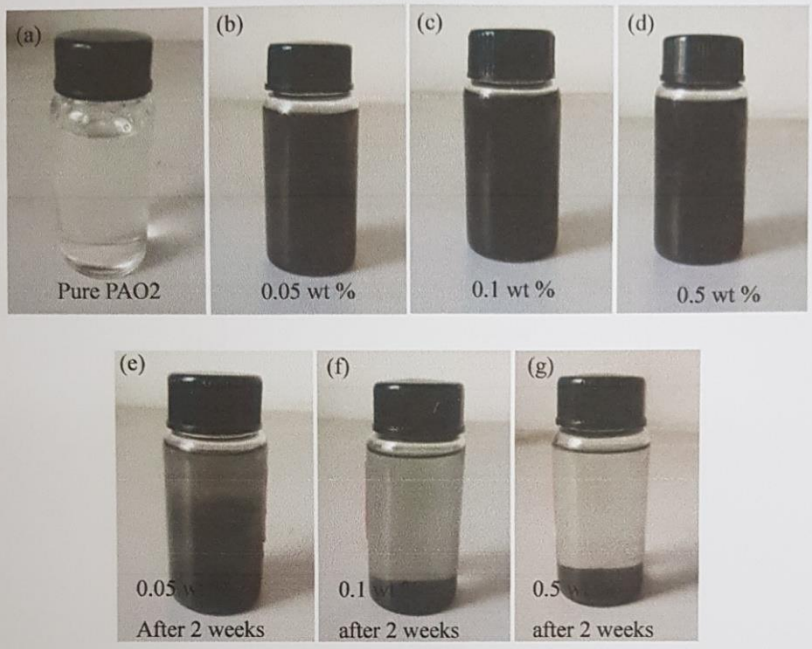


Figure 2. Digital pictures of pure polyalphaolefin-2 oil (PAO2) (**a**); and with different concentrations of graphene additives: 0.05 wt % (**b**); 0.1 wt % (**c**); and 0.5 wt % (**d**). After 2 weeks, the pictures of 0.05 wt %, 0.1 wt %, and 0.5 wt % are shown in (**e**), (**f**), and (**g**), respectively.

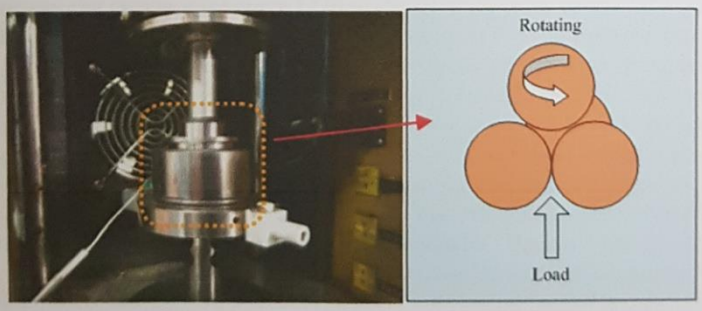


Figure 3. Schematic view of the four-ball assembly.

The effects of load and rotation speed on the lubricants of graphene additives were studied under different loads in the range 120–400 N, and different rotation speeds ranging from 100 rpm up to 400 rpm. In this study, each test was carried out twice under the above condition. New balls were used in every test, and all the tests were conducted at room temperature with a relative humidity of 25%.

In order to characterize the morphology of the scar surface, after the test, the worn scars were detected using scanning electric microscopy (SEM, FEI QUANTA 200F), energy dispersive spectroscopy

SOLUTIONS UNLIMITED

(EDS), and 3D white light interference (WLI). Besides, the viscosity of lubrication was measured using an MCR301 rotary rheometer, varying the shear rate from 1 s^{-1} to 10,000 s^{-1}.

3. Results and Discussion

3.1. Coefficients of Friction (COF)

The COF curves of lubricants with different graphene concentrations (wt %) under load of 120 N and rotation speed of 250 rpm are shown in Figure 4. It can be seen that the fluctuation of COF curves is gentle. Moreover, the values of COF decrease smoothly with the passage of time and are less than that of the pure lubricant. This shows that the graphene has obvious anti-friction properties. The lowest value of COF is found when the graphene concentration is 0.05 wt %, about 78% less than that of pure lubricant.

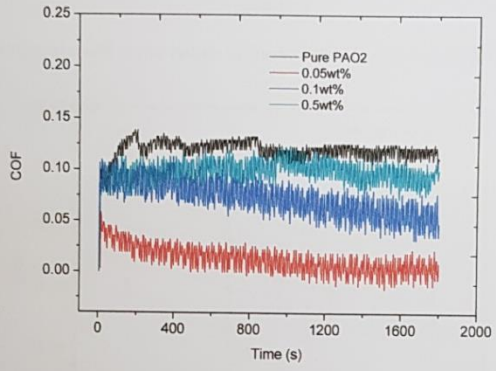


Figure 4. Friction coefficient curves of different additive concentrations of graphene in PAO2 (load 120 N, rotation speed 250 rpm).

Figure 5 shows the curves of average COF of different samples under different loads and a rotation speed of 250 rpm, along with the error bars denoting the standard deviation around the rolling mean. It was found that the COF increased with the loads from 120 N up to 400 N for the four samples. Furthermore, when the loads are below 240 N, the COF rises markedly with increasing loading force, and is then stable with increasing load. Furthermore, the COF of the samples under a series of rotation speeds from 100 rpm to 400 rpm with 120 N (Figure 6) shows that the COF of the sample with 0.05 wt % graphene has the lowest friction under different rotation speeds. A comparison among the four samples (PAO2 with different graphene concentrations) shows that reduction of the friction coefficient for the sample with graphene is remarkable (Figures 5 and 6). Additionally, as can be seen from Figure 6, the COF is decreasing with increasing rotation speeds, from 100 rpm to 400 rpm. From the friction curves, it is found that the lubrication regime is mainly boundary and mixed lubrication, and the friction coefficient decreases with increasing sliding speed [24]. In addition, for the graphene-added PAO2, more graphene would be entrained into the rubbing surfaces with the increasing of rotation speed. Moreover, the higher rotation speed is beneficial to the dispersibility of graphene in PAO2 and hinders the precipitation phenomenon.

SOLUTIONS UNLIMITED

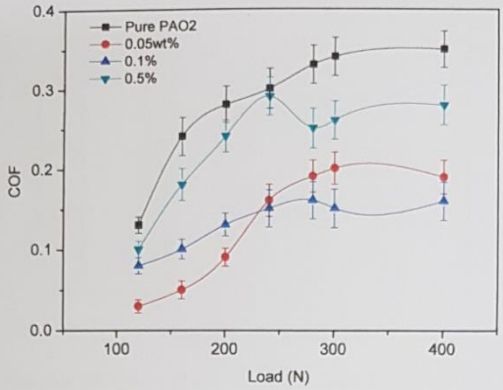


Figure 5. Friction coefficients versus different loads (rotation speed of 250 rpm).

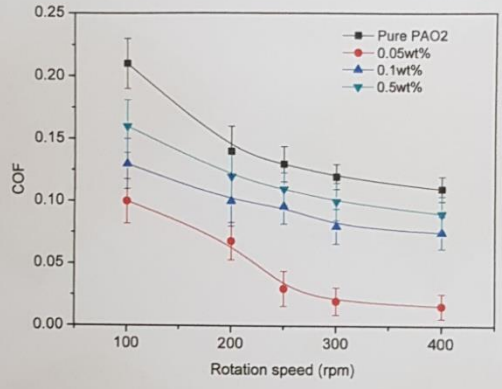


Figure 6. Coefficients of friction (COF) of different rotation speeds for different concentrations of graphene additive (load of 120 N).

3.2. *Anti-Wear Behaviors*

Wear scar diameter (WSD) is a key parameter to evaluate the anti-wear properties of the lubricants. The surface topographies of worn steel balls were investigated by 3D white light interference and the average WSDs were calculated from the surface topography. Figure 7 shows the average WSDs of ball samples under applied load of 120 N and rotation speed of 250 rpm with friction time of 30 min. It can be seen that the average WSD of pure lubricant is about 0.77 mm, which is larger than that of the other three samples. Figure 8 shows the 3D surface images of wear scars of different samples. As shown in Figure 8a, the worn surface in pure lubricant is rough with many wide and deep furrows, but the surface images of the other three samples are smooth except for a few scratches. This wear protective effect is attributed to increased tendency to form a protective film with graphene. The sample with 0.05 wt % graphene has a lower surface roughness than the pure lubricant. In contrast, when 0.5 wt % graphene was added, a number of scratches emerged on the surface with a greater surface roughness. Figure 8e,f shows the linear roughness curve. When 0.05 wt % of graphene was added, the reduction of the WSD is up to 16%. This result indicates that the addition of graphene could improve the anti-wear properties of the lubricants. This might be due to the present of graphene on the friction surface. However, when the concentration increases, the WSD becomes a little larger, perhaps due to abrasive wear occurring [28].

SOLUTIONS UNLIMITED

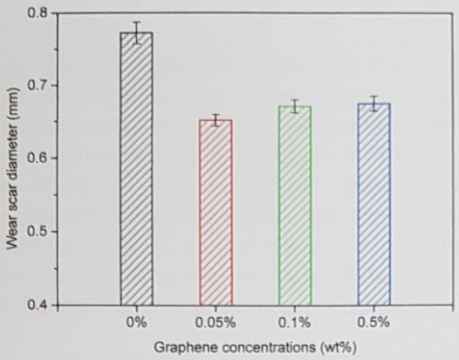


Figure 7. Wear scar diameter (WSD) of different concentrations of graphene additive (load 120 N, rotation speed 250 rpm).

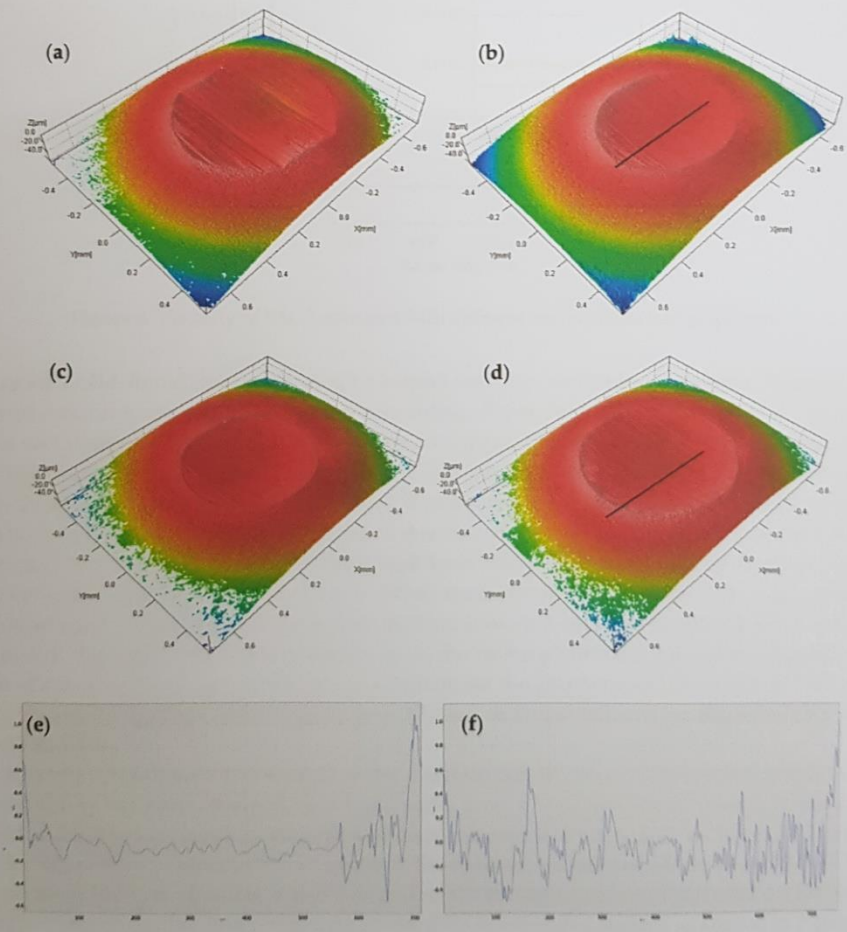


Figure 8. 3D optical micrographs of the abraded surface with pure PAO2 (**a**); 0.05 wt % (**b**); 0.1 wt % (**c**); 0.5 wt % (**d**) of graphene; linear roughness with (**e**) 0.05 wt % graphene in PAO2 and (**f**) 0.5 wt % graphene in PAO2, respectively.

SOLUTIONS UNLIMITED

3.3. Lubrication Mechanism

As stated above, with the addition of graphene additives in PAO2 is effective on the anti-friction and wear-resistant properties. It is well known that the rheological behavior is a key parameter of lubricants [32]. In order to investigate the effect of graphene additives on the rheological behavior of PAO2, the viscosity of samples was measured at 20 °C using a MCR301 rotary rheometer (Figure 9). It was found that the reduction of viscosity was the result of increasing shear rate for all samples. This can be explained by a shear-thinning phenomenon of the base liquids, and the addition of graphene does not change the characteristics of non-Newtonian liquid. Added to this, the addition of graphene causes a slight increase of the viscosity compared with pure PAO2, shown in the illustration insert in Figure 9. This indicated that the viscosity of the four samples were about the same.

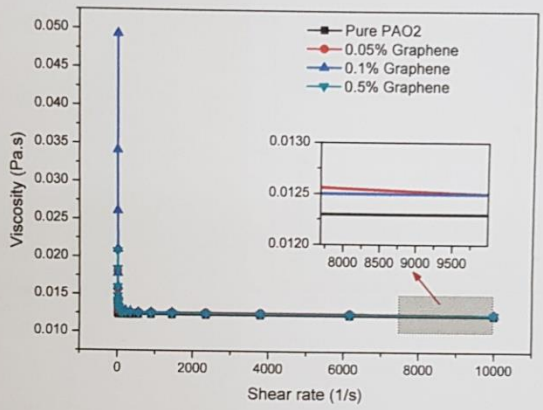


Figure 9. Viscosity of PAO2 solutions with different concentrations of grapheme.

Biphase (solid–liquid) lubricant could be helpful for better explaining the above. It is well known that liquid lubricants can reduce friction by preventing sliding contact interfaces from severe or more frequent metal-to-metal contacts or by forming a low-shear, high-durability film on rubbing surfaces. Depending on the sliding speed/rotation speed and other operating conditions, the lubricant can effectively separate the contacting surfaces and, thereby, reduce the direct metal-to-metal contact and thus friction and wear. In this study, if and when there is metal-to-metal contact, the graphene additives in PAO2 can form a protective film to provide additional safety. According with the Stribeck curve, the lubrication form is mainly mixed lubrication. When the concentration of graphene is appropriate, the favorable dispersive graphene additives into the base lubricant could be beneficial for the formation of lubrication film and persistence of additives on the rubbing surfaces. However, with the further increase of concentration of graphene, it is too difficult for the graphene additives to enter the rubbing surfaces due to the agglomeration of graphene. Moreover, it also reduces the dispersive behavior of graphene additive.

In this work, it has been shown that under a certain condition of multi-layered graphene, good anti-wear ability has been obtained, and at the same time, a very low friction coefficient is reached. The SEM and EDS of surface morphologies of three samples (0.0 wt %, 0.05 wt %, and 0.5 wt %) are shown in Figure 10a–c, respectively. In contrast, the rubbing surfaces of 0.0 wt % and 0.5 wt % have wide and deep furrows. Besides, some pits and spalls are non-uniformly covered on the surfaces. Furthermore, some coating (black region) appeared on the abraded surface as shown in Figure 10b,c. Especially for the sample with 0.05 wt % graphene, the region of coating extended as shown in Figure 10b. As presented in Figure 10b, the rubbing surface lubricated with PAO2 added 0.05 wt % multi-layered graphene is smoother. Thus, the mechanism of the reducing friction and anti-wear of graphene particles dispersed in PAO2 can be confirmed by results of SEM. As seen from Figure 10a–c,

SOLUTIONS UNLIMITED

the carbon content in the rubbed surface of the sample with 0.05 wt % graphene is the highest. Taking into account the fact that graphene is made of carbon, it can be deduced that the graphene content in contact surfaces of this sample is also the highest. This indicates that a thin tribofilm is formed on the metal surface. The tribofilms could not only bear the load of the steel ball, but also prevent the direct contact of two mating metal surfaces [21]. Therefore, the anti-wear ability of the PAO2 with graphene additives was improved, and the friction coefficient was reduced significantly. However, when the concentration of graphene further increased, the anti-wear and friction-reducing performance was weakened. This might be due to the agglomeration of graphene during the friction process. The SEM images of the sample with 0.5 wt % graphene after the friction test are shown in Figure 11. It was observed that the agglomeration of graphene appeared obviously.

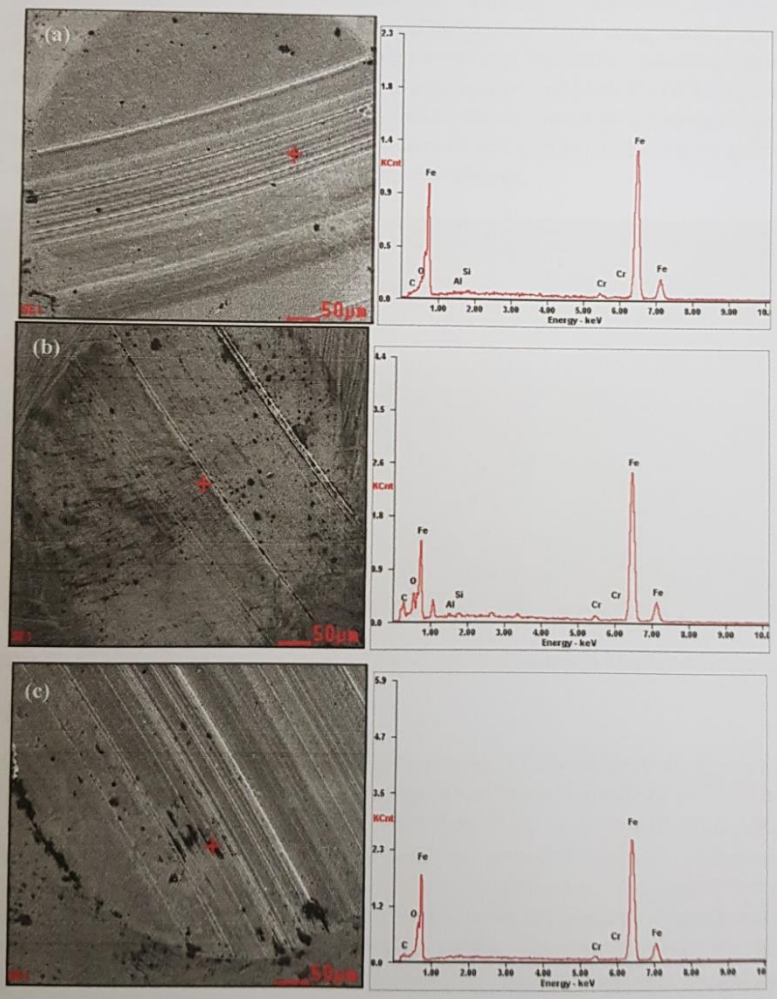


Figure 10. SEM surface morphologies and energy dispersive spectroscopy (EDS) of the wear scars. (**a**) 0.0 wt % (pure PAO2); (**b**) 0.05 wt %; and (**c**) 0.5 wt % of graphene.

In a real friction process, the contact surfaces were filled with the dispersed graphene, and then graphene sheets in PAO2 on contact surfaces can serve as spacers, preventing some real contact. In addition, the two-dimensional sheet shape of graphene could provide easy shear and more easily a

SOLUTIONS UNLIMITED

slider between the two contact surfaces. So, the friction coefficient of PAO2 with graphene decreased obviously. All the tribological behaviors mentioned above show that graphene is very attractive for demanding tribological applications to achieve low friction and wear regimes.

Results indicated that a thin tribofilm is formed on the metal surface during the friction test. The tribofilms could in some degree bear the load of the steel ball, but also prevent from some direct contact between contact surfaces. Therefore, the anti-wear ability of the PAO2 with graphene additives was improved, and the friction coefficient was reduced significantly. In addition, the rubbing surface lubricated with PAO2 added with multi-layered graphene is smoother than the pure PAO2 lubricant condition.

The friction-reduction ability of multi-layered graphene sheets as lubricant additive could be explained by better dispersion. It could be deduced that the high-concentration graphene presented poor dispersion, with large graphene bundles caused by agglomeration being easily formed in higher concentrations, resulting in the friction coefficient increasing. When the concentration of graphene increases, the agglomeration and shape change of graphene occurs with the friction process, which can be seen from Figure 11; it is difficult for larger additives to enter into the contact area during the rotation friction process. Therefore, the improvement of anti-friction and abrasive properties were weakened with the higher concentration of graphene additives.

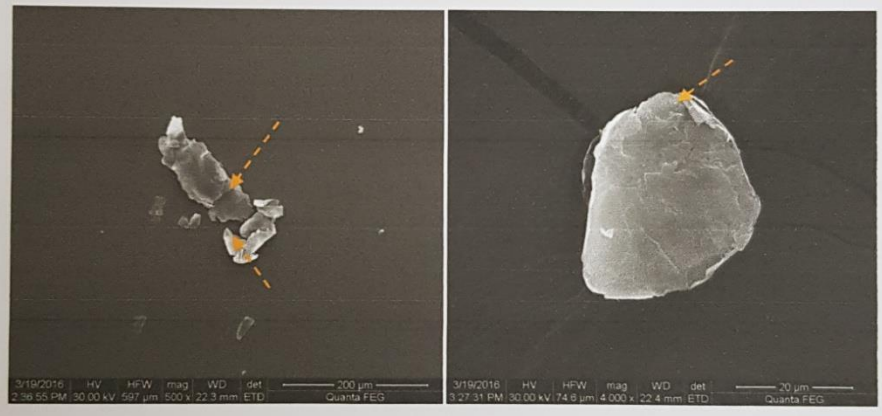


Figure 11. SEM images of agglomerated graphene after friction test (0.5 wt % concentration).

4. Conclusions

Multi-layered graphene sheets prepared by supercritical CO_2 exfoliation of graphite showed excellent performance of friction reduction and anti-wear as 0.05 wt % additives of PAO2 in steel–steel contacts in comparison with the pure lubricant. With the 0.05 wt % graphene additives, friction coefficient reduced by about 78% and wear scar diameter decreased markedly compared to that of pure PAO2 lubricant under a load of 120 N and rotation speed 250 rpm. The lubrication mechanism was presented, which indicated that the graphene additives with the lubricant entered into the rubbing surfaces, and a thin physical triofilm formed on the rubbing surfaces to prevent the direct contact of these surfaces. This could explain the improvement of friction and wear properties with the appropriate concentration of graphene additives. The test results show that multi-layered graphene is very attractive for demanding tribological applications to achieve low friction and wear regimes.

Acknowledgments: This research is supported by Beijing Natural Science Foundation (No. 3162024), the National Natural Science Foundation of China (No. 51305459), Tribology Science Foundation of State Key Laboratory of Tribology, Tsinghua University (No. SKLTKF14A08) and the Science Foundation of China University of Petroleum (No. 2462013YJRC032).

Author Contributions: All authors were involved in the preparation and correction of the manuscript.

SOLUTIONS UNLIMITED

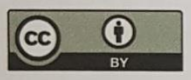
Conflicts of Interest: The authors declare no conflict of interest.

References

1. Berman, D.; Deshmukh, S.A.; Sankaranarayanan, S.K.R.S.; Erdemie, A.; Sumant, A.V. Macroscale superlubricity enabled by graphene nanoscroll formation. *Science* **2015**, *348*, 1118–1122. [CrossRef] [PubMed]
2. Berman, D.; Erdemir, A.; Sumant, A.V. Graphene: A new emerging lubricant. *Mater. Today* **2014**, *17*, 31–42. [CrossRef]
3. Zhang, S.W. Green tribology—The way forward to a sustainable society. In Proceedings of the International Tribology Congress—ASIATRIB, Perth, Australia, 5–9 December 2010; Volume 6.
4. Zhang, S.W. Green tribology: Fundamentals and future development. *Friction* **2013**, *1*, 186–194. [CrossRef]
5. Zhang, S.W. Recent developments of green tribology. *Surface Topogr. Metrol. Prop.* **2016**, *4*, 023004. [CrossRef]
6. Totten, G.E. *Handbook of Hydraulic Fluid Technology*; CRC Press: Boca Raton, FL, USA, 2011.
7. Adhvaryu, A.; Erhan, S.Z.; Perez, J.M. Tribological studies of thermally and chemically modified vegetable oils for use as environmentally friendly lubricants. *Wear* **2004**, *257*, 359–367. [CrossRef]
8. Erdemir, A. Advances In novel nanolubrication additives for improved friction and wear properties. In Proceedings of the 5th World Tribology Congress, Torino, Italy, 8–13 September 2013.
9. Novoselov, K.S.; Geim, A.K.; Morozov, S.V.; Jiang, D.; Zhang, Y.; Dubonos, S.V.; Grigorieva, I.V.; Firsov, A.A. Electric field effect in atomically thin carbon films. *Science* **2004**, *306*, 666–669. [CrossRef] [PubMed]
10. Nair, R.R.; Blake, P.; Grigorenko, A.N.; Novoselov, K.S.; Booth, T.J.; Stauber, T.; Peres, N.M.R.; Geim, A.K. Fine structure constant defines visual transparency of graphene. *Science* **2008**, *320*, 1308. [CrossRef] [PubMed]
11. Lee, C.; Wei, X.D.; Kysar, J.W.; Hone, J. Measurement of the elastic properties and intrinsic strength of monolayer graphene. *Science* **2008**, *321*, 385–388. [CrossRef] [PubMed]
12. Bolotin, K.I.; Sikes, K.J.; Jiang, Z.; Klima, M.; Fudenberg, G.; Hone, J.; Kim, P.; Stormer, H.L. Ultrahigh electron mobility in suspended graphene. *Solid State Commun.* **2008**, *146*, 351–355. [CrossRef]
13. Jia, Z.; Chen, T.; Wang, J.; Ni, J.; Li, H.; Shao, X. Synthesis, characterization and tribological properties of Cu/reduced graphene oxide composites. *Tribol. Int.* **2015**, *88*, 17–24. [CrossRef]
14. Liu, X.W.; Mao, J.J.; Liu, P.D.; Wei, X.W. Fabrication of metal-graphene hybrid materials by electroless deposition. *Carbon* **2011**, *49*, 477–483. [CrossRef]
15. Liu, W.; Chung, C.H.; Miao, C.Q.; Wang, Y.J.; Li, B.Y.; Ruan, L.Y. Chemical vapor deposition of large area few layer graphene on Si catalyzed with nickel films. *Thin Solid Films* **2010**, *518*, S128–S132. [CrossRef]
16. Sim, H.S.; Kim, T.A.; Lee, K.H.; Min, P. Preparation of graphene nanosheets through repeated supercritical carbon dioxide process. *Mater. Lett.* **2012**, *89*, 343–346. [CrossRef]
17. Pu, N.W.; Wang, C.A.; Sung, Y.; Liu, Y.M.; Ger, M.D. Production of few-layer graphene by supercritical CO_2 exfoliation of graphite. *Mater. Lett.* **2009**, *63*, 1987–1989. [CrossRef]
18. Lin, J.S.; Wang, L.W.; Chen, G.H. Modification of graphene platelets and their tribological properties as a lubricant additive. *Tribol. Lett.* **2011**, *41*, 209–215. [CrossRef]
19. Kinoshita, H.; Nishina, Y.; Alias, A.A.; Fujii, M. Tribological properties of monolayer graphene oxide sheets as water-based lubricant additives. *Carbon* **2014**, *66*, 720–723. [CrossRef]
20. Berman, D.; Erdemir, A.; Sumant, A.V. Few layer graphene to ewduce wear and friction on sliding steel surfaces. *Carbon* **2013**, *54*, 454–459. [CrossRef]
21. Song, H.J.; Li, N. Frictional behavior of oxide graphene nanosheets as water-base lubricant additive. *Appl. Phys. A Mater. Sci. Process.* **2011**, *105*, 827–832. [CrossRef]
22. Elomaa, O.; Singh, V.K.; Iyer, A.; Hakala, T.J.; Koskinen, J. Graphene oxide in water lubrication on diamond-like carbon vs. stainless steel high-load contacts. *Diam. Relat. Mater.* **2015**, *52*, 43–48. [CrossRef]
23. Min, C.; Nie, P.; Song, H.J.; Zhang, Z.; Zhao, K. Study of tribological properties of polyimide/graphene oxide nanocomposite films under seawater-lubricated condition. *Tribol. Int.* **2014**, *80*, 131–140. [CrossRef]
24. Senatore, A.; D'Agostino, V.; Petrone, V.; Ciambelli, P.; Sarno, M. Graphene oxide nanosheets as effective friction modifier for oil lubricant: Materials, methods, and tribological results. *ISRN Tribol.* **2013**, *2013*, 425809. [CrossRef]
25. Eswaraiah, V.; Sankaranarayanan, V.; Ramaprabhu, S. Graphene-based engine oil nanofluids for tribological applications. *ACS Appl. Mater. Interfaces* **2011**, *3*, 4221–4227. [CrossRef] [PubMed]

SOLUTIONS UNLIMITED

26. Juś, A.; Kamiński, M.; Radzikowska-Juś, W. Influence of graphene nanoflakes addition on grease tribological properties. In Proceedings of the 22th International Conference on Applied Physics of Condensed Matter, Štrbské Pleso, Slovakia, 22–24 June 2016; pp. 307–310.
27. Missala, T.; Szewczyk, R.; Winiarski, W.; Hamela, M.; Kamiński, M.; Dąbrowski, S.; Pogorzelski, D.; Jakubowska, M.; Tomasik, J. Study on tribological properties of lubricating grease with additive of graphene. In *Progress in Automation, Robotics and Measuring Techniques*; Springer International Publishing: Berlin/Heidelberg, Germany, 2015; pp. 181–187.
28. Zhang, W.; Zhou, M.; Zhu, H.; Tian, Y.; Wang, K.; Wei, J.; Ji, F.; Li, X.; Li, Z.; Zhang, P.; et al. Tribological properties of oleic acid-modified graphene as lubricant oil additives. *J. Phys. D Appl. Phys.* **2011**, *44*, 205303. [CrossRef]
29. Jia, Z.; Pang, X.; Li, H.; Ni, J.; Shao, X. Synthesis and wear behavior of oleic acid capped calcium borate/graphene oxide composites. *Tribol. Int.* **2015**, *90*, 240–247. [CrossRef]
30. Li, L.; Li, G.H.; Li, Y.F.; Gao, J.S.; Xu, C.M. Preparation of graphene from graphite by supercritical CO_2 exfoliation assisted with fluid shear. *Chin. Sci. Bull.* **2015**, *60*, 2561–2566. (In Chinese) [CrossRef]
31. Li, L.; Xu, J.; Li, G.; Jia, X.; Li, Y.; Yang, F.; Zhang, L.; Xu, C.; Gao, J.; Liu, Y.; et al. Preparation of graphene nanosheets by shear-assisted supercritical CO_2 exfoliation. *Chem. Eng. J.* **2016**, *284*, 78–84. [CrossRef]
32. Xiao, H.; Dai, W.; Kan, Y.; Clearfield, A.; Liang, H. Amine-intercalated α-zirconium phosphates as lubricant additives. *Appl. Surface Sci.* **2015**, *329*, 383–389. [CrossRef]



© 2016 by the authors; licensee MDPI, Basel, Switzerland. This article is an open access article distributed under the terms and conditions of the Creative Commons Attribution (CC-BY) license (http://creativecommons.org/licenses/by/4.0/).

SOLUTIONS UNLIMITED

materials

MDPI

Article

Tribological Behaviors of Graphene and Graphene Oxide as Water-Based Lubricant Additives for Magnesium Alloy/Steel Contacts

Hongmei Xie [1], Bin Jiang [2,3,*], Jiahong Dai [1], Cheng Peng [1,*], Chunxia Li [1,*], Quan Li [3] and Fusheng Pan [2,3]

1 College of Mechanical and Electrical Engineering, Yangtze Normal University, Chongqing 408100, China; xiehongmei@yznu.cn (H.X.); 20091008@yznu.cn (J.D.)
2 College of Materials Science and Engineering, National Engineering Research Center for Magnesium Alloys, Chongqing University, Chongqing 400044, China; fsPan@cqu.edu.cn
3 Chongqing Academy of Science and Technology, Chongqing 401123, China; liquan@cqu.edu.cn
* Correspondence: jiangbinrong@cqu.edu.cn (B.J.); pengcheng@yznu.cn (C.P.); lichunxia@yznu.cn (C.L.); Tel./Fax: +86-023-65111140 (B.J.)

Received: 3 January 2018; Accepted: 25 January 2018; Published: 29 January 2018

Abstract: The tribological behaviors of graphene and graphene oxide (GO) as water-based lubricant additives were evaluated by use of a reciprocating ball-on-plate tribometer for magnesium alloy-steel contacts. Three sets of test conditions were examined to investigate the effect of concentration, the capacity of carrying load and the endurance of the lubrication film, respectively. The results showed that the tribological behaviors of water can be improved by adding the appropriate graphene or GO. Compared with pure deionized water, 0.5 wt.% graphene nanofluids can offer reduction of friction coefficient by 21.9% and reduction of wear rate by 13.5%. Meanwhile, 0.5 wt.% GO nanofluids were found to reduce the friction coefficient and wear rate up to 77.5% and 90%, respectively. Besides this, the positive effect of the GO nanofluids was also more pronounced in terms of the load-carrying capacity and the lubrication film endurance. The wear mechanisms have been tentatively proposed according to the observation of the worn surfaces by field emission scanning electron microscope-energy dispersive spectrometer (FESEM-EDS) and Raman spectrum as well as the wettability of the nanofluids on the magnesium alloy surface by goniometer.

Keywords: graphene; graphene oxide; water-based; lubricant additives; magnesium alloy

1. Introduction

Magnesium and its alloys are attractive materials for a wide range of applications in such demanding fields as transportation, electronics or aerospace [1,2]. This is due to superior attributes such as low density, high thermal conductivity, and ease of manufacturing by conventional processes. Currently, most of the magnesium alloy usage in industry is limited to die-cast components [3]. In the future, the increasing demand for large-scale applications of wrought Mg alloy products, such as extruded profiles, rolled sheets and forgings, will determine the development of Mg alloys. The wrought Mg alloys offer better mechanical properties in comparison to cast Mg alloys because of the pronounced grain refinement without pores and uniform composition distribution after the deformation process [4]. However, the high friction between the workpiece and tool steel during the forming process cannot be avoided, thus resulting in relatively short tool life, high energy consumption and poor-quality products [5,6].

To address these issues, lubricants can be employed. So far, there are no suitable forming fluids for the forming process of Mg alloy; even in some conditions, the forming fluid used for Al alloy

SOLUTIONS UNLIMITED

is casually used and the result is not satisfied. The commonly used Al alloy forming lubricants relies heavily on sulfur-, chlorine- and phosphorous-containing organic compounds as additives. The discharge of these lubricants has caused a series of issues such as high cost, environmental pollution and others [7]. Furthermore, the effects of these additives on tribological properties can be complicated by the fact that the fast chemical degradation during friction process is often inevitably present in them and degrades their desired tribological behaviors [8]. Therefore, a new type of environmentally sustainable lubricant additives that do not compromise lubricant performances needs to be required to substitute the conventional additives. To ameliorate the tribological performances of magnesium alloys, several categories of advanced additives have been explored, such as N-containing compounds [9], borates [10] and ionic liquids [11]. Overall, these lubricant additives have exhibited excellent tribological properties during testing, mainly because of the formation of different types of tribofilm between the interacting surfaces. Although many nitrogen heterocyclics showed favorable wear resistance and corrosion inhibition, the friction reduction performance was limited [12]. The borate without active element, such as nitrogen, sulfur and chlorine, is ineffective at improving the tribological properties of magnesium alloy [13]. The ionic liquids are synthesized from expensive starting material, which results in the high cost to use these ionic liquids as lubricant additives [14]. Therefore, the search continues for novel materials that can potentially be used as lubricant additives for magnesium alloys.

Lately, a wide variety of nanomaterials as lubricant additives is a rapidly progressing field of research owing to their unique chemical and structural attributes [15–17]. Compared with conventional organic lubricant additives, the nanoparticles as lubricant additive possess several advantages; for example the small size allows the nanoparticles to readily enter the tribological interfaces [18]. More importantly, the excellent chemical stability of the nanoparticles contributes to less harmful emissions and dramatically lower toxicity than conventional organic additives, making them attractive with respect to the sustainable development of environmental. Among a variety of nanoparticles, the two-dimensional graphene and GO possess the desirable properties from a lubrication point of view, such as extreme strength, easy shear capability, excellent Young's modulus, high thermal stability and good conductivity, and have been extensively explored for their tribological behaviors as self-lubricating solids [19,20], as composites [21–23] and as lubricant additives. For example, Harshal P. Mungse et al. [24] evaluated the tribological properties of graphene oxide sheets as additives in conventional 10W-40 lube oil for steel/steel pairs. It was reported that GO nanosheets, used as a lubricant oil additive, played a positive role in remarkably lowering the friction and improving the anti-wear properties. The friction coefficient and wear volume were reduced by about 36.4% and 37.5% respectively. Yinglei Wu et al. [25] used a ball-on-ring tribometer to investigate the tribological behavior of GO sheets, which were dispersed in O/W base emulsion. Their results revealed 27.9% and 21.8% reductions in friction coefficient and wear volume, respectively, attributed to the formation of a GO-related lubricating tribofilm on the worn surface. Xiaoqiang Fan et al. [26] reported the use of graphene as a bentone-lubricating grease additive for the steel/steel pairs. The experimental measurements showed that friction-reducing and anti-wear properties of bentone-lubricating grease were both improved by the formation of a graphene-related lubricating boundary layer. Nevertheless, no improvement of the lubricating behaviors was observed for the copper alloy/steel contacts when graphene was dispersed into the hydraulic oil [27]. Previous studies demonstrate that the lubrication effectiveness of GO and graphene as additives are very sensitive to the tribological system properties such as based media and contact pairs. Clearly, water-based lubrication processes the advantage of cooling capabilities, reduced cleaning costs, lower toxicity and fire resistance. However, the low viscosity, corrosive properties and poor boundary lubrication properties limit the application of water lubrication in the process of metal forming, and extra additives are necessary for enhancing its lubricating properties. To date, the combination of graphene or GO water-based fluids and magnesium alloy are still waiting to be explored.

SOLUTIONS UNLIMITED

The aim of this study was to evaluate the tribological performances of graphene and GO as water-based lubricant additives for the magnesium alloy/steel contacts using a ball-on-plate tribotester. The lubrication mechanism was investigated by analyzing the worn surface using FESEM-EDS and Raman spectroscopy. It is anticipated that graphene or GO water-based nanofluids may find broad potential applications in the forming process of magnesium alloy.

2. Experimental

2.1. Materials

The graphene and GO used in this work were commercially obtained from Hengqiu Graphene technology Co., Ltd., Suzhou, China. The morphology and structure of the samples were observed with JEM 1200EX transmission electron microscope (TEM; JEOL Ltd., Tokyo, Japan) and VG model Escalab 250 X-ray photoelectron spectroscopy (XPS, VG Scientific Ltd., East Grinstead, UK). As shown in TEM images (Figure 1a,b), graphene is apparently transparent with the size of several micrometers, while the GO nanosheets with many folds are observed. These rippled morphologies can be attributed to the oxygen-containing groups on the GO nanosheets. These oxygen containing groups attracted to each other through hydrogen bond, resulting in folds in GO sheets. The high-resolution transmission electron microscope (HRTEM, JEM 1200EX, JEOL Ltd., Tokyo, Japan) lattice image as shown in Figure 1c,d clearly demonstrated that the thickness of graphene sheets and GO was 5 nm and 4.2 nm, respectively. Based on the reported interlayer distances for graphene and GO layers (0.34 nm and 0.7 nm), the graphene and GO were identified to be multi-layer [28]. XPS spectrum (Figure 1e,f) is demonstrated the difference in the carbon composition for graphene and GO, as well as to emphasize the oxidation level of GO. The C1s spectrum of GO as shown in Figure 1 consists of three different peaks: C–C in aromatic rings (284.7 eV), C–O (286.8 eV) and C=O (288.1 eV), indicating the existence of these oxygen-containing functional groups. The nanofluids were prepared by mixing the given additives (graphene and GO) into the water at different concentration i.e., 0.2, 0.5, 0.7 and 1.0 wt.%. In order to obtain a uniform mixture, the suspensions were stirred for 1 h, followed by ultrasonic bathing for 2 h. In this study, any extra dispersion or surfactant agents were not used so as to isolate the effects of the nanoparticles additives.

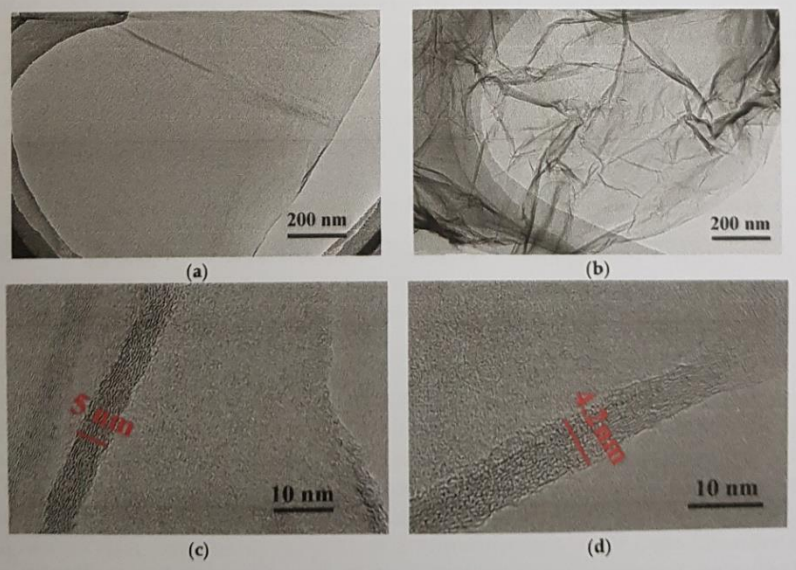


Figure 1. *Cont.*

SOLUTIONS UNLIMITED

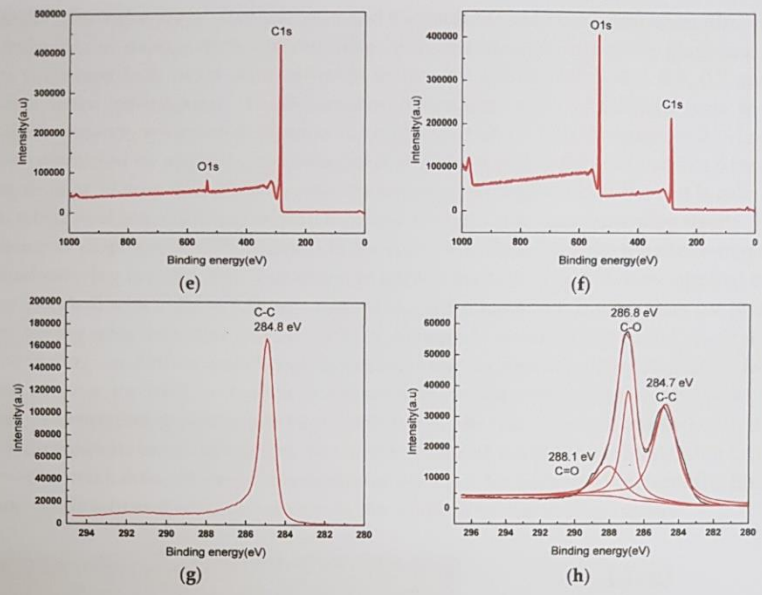


Figure 1. TEM images and XPS spectrum of graphene (**a**,**c**,**e**,**g**) and GO (**b**,**d**,**f**,**h**).

The commercial AZ31 (Mg–3.07Al–0.78Zn–0.38Mn in wt.%) magnesium alloy ingots with 82 mm in diameter were homogenized at 380 °C for 2 h, and then were extruded to plates with dimensions of 56 mm in width and 3 mm in thickness at 380 °C. Several tensile tests were performed by a CMT6305-300 KN universal testing machine (Skyan power equipment Ltd., Shenzhen, China) with an initial speed of 1.5 mm·min^{-1} at room temperature. In tensile test, at least three samples were tested for each condition and the average value was then obtained. The mechanical behaviors of the extruded AZ31 magnesium alloy are presented in Table 1. The as-extruded plates were then divided into samples with dimensions of 20 mm (Extrusion direction) × 10 mm (Transverse direction) × 3 mm (Normal direction). Prior to friction test, the samples were successively polished with 600 and 1000 grit silicon carbide paper, and then ultrasonic degreased in alcohol. The arithmetic average surface roughness (Ra) of the specimens tested was measured as 0.08 μm using the Olympus OLS4000 3D surface mapping profilometer (Olympus Ltd., Tokyo, Japan).

Table 1. Mechanical properties of extruded AZ31 magnesium alloy used in this study.

Material	0.2% YS/MPa	UTS/MPa	Elongation/%	$HV_{0.01}$
Extruded AZ31	142.1	305	18.5	66.7

2.2. *Tribological Tests*

The tribological properties of graphene and GO as water-based additives for AZ31 magnesium alloy/AISI 52100 steel contacts were investigated on a reciprocating tribometer with a ball-on-plate configuration (CSM Instruments, Peseux, Switzerland) in the ambient environment. Experimental set up of the tribotester is presented in Figure 2 along with schematic view of ball-on-plate assembly. The reference gives a detailed introduction to the principle of the tribometer [29]. The prepared AZ31 magnesium alloy was used as the stationary plate specimen while 6 mm diameter steel ball (hardness 690 $HV_{0.01}$, surface roughness Ra 0.05 μm) was sliding with a speed controlled by a DC servomotor. Three sets of test conditions (shown in Table 2) were examined to evaluate the effect of

SOLUTIONS UNLIMITED

concentration, the capacity of carrying load and the endurance of the lubrication film, respectively. For the influence of nanoparticle concentration on lubrication performance, graphene and GO as additives dispersed into water with different mass concentration of 0, 0.2, 0.5, 0.7 and 1.0 wt.%, respectively, were investigated. These concentration values were established from the results of bibliographic research, where concentration of graphene or GO was in the range of 0.1–1 wt.% [30,31]. Tests were conducted by applying a normal load of 3 Nat speed of 0.08 m/s with a 6 mm stroke for a rubbing time of 30 min. The Hertzian contact stress at the beginning of the test is calculated to be 312 MPa, which is at least 30% higher than the yield strength of magnesium alloy sheets. The optimal concentration of graphene or GO dispersed in the water was obtained from the above-mentioned tests. For the load-carrying capacity test, four different normal loads (1, 3, 5, 8 N) were applied to the upper stationary steel ball which slid at 0.08 m/s against the lower magnesium alloy plate for 30 min. Finally, some long lasting wear tests were carried out by applying 8 N of normal load at 0.03 m/s sliding speed. This set of testing conditions was chosen to evaluate the endurance of the lubrication film. During the sliding process, the friction coefficient was recorded in situ and a sudden increase in the friction coefficient was regarded as lubrication-film breakdown. The lubricant was applied onto the plates as droplets with a pipette before operation. The droplets formed a continuous lubricating layer covering the entire wear track area. At least three replicates were run for each lubricant and the final results of the friction coefficient and wear rate shown in this study were the average value.

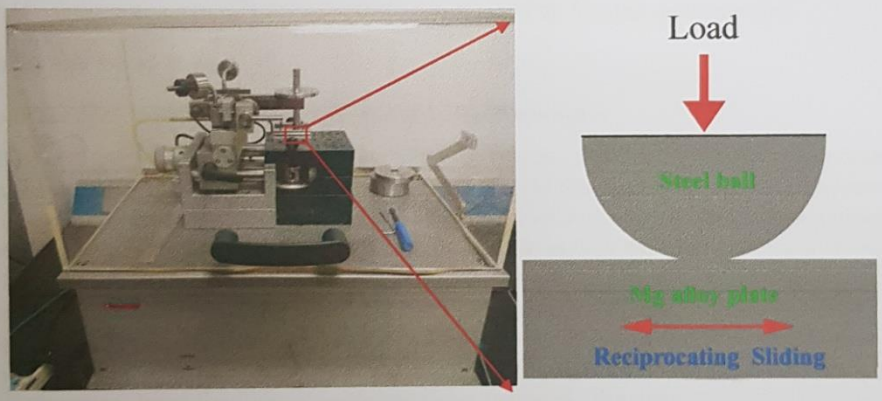


Figure 2. The ball-on-flat reciprocating sliding tester and schematic of ball-pot assembly in ball-on-flat tribotester.

Table 2. Testing conditions.

Test	Load (N)	Contact Pressure (MPa)	Sliding Speed (m/s)	Sliding Time (h)	Lubricants
The effect of concentration	3	312	0.08	0.5 h	Water Graphene nanofluids with different concentration GO nanofluids with different concentration
Carrying capacity	1 3 5 8	223 312 381 446	0.08	0.5 h	Water 0.5 wt.% Graphene nanofluids 0.5 wt.% GO nanofluids
Endurance of lubrication film	8	446	0.03	1.5 h	Water 0.5 wt.% Graphene nanofluids 0.5 wt.% GO nanofluids

SOLUTIONS UNLIMITED

2.3. Surface Characterization

The plate samples were cleaned in an alcohol ultrasonic bath for 5 min to eliminate the contaminants prior to the surface analysis. The rubbing surfaces on the magnesium alloys were analyzed by Zeiss AURIGA field emission scanning electron microscope (SU8010, Hitachi Ltd., Tokyo, Japan) integrated with energy dispersive spectrometer (FESEM-EDS; ESCA+, OXFORD instrument Ltd., London, UK). The Raman spectroscopy (Lab RAM HR800, with 532 nm laser excitation; Horiba Jobin Yvon S.A.S Ltd., Pairs, France) of the wear tracks on the plates was used to analyze the characteristics of the graphene or GO residue. The wettability of the sliding counterparts was evaluated by determining the static contact angle of pure water and nanofluids droplets on the magnesium alloy surface (Ra ~0.08 μm) using JC-2000C1 goniometer (Zhongchen Digital Technic Apparatus Ltd., Shanghai, China). A 5 μL volume droplet was placed on the magnesium alloy surface using a syringe, and the reported values in this study were reproducible for five identical samples. The wear volume of the lower magnesium alloy plate was measured by Olympus OLS4000 laser scanning confocal microscope (Olympus Ltd., Tokyo, Japan). Three replicates of friction and wear measurements were performed to minimize data scattering. In addition, then, the wear rate w was estimated by Equation (1):

$$w = \frac{V}{F_N \times S} \quad (1)$$

where V = wear volume (mm^3), F_N = applied normal load (N), S = slidingdistance (m).

3. Results and Discussion

3.1. Influence of Nanoparticle Concentration on Lubrication Performance

It is well known that the concentration of nanoparticles in the base lube plays a predominant role to control the friction coefficient and wear rate [32]. In this study, the effect of graphene and GO concentrations in the water ranging from 0.2 to 1.0 wt.% on the tribological properties was performed for magnesium alloy/steel contacts under 0.08 m/s at the load of 3 N for 30 min test duration. The pure water lubrication was chosen as a benchmark compared with the lubrication effects of nanofluids. The average friction coefficient as a function of nanoparticles concentration in water is displayed in Figure 3a. The correlation between friction coefficient and sliding time is given in Figure 3b. Accordingly, testing the pure water produced a high maximum friction coefficient and large fluctuations about the friction coefficient curve persisted. The main reason for this is that the low viscosity and pressure viscosity index of water was hard to form a sufficiently thick lubrication film between the contact interfaces. Both graphene and GO dispersed in water at the concentration of 0.5 wt.% showed best friction reducing in contrast with those at lower and higher concentrations due to negative lubrication effects caused by insufficient or excess amounts of graphene or GO in the contact area. Meanwhile, the effect of GO as lubricant additive on friction reducing was particularly noticeable. The 0.5 wt.% GO addition into the water reduced the friction coefficient by 77.5% (from 0.169 to 0.038 in average value) when compared with the pure water. Instead, there was slight improvement in the friction-reducing ability of the water in the presence of graphene, which reduced the value of friction coefficient by only 21.9% (from 0.169 to 0.132 in average value). In addition, it needs to be emphasized that the friction coefficient of the 0.5 wt.% graphene nanofluids during the initial few minutes of the sliding time has little difference from that of the pure water. Upon further increasing sliding time, the friction coefficient gradually drops. It can be inferred that the graphene additive in the water have not taken any effect on the friction coefficient at the early stage of the test, the water plays the major role between the rubbing pairs. Compared with 0.5 wt.% grapheme nanofluids, the high initial friction coefficient value was eliminated when 0.5 wt.% GO nanofluids were used. Moreover, the 0.5 wt.% graphene oxide nanofluids exhibited stability and consistent low friction coefficient within overall sliding time, which indicated a more positive effect from the friction reducing throughout the testing process.

SOLUTIONS UNLIMITED

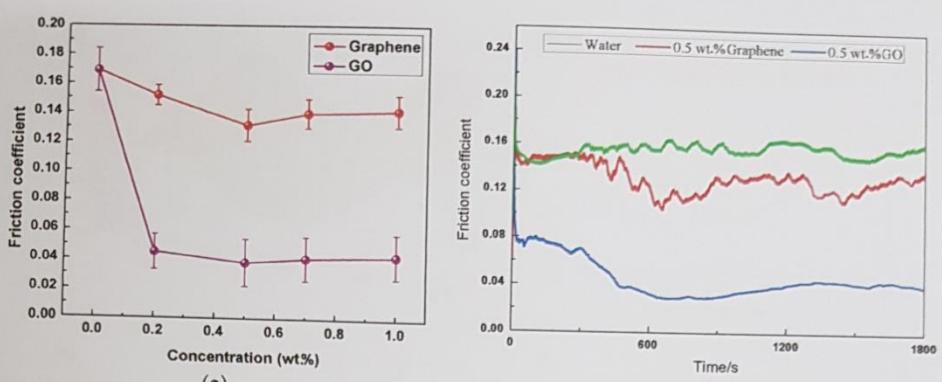


Figure 3. (**a**) The average friction coefficientas a function of nanoparticles concentration in water and (**b**) the friction coefficient relative to sliding time (3 N, 0.08 m/s, 30 min).

For a prospective lubricant to be considered effective, it is also necessary to safeguard the underlying surface from wear and damage. The steel ball experienced little wear because its hardness is much greater than that of the magnesium alloy plates. Therefore, the worn scars on the AZ31 magnesium alloy plate were mainly analyzed in the present study. The variation of wear rate in Figure 4 reveals similar change in the friction coefficient. The best wear resistance results found at 0.5 wt.%, and smaller improvements at higher concentration (e.g., 0.7 wt.%, 1.0 wt.%). When the concentration of nanoparticles is too high, the redundant nanoparticles will aggregate, which limits the amount of nanoparticles from supply zone to transition zone and further hinders the formation of tribofilm on the worn surfaces [33]. The addition of 0.5 wt.% graphene into the water reduced the wear rate by 13.5% compared with the pure water. In marked contrast, the wear rate lubricated with 0.5 wt.% GO nanofluids was nearly an order of magnitude smaller than that of pure water. These results demonstrated the beneficial contribution of graphene and GO in promoting anti-wear property of pure water, and the advantage of GO over graphene can be clearly seen. Figure 5 presents the 3D topography images and 2D profiles of the wear tracks on the plate. The wear track lubricated with pure water was obviously deeper than the tracks lubricated with the nanofluids. The optimal lubrication was 0.5 wt.% GO nanofluids, which was confirmed by the shallower wear tracks. According to demonstration research above, the optimized nanoparticles concentration in the water has been found to be 0.5 wt.%.

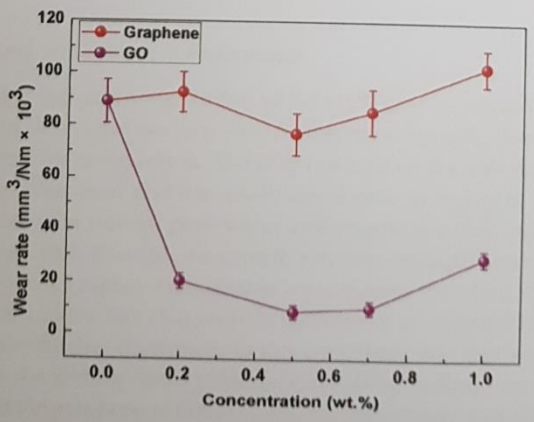


Figure 4. The average wear rate as a function of nanoparticles concentration in water (3 N, 0.08 m/s, 30 min).

SOLUTIONS UNLIMITED

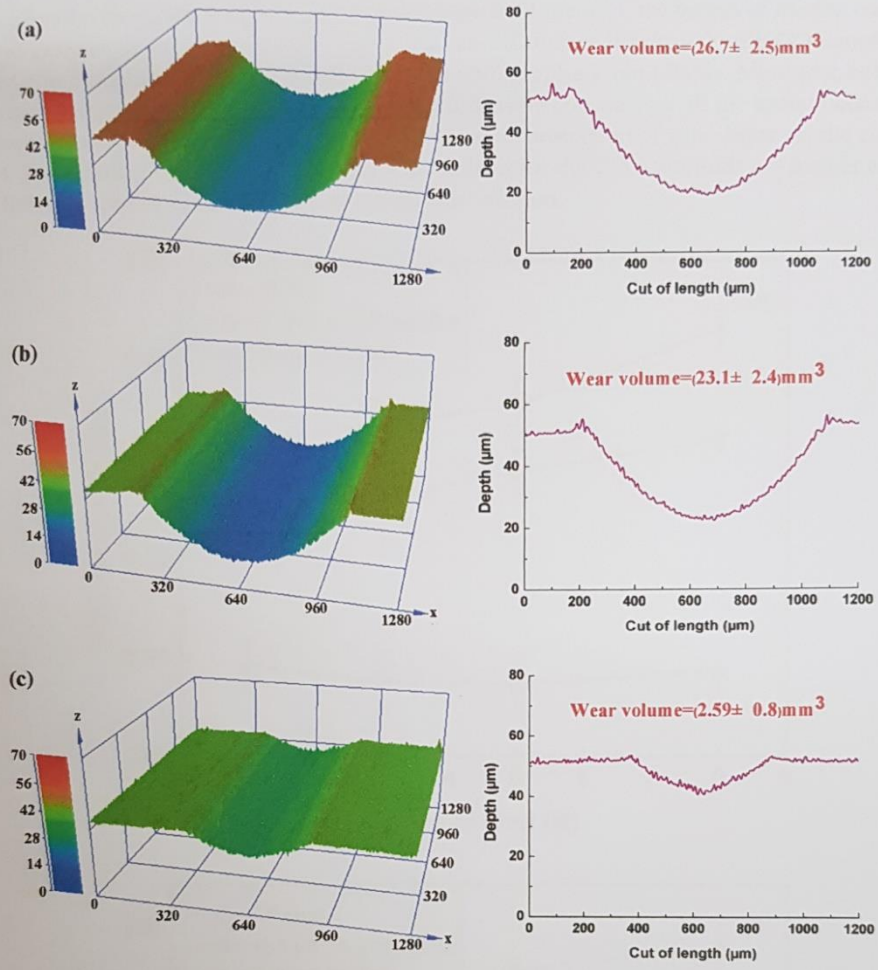


Figure 5. 3D topography images and 2D profiles across the wear tracks for flat specimens after wear tests with (**a**) pure water; (**b**) 0.5 wt.% graphene nanofluids; (**c**) 0.5 wt.% GO nanofluids (3 N, 0.08 m/s, 30 min).

3.2. *Influence of Normal Load on Lubrication Performance*

The friction-reducing and anti-wear ability of 0.5 wt.% graphenenanofluids and 0.5 wt.% GO nanofluids for magnesium alloy/steel contacts were further investigatedin detail. Except for nanofluids, the pure water was chosen for comparison. The effect of load on the tribological properties of pure water and nanofluids are discussed and the results are shown in Figure 6. It can be seen that both the friction coefficient and wear rate for pure water and graphene nanofluids remarkably increased with increasing the normal load. Even so, the growth rate was quite different. The friction coefficient and wear rate for the 0.5 wt.% graphene nanofluids were smaller than that of pure water under each load. This may be ascribed to the fact that with an increase of the normal load, the micro-intervals between two rubbing pairs further decreased. In this case, there was less water at a molecular level that could be drawn into the sliding contact interface, resulting in significantly reduced lubrication property. As for the test of the graphene nanofluids, the graphene-based tribofilm forms on the rubbing surfaces can avoid the metal-metal contact interface [34]. Therefore, there is slight enhancement in the friction-reducing and anti-wear performances of the pure water in the presence of graphene. Even so, observation of the increase in friction coefficient and wear rate with load may be attributed to relatively

SOLUTIONS UNLIMITED

thinner tribofilm formation and its removal under high load. Instead, the values of friction coefficient and wear rate are found to be much lower in the case of surface lubricated with GO nanofluids at the same operating load than the surface lubricated with graphene nanofluids. Moreover, both of the friction coefficient and wear rate for the GO nanofluids were constant for all the tested normal loads. This was ascribed to the stable existence and continuous protection of tribo-layer on the contacted surfaces. The possible tribological enhancing mechanisms for the GO nanofluids are further analyzed in the "Related tribological mechanism of nanofluids" section.

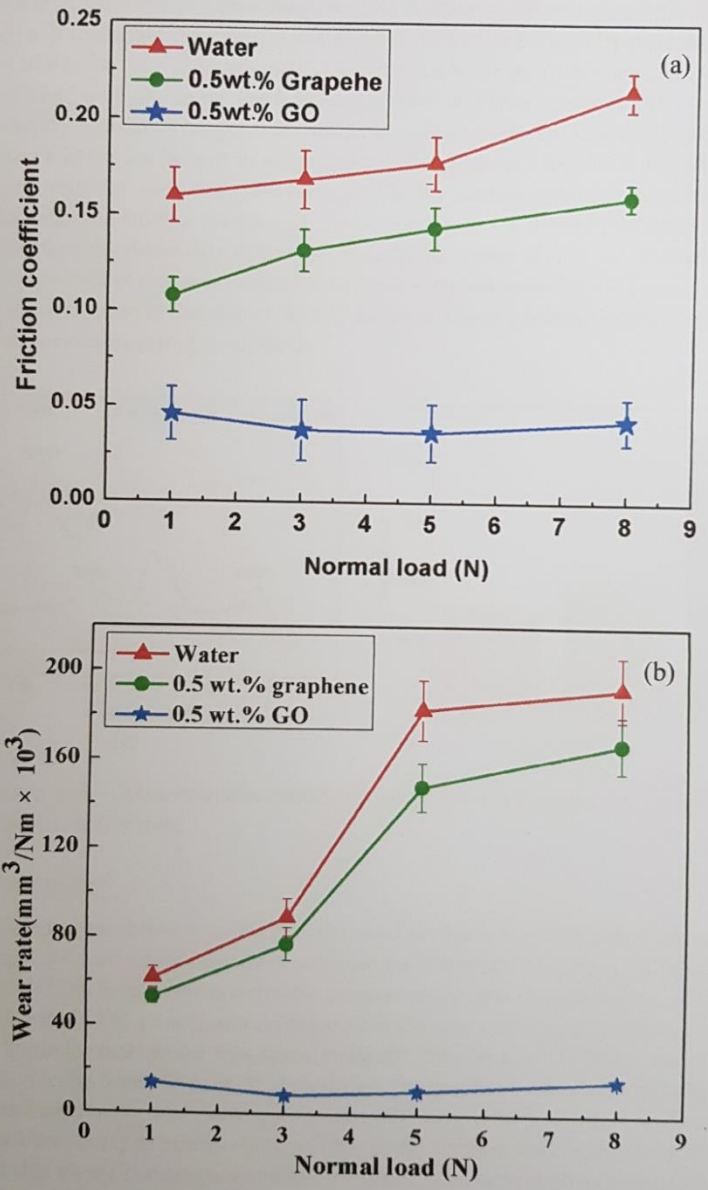


Figure 6. Effects of loads on average friction coefficient (**a**) and wear rate (**b**) of magnesium alloy specimens lubricated by the water with and without nanoparticles (0.08 m/s, 30 min).

SOLUTIONS UNLIMITED

3.3. The Endurance of Lubrication Film

The stability of the lubrication film with time is a very important property in mechanical systems needed for their functionality during their service life. In order to evaluate the lubrication film endurance during sliding, the severity of the contact conditions was increased by increasing the applied normal load and sliding time and reducing the sliding velocities. Figure 7 summarizes the tribological results conducted under a normal load of 8 N and sliding speed of 0.03 m/s for 90 min test duration. As can be observed in Figure 7, the lubrication film could not survive for a long period of time in the case of pure water lubrication, and its friction coefficient abruptly increased to 0.35 after about 1600 s. It indicated the rupture of the lubrication film formed by pure water on the wear track, resulting in a break in the steady state. Adding 0.5 wt.% graphene into the water decreased the friction coefficient and prolonged the lubrication film's stability to about 2000 s of sliding, which lasted approximately 1.25 times longer than that of the pure water. Though the graphene nanofluids can decreased the friction coefficient to some degree and protected the AZ31 Mg alloy temporarily, the durability and stability were not good enough. On the contrary, the GO nanofluids cannot only significantly decrease the friction coefficient, but also possess excellent lubrication film endurance. The graph shows that the durability of the GO nanofluids lasted 4500 s, which was approximately 2.8 times longer than that of the pure water. These results demonstrated the superior friction-reducing performance and lubrication endurable of the GO as water-based additive for magnesium alloy/steel pairs even under severe operating conditions.

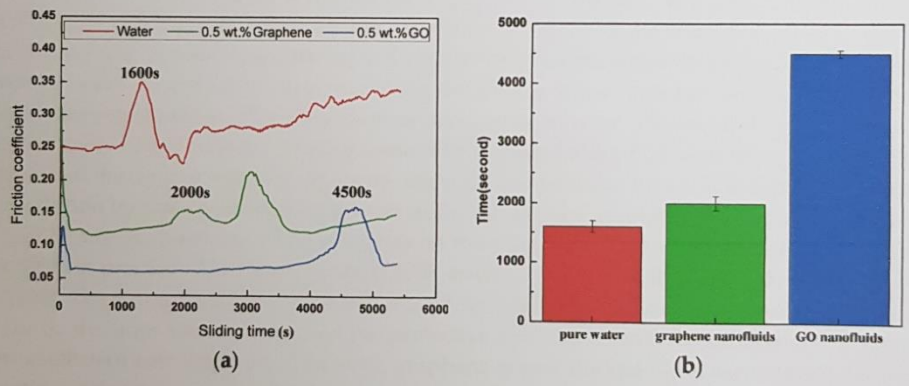


Figure 7. Sliding time to lubrication-film breakdown (**a**) and the average time of the lubrication films fails; (**b**) (8 N, 0.03 m/s, 90 min).

3.4. Surface Wettability Test

The wetting of the water-based nanofluids on the metal surface is very critical to lubricant performances. Generally, the excellent wettability intends to promote the formation of a tribofilm, which can separate the asperity contact [28]. Figure 8 illustrates the contact angle data of pure water, 0.5 wt.% graphene nanofluids and 0.5 wt.% GO nanofluids on the polished magnesium alloy surface. It was observed that the contact angle for pure water was found to be 89°. The addition of GO in water has markedly reduced the contact angle from 89° to 46.5°. In contrast, the graphene nanofluids did not show obvious change in contact angle in contrast with pure water (89° versus 88°). Contact angle values provide information about the ability of lubricants to wet the metal surfaces and to interact with them to form surface films. In this study, the magnesium alloy surface is more wettable for the GO nanofluids in comparison with pure water and graphene nanofluids. Therefore, we can deduce that it is more facile for the GO nanofluids than the graphene nanofluids to form the protective layer due to their different wettability of the contact sliding interfaces. The obtained results are showing good agreement with the tribological performances.

SOLUTIONS UNLIMITED

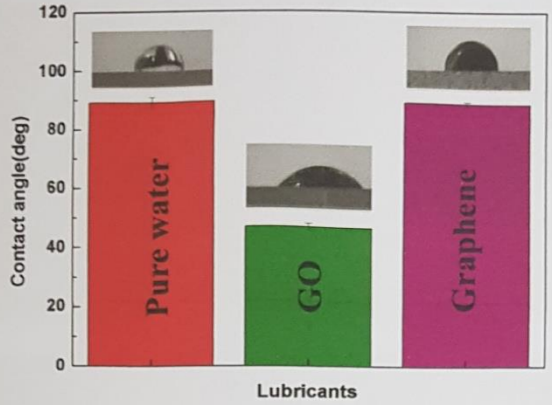


Figure 8. The contact angle of AZ31 magnesium alloy surface for pure water, 0.5 wt.% graphene nanofluids and 0.5 wt.% GO nanofluids.

3.5. *The Worn Surface Analysis*

Figure 9 exhibits the FESEM micro-morphologies and the corresponding EDS analysis of the worn surface lubricated by pure water, 0.5 wt.% graphene nanofluids and 0.5 wt.% GO nanofluids under 0.08 m/s at the load of 3 N for 30 min. As shown in Figure 9a, the worn surface lubricated with pure water showed signs of deep grooves and significantly desquamation from body surface, possibly because the water caused tribo-corrosion during the sliding. It was therefore reasonable to infer that this condition was dominated by abrasive wear and corrosion wear. Therefore, the pure water failed to act effectively under constant loading cycle. The corresponding EDS analysis in the spectrum A displayed that the content of C element on the worn surface was only 0.2 wt.%, which may be ascribed to the pollution by carbon containing species in the air. For the graphene nanofluids lubrication as shown in Figure 9b, there were few scratches on the worn surface, and dark patches was formed during sliding process. The corresponding EDS analysis (spectrum B) was made to ascertain the ingredients. The strong signal of C element (28.2 wt.%) from EDS spectrum confirmed the presence of graphene on the worn surface. The graphene protective layer can smooth the surfaces and thus reduce friction coefficient and wear rate. However, graphene sheets stacked upon each other and showed no effective uniform coverage on the worn surface, and thus the lubricant performance of graphene sheets as a lubricant additive was limited. Compared with graphene nanofluids, it was clear that GO platelets were homogeneous distributed on the contact surface and that the surface had nearly none of scratch traces observed in Figure 9c. Moreover, the content of C element on the worn surface was up to 55.3 wt.% (spectrum C), which was almost 2-fold higher than that shown in spectrum B. It can be reasonably inferred that GO in dispersed water is able to form a block deposition film with good coverage on the rubbing surfaces, which finally leads to the significant improvement in tribological performance of the pure water. The results are in good accordance with the previous findings in Figures 4 and 5, further verifying the best anti-wear ability of GO nanofluids among all samples.

SOLUTIONS UNLIMITED

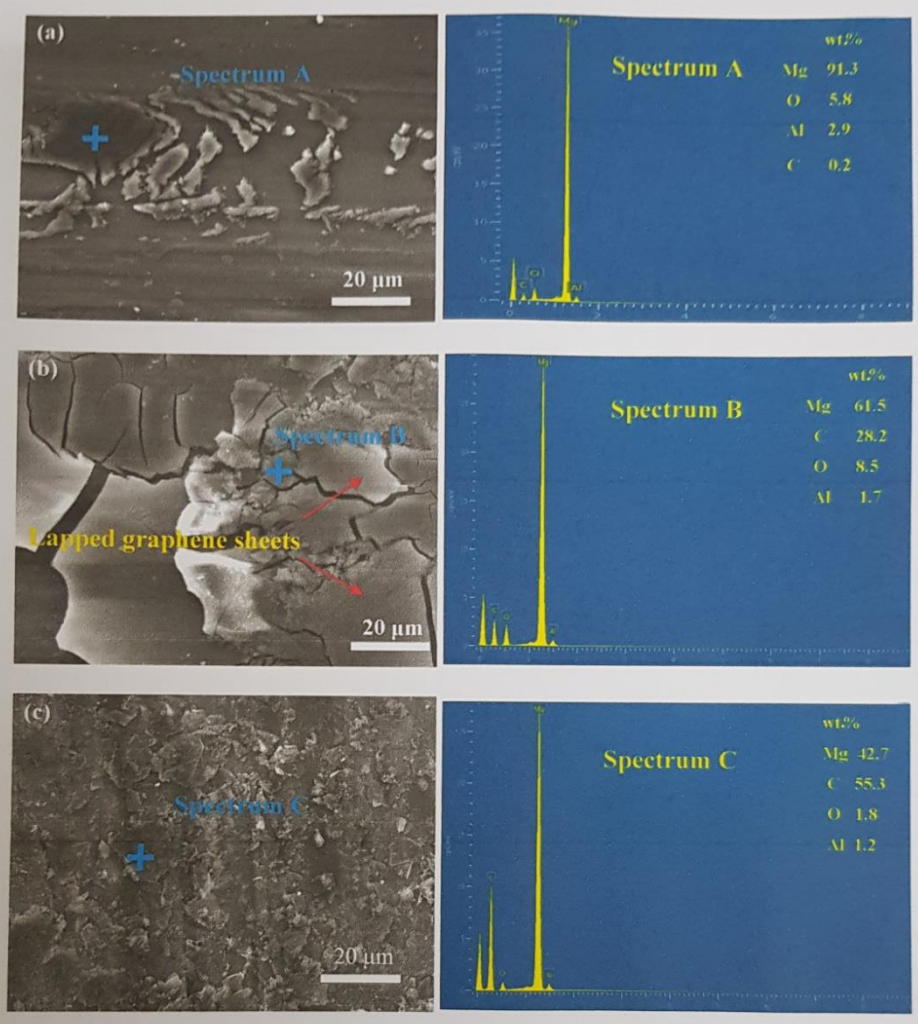


Figure 9. FESEM-EDS results for the wear surface lubricated with (**a**) pure water; (**b**) 0.5 wt.% graphene nanofluids; (**c**) 0.5 wt.% GO nanofluids (3 N, 0.08 m/s, 30 min).

Raman spectroscopy was carried out to further confirm that the excellent tribological performance is attributed to the presence of graphene or GO on the worn surface. Figure 10 exhibits the Raman spectrum measured in the wear track on the magnesium alloy surface lubricated with 0.5 wt.% graphene nanofluids and 0.5 wt.% GO nanofluids, compared with the corresponding spectrum of the pristine powder. According to Figure 10a, the Raman spectrum of the worn surface lubricated with graphene nanofluids exhibited three characteristic peaks of the D-band at 1350 cm^{-1}, 2D-band at 2712 cm^{-1} and a G-band at 1580 cm^{-1}, which are the typical Raman signals of graphene. This means that some graphene would be inlaid into the worn surface of the specimen to improve the tribological behaviors. However, the Raman spectrum for the deposited graphene on the worn surface is some different characteristics in comparison with the pristine powder. The intensity ratio of D to G band increased as compared to that of the pristine graphene powder, illustrating significant modification had occurred to graphene during sliding by converting it into the disordered graphitic structure.

SOLUTIONS UNLIMITED

The GO on the worn surface was confirmed by the Raman spectra analysis of the two most intense features of the D band (1345 cm^{-1}) and G band (1587 cm^{-1}) as shown in Figure 10b. Similar to the graphene nanofluids lubricated surface, the GO on the worn surface also presented the strengthening of the intensity ratio of I_D/I_G, in contrast that of the pristine GO powder. This should not be a surprise considering that those flakes were lying in between the two sliding surfaces standing a pressure of several hundred MPa. Such phenomenon has been well documented in the previous reports [35,36].

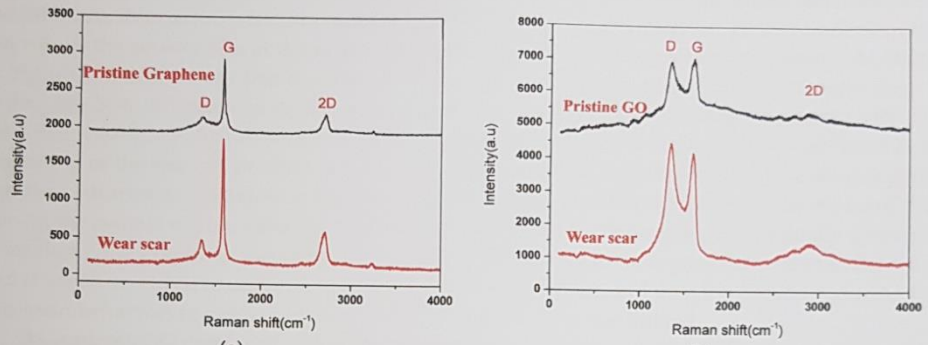


Figure 10. Raman results for the wear surface lubricated with (**a**) 0.5 wt.% graphene nanofluids; (**b**) 0.5 wt.% GO nanofluids (3 N, 0.08 m/s, 30 min).

3.6. Related Tribological Mechanism of Nanofluids

The tribological properties of potentially useful graphene and GO as water-based lubricant additives for magnesium alloy/steel contacts have been investigated in the present study. It is observed that both of the friction reduction and anti-wear ability of graphene or GO nanofluids were improved compared with those of pure water. Prior to any speculation of the friction-reducing and anti-wear mechanism, it is necessary to investigate the lubrication regime of the test situation. The lubrication regime in the tribological contacts can be divided into three categories, including boundary lubrication, mixed lubrication and hydrodynamic lubrication. The corresponding lubrication regime should be evaluated based on the value of λ in Equation (2), where h_{min} refers to the theoretical minimum film thickness separating the contact interfaces. The h_{min} can be calculated by the Hamrock-Dowson model displayed in Equation (3), and R_q is the combined surface roughness determined according to Equation (4) [37].

$$\lambda = \frac{h_{min}}{R_q} \tag{2}$$

$$h_{min} = 2.8R'\left(\frac{\eta u_e}{E'R'}\right)^{0.65}\left(\frac{W_y}{E'R'^2}\right)^{-0.21} \tag{3}$$

$$R_q = \sqrt{R_{ball}{}^2 + R_{flat}{}^2} \tag{4}$$

Of which W_y is the applied normal load, u_e is the linear velocity, η is the bulk viscosity of the nanofluids, E' is the effective elastic modulus, and R' is the radius of the ball. On the basis of the material characteristics and test condition, the thickness of the lubricant film at the point of contact is 25, 20, 18, 16 nm for 1, 3, 5, 8 N, respectively. The corresponding λ values were confirmed to be 0.26, 0.21, 0.19, 0.17, respectively. The lubrication regime is usually defined by the following regulations: boundarylubrication ($0.1 < \lambda < 1$), mixed lubrication ($1 \leq \lambda \leq 3$), elastohydrodynamic lubrication ($\lambda > 3$) [38]. It is suggested that the test condition in this study is within the boundary lubrication regime.

The high friction generally occurs in the boundary lubrication regime where a beneficial fluid lubricant film is unable to form and separate the rubbing surfaces. Therefore, the addition of nanoparticles

SOLUTIONS UNLIMITED

in the base media is essential to provide a surface protective layer. In this study, when 0.5 wt.% graphene is dispersed into water, the friction coefficient and wear rate are respectively reduced by 21.9% and 13.5% as compared to that of the benchmark water. We know that, during sliding process, graphene with water tends to penetrate into the interface of contact pairs and gradually accumulate on the magnesium alloy surface, resulting in the formation of a transfer films between the rubbing surfaces. This outlook was supported by the FESEM–EDS spectra and Raman imaging shown in Figures 9a and 10a, respectively. Undoubtedly, the tribo-layer alleviates the metal-metal contact at the interface, thus reduces friction coefficient and wear rate [31,39]. Even so, further understanding the role of the protect film at disparate stage of the whole test is crucial and necessary. As shown in Figure 3, it is apparent that the friction coefficient for graphene nanofluids at the early stage of sliding has little difference from that of pure water. Similar evolution of friction coefficient with time for a steel-cast iron pairs lubricated by graphene nanofluids, where a higher friction coefficient at the beginning of the test can be observed, was reported by Dan Zheng et al. [36]. The authors explain that the high friction coefficient at the early stage of the tests could be attributed to the absent of tribo film on the contact region. Once the tribofilm generated, the friction coefficient gradually decreased. In addition, the graphene sheets stacked upon each other due to their poor dispersion in the water and showed no effective uniform coverage on the worn surface, and thus the friction-reducing and anti-wear behaviors of graphene sheets as a lubricant additive was limited.

In contrast, GO displayed higher friction-reducing and anti-wear capability than graphene did. The 0.5 wt.% addition of GO in the water offered reduction of friction coefficient by 77.5% and reduction of wear rate by 90% compared with the pure water, which is also larger than the reported values for other nanomaterial water-based additives, e.g., Al_2O_3 (27% friction and 22% wear reduction with the addition of 1 wt.%) [40], TiO_2 nanoparticles (50% friction and 27% wear reduction with the addition of 0.8 wt.%) [41], and nanographite (44% friction and 49% wear reduction with the addition of 1.0 wt.%) [42]. It can be considered that the superior tribological performances of GO nanofluids results from the intrinsic surface oxygen-containing functionalized groups, such as carbonyl (C=O), hydroxide (C–OH) and carboxyl (COOH). Firstly, GO with the oxygen-containing functionalized groups, due to chemistry nature and polarity, favorably attach on the metal surface, resulting in the improved adhesion between the GO and the magnesium alloy. Therefore, GO shows a great advantage in achieving long-term stability and load bearing capacity compared with graphene as shown in Figures 6 and 7. Secondly, the relatively low interfacial strength within the GO layers may have also contributed to the significant improvement in the tribological properties. The literature [43] demonstrated that the increase of the oxygen-containing functionalized groups in the pristine graphene lead to the degradation of the interlayer bond strength by molecular dynamics (MD) simulation. Also, the increase in the interplanar spacing between the GO layers may have increased the possibility of water molecules to be penetrated into the gap [44]. Thus, it was claimed that the low interfacial strength of GO layers and the water molecules in between the GO layers were responsible for the reduction of the shear strength during sliding. Thirdly, the oxygen-based groups arehydrophilic, resulting in excellent dispersion stability [45,46] and wetting property as shown in Figure 8. The superior dispersion stability of the GO in the water ensures its uninterrupted supply to the contact area followed the water. So the running-in time required to obtain very low friction values for GO nanofluids is shorter than graphene nanofluids as shown in Figure 3. Meanwhile, the excellent wetting property of GO nanofluids promotes the formation of the protective layer on the worn surfaces. This is supported by the EDS spectra (Figure 9), which shows that the content of C element on the GO nanofluids lubricated surface is nearly 2-fold higher than that of the graphene nanofluids lubricated surface. Even so, the acidity of the GO nanofluids could be concerned for metal lubrication. In this study, the pH value of the GO suspension measured by a digital calibrated pH meter was at 3.8, which is close to weak acid. In addition, no obvious corrosive wear on the worn surface as shown in Figure 9c. Therefore, the GO water-based nanofluids with the superior property can be readily available for potential industrial applications.

SOLUTIONS UNLIMITED

4. Conclusions

In this paper, the tribological behaviors of graphene or GO as water-based lubricant additives for magnesium alloy/steel contacts were evaluated by a reciprocating sliding ball-on-plate contact configuration. According to the analysis of the experimental results, the following conclusions can be drawn.

(1) Graphene and GO as water-based lubricant additives improved the friction-reducing and anti-wear abilities. The best tribological response of the magnesium alloy/steel pairs evaluated was obtained when graphene or GO at a concentration of 0.5 wt.% was added to water.

(2) Graphene and GO exhibited different friction-reducing and anti-wear efficiencies, and the tribological performances of GO are superior to that of graphene. Meanwhile, the positive effect of the GOnanofluids was also more pronounced in terms of the load-carrying capacity and the lubrication film endurance.

(3) The prominent lubricant performance of GO nanofluids can be attributed to the strong affinity between GO sheets and magnesium alloy surface, superior dispersion in the water and excellent wetting of the GO nanofluids on the magnesium alloy surface.

Acknowledgments: The authors are supported by Scientific and Technological Research Program of Chongqing Municipal Education Commission (Grant No. KJ1601203, KJ1712301) and Fuling Science and Technology Commission (Grant No. FLKW2017ABA1013) and Chongqing Science and Technology Commission (Grant No. cstc2017jcyjAX0301, csct2017jcyjAX0394) and Research Founds for the Yangtze Normal University (Grant No. 2016XJQN31, 2017KYQD41).

Author Contributions: Hongmei Xie and Bin Jiang carried out the design and drafted the manuscript. Jiahong Dai, Quan Li and Chunxia Li prepared samples and carried out tribo-tests. Cheng Peng and Fusheng Pan commented on the results and revised the manuscript. All authors read and approved the final version of the manuscript.

Conflicts of Interest: The authors declare that they have no competing interests.

References

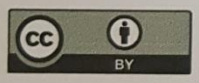
1. Aatthisugan, I.; Rose, A.R.; Jebadurai, D.S. Mechanical and wear behaviour of AZ91D magnesium matrix hybrid composite reinforced with boron carbide and graphite. *J. Magnes. Alloys* **2017**, *5*, 20–25. [CrossRef]
2. Li, Q.; Huang, G.J.; Huang, X.D.; Pan, S.W.; Tan, C.L.; Liu, Q. On the texture evolution of Mg–Zn–Ca alloy with different hot rolling paths. *J. Magnes. Alloys* **2017**, *5*, 166–172. [CrossRef]
3. Griffiths, D. Explaining texture weakening and improved formability in magnesium rare earth alloys. *Mater. Sci. Technol.* **2014**, *31*, 10–24. [CrossRef]
4. Selvam, B.; Marimuthu, P.; Narayanasamy, R.; Senthilkumar, V.; Tun, K.S.; Gupta, M. Effect of temperature and strain rate on compressive response of extruded magnesium nano-composite. *J. Magnes. Alloys* **2015**, *3*, 224–230. [CrossRef]
5. Podgornik, B.; Kosec, T.; Kocijan, A.; Donik, Č. Tribological behaviour and lubrication performance of hexagonal boron nitride (h-BN) as a replacement for graphite in aluminium forming. *Tribol. Int.* **2015**, *81*, 267–275. [CrossRef]
6. Brostow, W.; Lobland, H.E.H. *Materials: Introduction and Applications*; John Wiley & Sons: New York, NY, USA, 2017.
7. St. Dennis, J.E.; Jin, K.; John, V.T.; Pesika, N.S. Carbon Microspheres as Ball Bearings in Aqueous-Based Lubrication. *ACS Appl. Mater. Interfaces* **2011**, *3*, 2215–2218. [CrossRef] [PubMed]
8. Xie, H.; Jiang, B.; Wang, Q.; Xia, X.; Pan, F. Effects of combined additions of SiO_2 and MoS_2 nanoparticles as lubricant additive on the tribological properties of AZ31 magnesium alloy. *Sci. China Technol. Sci.* **2016**, *59*, 689–698. [CrossRef]
9. Huang, W.; Du, C.; Li, Z.; Liu, M.; Liu, W. Tribological characteristics of magnesium alloy using N-containing compounds as lubricating additives during sliding. *Wear* **2006**, *260*, 140–148. [CrossRef]
10. Huang, W.; Fu, Y.; Wang, J. Effect of chemical structure of borates on the tribological characteristics of magnesium alloy during sliding. *Tribol. Int.* **2005**, *38*, 775–780. [CrossRef]
11. Xia, Y.Q.; Jia, Z.F.; Jia, J.H. *Advanced Tribology*; Springer: Berlin/Heidelberg, Germany, 2010.

SOLUTIONS UNLIMITED

12. Yan, L.; Yue, W.; Wang, C.; Wei, D.; Xu, B. Comparing tribological behaviors of sulfur- and phosphorus-free organomolybdenum additive with ZDDP and MoDTC. *Tribol. Int.* **2012**, *53*, 150–158. [CrossRef]
13. Li, Z.; Li, X.; Zhang, Y.; Ren, T.; Zhao, Y.; Zeng, X.; van der Heide, E. Tribological study of a highly hydrolytically stable phenylboronic acid ester containing benzothiazolyl in mineral oil. *Appl. Surf. Sci.* **2014**, *308*, 91–99. [CrossRef]
14. Cai, M.; Liang, Y.; Zhou, F.; Liu, W. Tribological properties of novel imidazolium ionic liquids bearing benzotriazole group as the antiwear/anticorrosion additive in poly(ethylene glycol) and polyurea grease for steel/steel contacts. *ACS Appl. Mater. Interfaces* **2011**, *3*, 4580–4592. [CrossRef] [PubMed]
15. Zhang, X.; Xu, H.; Wang, J.; Ye, X.; Lei, W.; Xue, M.; Tang, H.; Li, C. Synthesis of Ultrathin WS_2 Nanosheets and Their Tribological Properties as Lubricant Additives. *Nanoscale Res. Lett.* **2016**, *11*, 442–451. [CrossRef] [PubMed]
16. Yi, M.; Zhang, C. The synthesis of MoS_2 particles with different morphologies for tribological applications. *Tribol. Int.* **2017**, *116*, 285–294. [CrossRef]
17. Podgornik, B.; Kafexhiu, F.; Kosec, T.; Jerina, J.; Kalin, M. Friction and anti-galling properties of hexagonal boron nitride (h-BN) in aluminium forming. *Wear* **2017**, *388–389*, 2–8. [CrossRef]
18. Xie, H.; Jiang, B.; Liu, B.; Wang, Q.; Xu, J.; Pan, F. An Investigation on the Tribological Performances of the SiO_2/MoS_2 Hybrid Nanofluids for Magnesium Alloy-Steel Contacts. *Nanoscale Res. Lett.* **2016**, *11*, 329–346. [CrossRef] [PubMed]
19. Berman, D.; Erdemir, A.; Sumant, A.V. Reduced wear and friction enabled by graphene layers on sliding steel surfaces in dry nitrogen. *Carbon* **2013**, *59*, 167–175. [CrossRef]
20. Li, P.F.; Zhou, H.; Cheng, X. Investigation of a hydrothermal reduced graphene oxide nano coating on Ti substrate and its nano-tribological behavior. *Surf. Coat. Technol.* **2014**, *254*, 298–304. [CrossRef]
21. Min, C.; Nie, P.; Song, H.-J.; Zhang, Z.; Zhao, K. Study of tribological properties of polyimide/graphene oxide nanocomposite films under seawater-lubricated condition. *Tribol. Int.* **2014**, *80*, 131–140. [CrossRef]
22. Lahiri, D.; Hec, F.; Thiesse, M.; Durygin, A.; Zhang, C.; Agarwal, A. Nanotribological behavior of graphene nanoplatelet reinforced ultra high molecular weight polyethylene composites. *Tribol. Int.* **2014**, *70*, 165–169. [CrossRef]
23. Shah, R.; Datashvili, T.; Cai, T.; Wahrmund, J.; Menard, B.; Menard, K.P.; Brostow, W.; Perez, J. Effects of functionalised reduced graphene oxide on frictional and wear properties of epoxy resin. *Mater. Res. Innov.* **2014**, *19*, 97–106. [CrossRef]
24. Mungse, H.P.; Khatri, O.P. Chemically Functionalized Reduced Graphene Oxide as a Novel Material for Reduction of Friction and Wear. *J. Phys. Chem. C* **2014**, *118*, 14394–14402. [CrossRef]
25. Wu, Y.; Zeng, X.; Ren, T.; de Vries, E.; van der Heide, E. The emulsifying and tribological properties of modified graphene oxide in oil-in-water emulsion. *Tribol. Int.* **2017**, *105*, 304–316. [CrossRef]
26. Fan, X.; Xia, Y.; Wang, L.; Li, W. Multilayer Graphene as a Lubricating Additive in Bentone Grease. *Tribol. Lett.* **2014**, *55*, 455–464. [CrossRef]
27. Zhao, J.; He, Y.; Wang, Y.; Wang, W.; Yan, L.; Luo, J. An investigation on the tribological properties of multilayer graphene and MoS_2 nanosheets as additives used in hydraulic applications. *Tribol. Int.* **2016**, *97*, 14–20. [CrossRef]
28. Liang, S.; Shen, Z.; Yi, M.; Liu, L.; Zhang, X.; Ma, S. In situ exfoliated graphene for high-performance water-based lubricants. *Carbon* **2016**, *96*, 1181–1190. [CrossRef]
29. Brostow, W.; Kovačević, V.; Vrsaljko, D.; Whitworth, J. Tribology of polymers and polymer-based composites. *J. Mater. Educ.* **2010**, *32*, 273–290.
30. Song, H.; Wang, Z.; Yang, J. Tribological properties of graphene oxide and carbon spheres as lubricating additives. *Appl. Phys. A* **2016**, *122*, 933–941. [CrossRef]
31. Zin, V.; Barison, S.; Agresti, F.; Colla, L.; Paguraa, C.; Fabrizioa, M. Improved tribological and thermal properties of lubricants by graphene-based nano-additives. *RSC Adv.* **2016**, *6*, 59477–59486. [CrossRef]
32. Jaiswal, V.; Kalyani; Umrao, S.; Rastogi, R.B.; Kumar, R.; Srivastava, A. Synthesis, Characterization, and Tribological Evaluation of TiO_2-Reinforced Boron and Nitrogen co-Doped Reduced Graphene Oxide Based Hybrid Nanomaterials as Efficient Antiwear Lubricant Additives. *ACS Appl. Mater. Interfaces* **2016**, *8*, 11698–11710. [PubMed]
33. Meng, Y.; Su, F.; Chen, Y. Au/Graphene Oxide Nanocomposite Synthesized in Supercritical CO_2 Fluid as Energy Efficient Lubricant Additive. *ACS Appl. Mater. Interfaces* **2017**, *9*, 39549–39559. [CrossRef] [PubMed]

SOLUTIONS UNLIMITED

34. Tripathi, K.; Gyawali, G.; Lee, S.W. Graphene Coating via Chemical Vapor Deposition for Improving Friction and Wear of Gray Cast Iron at Interfaces. *ACS Appl. Mater. Interfaces* **2017**, *9*, 32336–32351. [CrossRef] [PubMed]
35. Ismail, N.A.; Bagheri, S. Highly oil-dispersed functionalized reduced graphene oxide nanosheets as lube oil friction modifier. *Mater. Sci. Eng. B* **2017**, *222*, 34–42. [CrossRef]
36. Zheng, D.; Cai, Z.-B.; Shen, M.-X.; Li, Z.-Y.; Zhu, M.-H. Investigation of the tribology behaviour of the graphene nanosheets as oil additives on textured alloy cast iron surface. *Appl. Surf. Sci.* **2016**, *387*, 66–75. [CrossRef]
37. Hamrock, B.J.; Dowson, D. Isothermal Elastohydrodynamic Lubrication of Point Contacts: Part III—Fully Flooded Results. *J. Lubr. Technol.* **1977**, *99*, 264–302. [CrossRef]
38. Hamrock, B.J.; Dowson, D. *Ball Bearing Lubrication: The Elastohydrodynamics of Elliptical Contacts;* John Wiley & Sons: Hoboken, NJ, USA, 1981.
39. Qu, J.; Wang, J.; Liu, S.; Mu, B.; Ren, J.; Wang, H.; Yang, S. Tribology Study of Reduced Graphene Oxide Sheets on Silicon Substrate Synthesized via Covalent Assembly. *Langmuir* **2010**, *26*, 15830–15836.
40. He, A.; Huang, S.; Yun, J.-H.; Wu, H.; Jiang, Z.; Stokes, J.; Jiao, S.; Wang, L.; Huang, H. Tribological Performance and Lubrication Mechanism of Alumina Nanoparticle Water-Based Suspensions in Ball-on-Three-Plate Testing. *Tribol. Lett.* **2017**, *65*, 40–45. [CrossRef]
41. Wu, H.; Zhao, J.; Xia, W.; Cheng, X.; He, A.; Yun, J.H.; Wang, L.; Huang, H.; Jiao, S.; Huang, L.; et al. A study of the tribological behaviour of TiO_2 nano-additive water-based lubricants. *Tribol. Int.* **2017**, *109*, 398–408. [CrossRef]
42. Chen, Q.; Wang, X.; Wang, Z.; Liu, Y.; You, T. Preparation of water-soluble nanographite and its application in water-based cutting fluid. *Nanoscale Res. Lett.* **2013**, *8*, 52–60. [CrossRef] [PubMed]
43. Zhang, J.; Jiang, D. Molecular dynamics simulation of mechanical performance of graphene/graphene oxide paper-based polymer composites. *Carbon* **2014**, *67*, 784–791. [CrossRef]
44. Kim, H.J.; Kim, D.E. Water Lubrication of Stainless Steel using Reduced Graphene Oxide Coating. *Sci. Rep.* **2015**, *5*, 17034–17047. [CrossRef] [PubMed]
45. Rasheed, A.K.; Khalid, M.; Rashmi, W.; Gupta, T.C.S.M.; Chan, A. Graphene-based nanofluids and nanolubricants—Review of recent developments. *Renew. Sustain. Energy Rev.* **2016**, *63*, 346–362. [CrossRef]
46. Xiao, H.; Liu, S. 2D nanomaterials as lubricant additive: A review. *Mater. Des.* **2017**, *135*, 319–332. [CrossRef]



© 2018 by the authors. Licensee MDPI, Basel, Switzerland. This article is an open access article distributed under the terms and conditions of the Creative Commons Attribution (CC BY) license (http://creativecommons.org/licenses/by/4.0/).

The 'Wonder Material': How Graphene Is Set to Change the World

Posted on 27/03/201929/03/2019 by Tibi Puiu

In 2010, Andre Geim and Konstantin Novoselov were awarded the Nobel Prize in Physics "for groundbreaking experiments regarding the two-dimensional material graphene." Konstantin Novoselov will participate in the 69th Lindau Nobel Laureate Meeting next summer. Learn more about the many ways how the 'wonder material' graphene could better our lives and which hurdles have to be overcome to do so.

The 'Wonder Material'

Since it was first forged in 2004 by a group of researchers at the University of Manchester led by Andre Geim and Konstantin Novoselov, graphene has emerged as one of the most promising nanomaterials due to its unique combination of properties. Before the groundbreaking discovery, scientists used to think that two-dimensional crystalline materials couldn't exist due to thermodynamic instability. Remarkably, using ordinary Scotch tape, Geim and Novoselov were able to isolate monolayer graphene from a piece of graphite. To this day, mechanical exfoliation is the simplest way to produce graphene flakes, although more recent methods have produced graphene with fewer impurities. For their work, Geim and Novoselov were awarded the Nobel Prize in Physics in 2010.



Andre Geim and Konstantin Novoselov, Nobel Laureates in Physics 2010, photographed for the serie 'Nobel Laureates in Portrait'. © Peter Badge/typos 1 in coop. with Lindau Nobel Laureate Meetings

A honeycomb lattice made of a single layer of carbon atoms sounds fragile; however, graphene most certainly doesn't fit that description. Not only is it the thinnest material (0.345 nanometers), but it's also the strongest – 200 times stronger than steel. Graphene's remarkable mechanical properties don't stop here. For instance, graphene is also elastic and lightweight (0.77 milligrams per square meter), which means you would only need a single gram of graphene to cover an entire football pitch. As such, graphene could become an indispensable component in composites or coatings for anything from aircraft and spaceships to buildings.

Graphene is also an excellent electrical and thermal conductor thanks to its crystal and band structures. Even at room temperature, the 'wonder material' is a zero-overlap semimetal with remarkable electron mobility. This makes it a promising material for flexible electronics, solar cells, batteries, and high-speed transistors – all of which have very practical applications.

Here are just a few ways researchers around the world are planning to use graphene to enrich and better our lives.



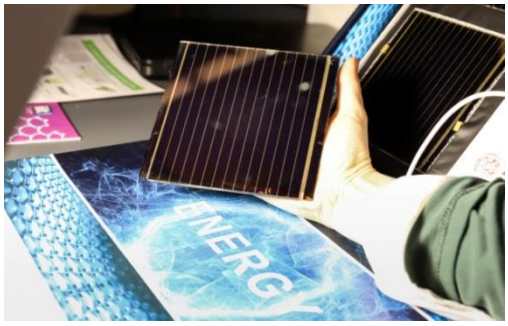
Graphene has remarkable properties: it is not just the thinnest but also the strongest material, it is elastic and lightweight and an excellent electrical and thermal conductor. © iStock/BONNINSTUDIO

Energy

Graphene is poised to become a central component of the energy infrastructure. For example, one important application is something that you likely interact with on a daily basis: your phone. Researchers at the Northwestern University experimented with graphene-based electrodes for lithium-ion batteries that could allow phones to hold a charge up to ten times longer and load ten times faster than current technology. Elsewhere, in Australia, researchers at RMIT University devised a graphene-based electrode for supercapacitors that could boost current solar energy storage by an astonishing 3,000%. Speaking of which, since it transports charge much faster than most other materials, graphene could also become an indispensable material for ultrathin, flexible, inexpensive solar cells (once the problem of graphene's short carrier lifetime is solved). Multifunction graphene mats could also prove valuable for catalytic systems for fuel cells.

Electronics

Many believe graphene will replace silicon in computer chips since charge can move faster through the 2D material than through silicon. According to estimates, graphene might one-day enable terahertz computing – computers that are 1,000 times faster than today. However, in order for graphene to be employed in transistors, it needs to be doped with impurities because it lacks the necessary band gap – it's just too good of conductor in its purest form. Other research groups are thinking about applying a magnetic field to graphene ribbons in order to change the resistance of current flowing through them. Much like a valve controlling the flow of water through a pipe, transistors act as on and off switches for electricity. Although graphene transistor isn't ready yet, research groups around the world are converging towards this goal, so it might be only a matter of time before computing is reinvented.



Australian researchers devised a graphene-based electrode for supercapacitors that could boost current solar energy storage by an astonishing 3,000%. © Graphene Flagship.

Environment

Today, one in nine people lack access to safe water and one in three people lack access to a toilet. In order to bridge the gap, scientists at Australian research center CSIRO have used graphene to create a simple filtration system that allows water molecules to pass through nanochannels on a membrane's surface while stopping pollutants with larger molecules. Meanwhile, Researchers at MIT say that graphene could provide a revolutionary way of turning saltwater into clean drinking water.

In 2013, Chinese researchers announced they had developed the most lightweight material ever – a sponge-like material made by fusing freeze-dried carbon with graphene oxide. Called the Graphene Aerogel, the graphene-based sponge weighs only 0.16 milligrams per cubic centimeter and is capable of absorbing oil in quantities up to 900 times its own weight. In the future, such sponges could prove indispensable to clean oil spills.

Looking towards the future

Is all of this hype justified? Graphene's properties are truly remarkable and versatile, but there are still some challenges that need to be addressed before the material enters consumers' lives. The rate of progress that graphene-based technology can hope to achieve is directly tied to manufacturing. Some applications require single-layer graphene with as few impurities as possible, but right now, the most effective methods (mechanical exfoliation and chemical vapor deposition) are not cost-effective enough yet to be suitable for production at scale. However,

manufacturing of graphene flakes (few-layer or multi-layer) has started to get off the ground, which means less demanding applications could soon bring their graphene-based products to the market in increasing numbers.
Although it's been fifteen years since graphene was first isolated, the material is still in its 'baby years'. Most of the components in your smartphone, from the microprocessor to touchscreen, were first invented in the 1960s or prior to that time but it took many decades before the technology was mature enough to transition into the consumer market. In many respects, graphene research is growing at an astonishing rate with respect to other novel materials. For instance, there are now nearly 60,000 graphene-related patents, half of which were filed in the last three years.

Investments in graphene R&D are also riding an exponential curve. For instance, the European Commission has launched the Graphene Flagship initiative, which aims to bring together "academic and industrial researchers to take graphene from the realm of academic laboratories into European society in the space of 10 years." With a budget of €1 billion, the consortium consists of over 150 academic and industrial research groups in 23 countries.
Although graphene is still way ahead of its time, there are reasons to believe that it won't be very long before almost every industry is disrupted by it.

We should all be very excited about a future spearheaded by graphene.

Additional information: Graphene will be the main topic during a Science Breakfast at the 69th Lindau Nobel Laureate Meeting; this programme session will be hosted by the Graphene Flagship, Europe's biggest ever research initiative.



Materials (Basel). 2018 Nov; 11(11): 2110.
Published online 2018 Oct 26. doi: 10.3390/ma11112110
PMCID: PMC6266351
PMID: 30373190

Lubrication Performance of Graphene as Lubricant Additive in 4-n-pentyl-4′-cyanobiphyl Liquid Crystal (5CB) for Steel/Steel Contacts

Zhiliang Li,[1] Chonghai Xu,[1,2,*] Guangchun Xiao,[1] Jingjie Zhang,[1] Zhaoqiang Chen,[1] and Mingdong Yi[1]
Author information Article notes Copyright and License information Disclaimer
Go to:

Abstract

The lubrication performance of graphene used as additive in 4-n-pentyl-4′-cyanobiphyl liquid crystal (5CB) for steel/steel contacts was studied on a ball-on-plate tribotester. The friction test results show that when the graphene content in the 5CB was 0.15 wt.%, and the lubricant and friction pairs were heated to 44–46 °C before friction tests, the lubrication performance of the 5CB was most improved. Compared with pure 5CB, 5CB+0.15 wt.% graphene suspension reduced the friction coefficient and wear scar diameter by up to 70.6% and 41.3%, respectively. The lubrication mechanisms have been tentatively proposed according to the test results. We speculate that the excellent lubrication performance of graphene/5CB suspensions may be attributed to the low shear resistance adsorption layer formed by graphene and 5CB molecules on the sliding surfaces. As the protective layer, it not only prevents direct contact between the rough sliding surfaces but also is easy to slide.

Keywords: graphene, 5CB, lubricant additive, lubrication performance

Go to:

1. Introduction

Friction and wear between mechanical parts widely exist in mechanical systems. Friction consumes a lot of energy, and wear will lead to premature failure of parts [1]. In order to improve the service efficiency and life of mechanical equipment, friction and wear between parts must be reduced. Lubrication technology is the key technology to solve friction and wear and prolong the service life of equipment. Lubricants are widely used in industry to protect products and machinery equipment from wear. In addition, the application of lubricants also reduces the friction coefficient of the manufacturing process and eliminates excess heat accumulated in the mechanical system. Therefore, improving lubricant performance is important for protecting machinery from severe damage and reducing energy consumption [2].

Liquid crystals exhibit mesophase between liquid and crystal phase, which have both crystal anisotropy and liquid fluidity. Liquid crystals can be classified in two categories: (1) monomer liquid crystals, irrespective of whether they are able to polymerize, and (2) polymer liquid crystals [3]. 5CB belongs to monomer liquid crystals. When liquid crystals are used as lubricants, their molecules exhibit a crystal characteristic with a strong carrying capacity in the direction perpendicular to the friction surface. In the sliding shear direction, the liquid crystal exhibits a low viscosity liquid characteristic with a low friction coefficient [4]. It is believed that the liquid crystal with nematic phase (internal molecules aligned in one direction) has the best lubricity. The molecule of 5CB consists of a rigid biphenyl/cyano backbone with a flexible alkyl chain and presents a nematic phase at room temperature [5,6]. 5CB is expected to be widely used in industrial production due to its high bearing capacity and low shear resistance when used as lubricant.

Recently, nanoparticles have been introduced into industry as a new lubricant additive [7,8,9]. The performance of some lubricants can be significantly improved by the addition of suitable nanoparticle additives, especially some flake nanoparticle additives. Among various flaky nanoparticles, graphene and graphene oxide (GO) have attracted worldwide attention since their discovery [10,11]. The unique sheet structure makes graphene and GO easily enter the friction contact surfaces. Graphene and GO have strong mechanical properties and stable chemical properties [12]. So they have excellent antiwear properties and may become effective lubricant additives [13,14]. In recent decades, many studies have been conducted on the lubricating properties of graphene and GO [15].

Multilayer graphene can be well dispersed in some specific lubricants, and shows its antifriction and antiwear properties. For instance, Fan et al. [16] reported that the multilayer graphene can be well dispersed in bentonite grease and provides lower friction and wear compared with graphite. This antifriction ability mainly depends on the lubricating films formed on the friction surfaces. Guo et al. [17] prepared multilayer graphene by supercritical CO_2 stripping of graphite. The antifriction and antiwear properties of the multilayer graphene as an additive of polyalphaolefin-2 (PAO2) oil were studied by using four-ball test method. They pointed out that the PAO2 with 0.05 wt.% multilayer graphene showed the best lubrication performance. By analyzing the worn surfaces, it was found that the excellent lubrication performance of the multilayer graphene additives can be attributed to its small sheet diameter and layered structure, which make the multilayer graphene easily enter the friction interfaces and form a protective layer, thus preventing the friction surfaces from directly contacting.

Besides multilayer graphene, few-layer graphene also has been reported as lubricant additive. For instance, Eswaraiah et al. [18] evaluated the lubricating properties of ultra-thin graphene. The results showed that the friction coefficient and the wear scar diameter of the steel ball were reduced by 80% and 33%, respectively, at the optimum graphene concentration. Xie et al. [19] evaluated the lubrication performance of graphene used as additive in water. It was reported that graphene played a positive role in reducing friction and wear. They pointed out that the water added with 0.5 wt.% graphene showed best lubrication performance. Berman et al. [20] reported that the friction surfaces covered with the few-layer graphene significantly reduced friction and wear on steel/steel contacts. Restuccia et al. [21] reported that graphene can effectively lubricate steel-steel sliding contact. It was also confirmed that the lubrication mechanism of graphene is that the metal surfaces covered by graphene become almost inert and show very low adhesion and shear strength when mated in a sliding contact. Marchetto et al. [22] reported that graphene can significantly reduce the friction coefficient of steel-steel sliding contact. Raman spectroscopy results proved that graphene reduced the adhesion of the iron interface by making the surfaces inert, which further reduced the coefficient of friction.

To exert the lubricating properties of graphene in a lubricant, the dispersibility of graphene in the lubricant must be considered. The dispersity of graphene in most lubricants is very poor [23]. Chemical modification is usually used to improve its dispersity. For instance, Lin et al. [24] reported that after chemical modification by stearic acid and oleic acid, the dispersibility of graphene in base oil was obviously improved. The lubrication performances of the modified graphene lubricant were studied. The results showed that the addition of 0.075 wt.% of modified graphene can obviously enhance the antiwear and bearing capacity of the oil. Gupta et al. [25] added functionalized aged reduced GO

additives to polyethylene glycol. The results showed that adding functionally aged reduced GO significantly improved the lubricating performance of steel–steel contact. The study found that the main reason for improving the lubricating performance was that many oxygen functional groups in the reduced GO structure after aging promoted its effective dispersion in polyethylene glycol. Choudhary et al. [26] prepared alkyl amine covalently modified GO, which was easily dispersed in nonpolar organic solvents (especially aliphatic hydrocarbon solvents). By analyzing the friction test results, it was found that when alkyl amine covalently modified GO was added to n-hexadecane lubricating oil at the optimum concentration, the friction coefficient and wear scar diameter of n-hexadecane lubricating oil were reduced by 26% and 9%, respectively, compared with the base oil. Zhang et al. [27] used oleic acid to modify graphene and dispersed it as an additive in the polyalphaolefin lubricating oil. The lubrication performances of the graphene oil were studied. When the concentration of graphene is 0.02–0.06 wt.%, the friction coefficient and the wear scar diameter were reduced by 17% and 14%, respectively, compared with the pure polyalphaolefin lubricating oil. Bordignon et al. [28] reported that the plasma functionalization of multilayer graphene can make it be well dispersed in polyolester oil and provides lower friction coefficient and lower wear loss compared with pure polyolester oil.

In addition to using chemical modification to improve the dispersion of graphene, it has also been reported to improve dispersion by changing the shape of graphene to prevent adsorption and agglomeration between sheets. Inspired by the fact that crumpled paper sheets are not easily adhered to each other, Dou et al. [29] used capillary compression to quickly evaporate aerosol droplets of GO flakes to produce crumpled graphene balls. Experiments showed that graphene balls can be stably dispersed in polyalphaolefins type 4 (PAO4) oil without obvious aggregation. The lubrication performances of the graphene balls in PAO4 oil were studied by using a pin-disk friction meter. Compared with PAO4 oil, the friction coefficient and wear coefficient with graphene balls were reduced by about 20% and 85% respectively, mainly due to their anti-aggregation properties.

The dispersion effect of graphene in base oil will directly affect its lubrication performance. However, using chemical modification to improve the dispersion of graphene will affect its chemical properties. At the same time, changing the morphology of graphene through external force to improve its dispersion will destroy the physical structure of graphene.

In order to achieve the good dispersion of graphene in lubricating oil without changing its physical and chemical properties, we chose 5CB as the basic lubricant in this study. Since the rod-shaped molecules of 5CB tend to be arranged along the surface of the nanostructure that graphene provides

[30,31,32], the alternate positions on the hexagons within the graphene surface and the alkyl chains of 5CB geometrically match well [33]. Therefore, when graphene is added to 5CB, 5CB molecules will be adsorbed on graphene [34]. However, few studies have been carried out to achieve the good dispersion of graphene and improve the lubricating performance of lubricants by using the adsorption between lubricating molecules and graphene.

In this study, the adsorption between the 5CB molecules and graphene was fully utilized. Considering the fact that the higher the temperature, the more intense the thermal movement of the liquid molecules and the more fierce the Brownian movement, we have achieved good dispersion of graphene in 5CB by heating the graphene/5CB suspension. The lubrication properties of the suspension were tested on a tribometer with a ball-on-plate configuration. Transmission electron microscopy (TEM), optical microscopy, scanning electron microscopy (SEM), energy dispersive spectroscopy (EDS) and Raman spectroscopy were used to characterize graphene and study the wear surfaces. Based on the above tests and analysis results, we deduced the possible antifriction and antiwear mechanism of graphene as additive in 5CB.

Go to:

2. Experimental

2.1. Materials

The 5CB was supplied by the Shijiazhuang Huarui Scientific and Technological Co. (Shijiazhuang, China). This liquid crystal exhibits a nematic phase at 22–35 °C [5,6]. The graphene was provided by Pioneer Nanotechnology Co. (Nanjing, China) with the specification of 0.2–2 μm in sheet diameter and 0.8–1.2 nm in thickness. The anhydrous ethanol and acetone were purchased from Tianjin Guangfu Technology Development Co. (Tianjin, China).

2.2. Preparation of Graphene/5CB Suspension

The preparation procedures of Graphene/5CB suspension are as follows: Firstly, 5 mg of graphene was added in 10 ml of anhydrous ethanol with ultrasonic dispersion for 1 h to ensure that graphene was uniformly dispersed the solution. Secondly, 10 g of 5CB was added to graphene/anhydrous ethanol solution in 40–50 °C water bath with ultrasonication for 1 h to obtain a homogeneous suspension. After that, the suspension was put in vacuum at 50 °C for 12 h to completely evaporate the anhydrous ethanol. Finally the suspension of 0.05 wt.% graphene in 5CB (5CB+0.05 wt.% G suspension) was obtained. According to the above method, 5CB+0.15 wt.% G suspension,

5CB+0.25 wt.% G suspension and 5CB+0.35 wt.% G suspension were prepared respectively. No additional dispersion or surfactant was used to improve the dispersion of graphene in 5CB.

2.3. Friction Tests

The friction tests were carried out on a high temperature tribometer (Anton Paar, Buchs, Switzerland) with a ball-on-plate configuration, in indoor air conditions (24–26 °C, 37–46% RH). The tribometer is shown in Figure 1. Steel balls and plates were all made of GCr15 steel. The diameter of the steel ball was 6 mm, with roughness Ra = 25 nm. The steel plate with 55 mm in diameter, 12 mm in thickness and roughness Ra < 110 nm was used as counter-sample.

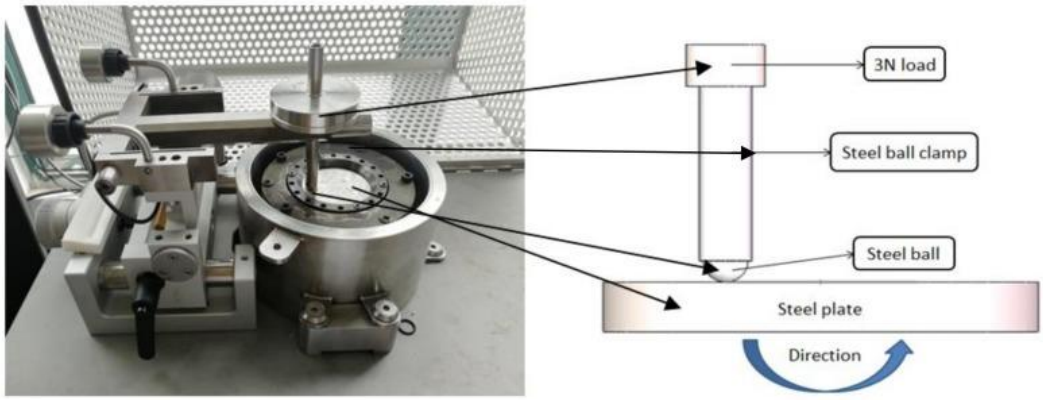


Figure 1

The high temperature tribometer and schematic view of ball-on-plate assembly.

Before conducting the friction tests, the steel balls and steel plates were ultrasonically washed with acetone, washed with anhydrous ethanol and dried. During the tests, the steel plate rotated at a speed of 200 rpm and the friction track radius was 18 mm, which was equivalent to sliding at a speed of 0.38 ms^{-1}. The normal load applied to the steel ball was 3 N. The duration for each sliding friction test was 1 h.

It is well known that the concentration of additives in basic lubricants plays an important role in reducing friction and wear [35]. In order to investigate the influence of graphene concentration on lubrication performance, graphene/5CB suspensions with graphene concentrations of 0 wt.%, 0.05 wt.%, 0.15 wt.%, 0.25 wt.%, and 0.35 wt.% were investigated, respectively.

For the influence of temperature on lubrication performance of the graphene/5CB suspension, three different temperature conditions were investigated. The first temperature condition: the steel plate was heated to 44–

46 °C while the graphene/5CB suspension lubricant was stirred at 44–46 °C for 120 s, to achieve good dispersion of the graphene in the 5CB, then the graphene/5CB suspension lubricant was applied to the plate and immediately stopping heating at the beginning of the friction test. The heating was stopped at the beginning of the friction test to make the 5CB return to the nematic phase, thus restoring the lubrication properties of the 5CB as a liquid crystal lubricant. After the friction test started, the shear force caused the graphene to be uniformly distributed on the surface of the friction region. Therefore, it is not necessary to rely on continuous heating to maintain a good dispersion state of graphene. The second temperature condition was at room temperature (24–26 °C). The third temperature condition was at 44–46 °C.

Before the friction tests, the lubricant was dripped onto the steel plate with a dropper. Then the wear track surface was fully covered with a lubricating layer formed by the lubricant droplets. Each test condition was repeated at least three times, and the final results of friction coefficient and wear scar diameter were the average values.

2.4. Surface Analyses

Before analyzing the friction surfaces, the steel balls and steel plates were washed with anhydrous ethanol to remove contaminants. An optical microscope (VHX-5000, Keyence, Osaka, Japan) was used to observe wear profile and measure diameter of wear scar. Scanning electron microscopy (SEM, JEM-5600 LV, JEOL, Tokyo, Japan) was used to further analyze the surface textures of steel ball wear scar. Energy dispersive spectroscopy (EDS) was used to analyze the content of various elements on the wear surfaces. Raman microscope (Renishaw, London, UK) was used to study Raman spectra of the graphene and wear scar. The transmission electron microscope (TEM, JEM-2100, JEOL Ltd, Tokyo, Japan) was used to analyze the structure and morphology of graphene before and after the friction tests.

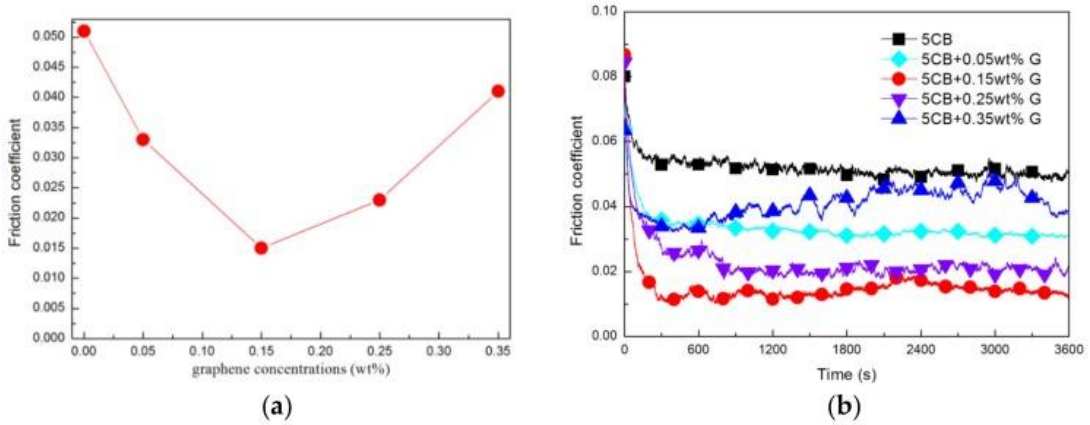
Go to:

3. Results and Discussion

3.1. Influence of Graphene Concentration on Lubrication Performance

In order to achieve good dispersion of graphene in the 5CB and make sure the 5CB exhibits a nematic phase during the rubbing process, the friction tests were performed in the first temperature condition. The friction coefficient and the wear scar diameter at different graphene concentrations were studied.

The relationship between the concentration of graphene in 5CB and the average friction coefficient is shown in Figure 2a. Clearly, compared with pure 5CB (μ = 0.051), all the graphene/5CB suspensions show lower friction coefficient. The coefficient of friction decreases as the concentration of graphene increases, when the addition amount is less than 0.15 wt.%. However, as the concentration increases, the friction coefficient increases, when the graphene concentration is higher than 0.15 wt.%. So the lowest value of friction coefficient (μ = 0.015, about 70.6% less than that of pure 5CB) is achieved when the graphene concentration is 0.15 wt.%.



Open in a separate window

Figure 2

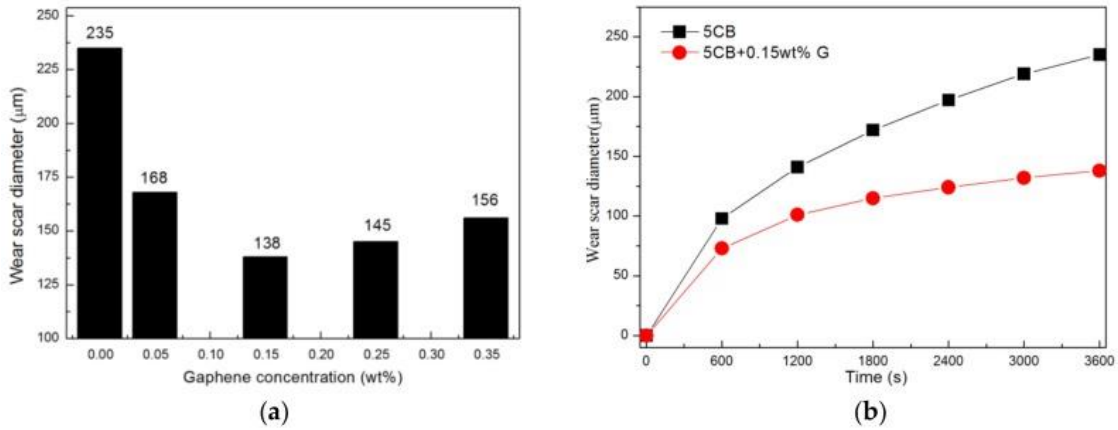
(a) Relationship between average friction coefficient and graphene concentration in 5CB, (b) relationship between friction coefficient and time at various graphene concentrations.

The relationship between the friction coefficient and the time is shown in Figure 2b. It can be found that in the first 300 s, the friction coefficient of all lubricants decreased significantly with time. All the graphene/5CB suspensions show a greater reduction in friction coefficient than pure 5CB. Observing the temperature change of the steel plate, it was found that when the friction test was carried out for 300 s, the temperature of the steel plate decreased to room temperature (24–26 °C). This indicates that the friction coefficient decreases and tends to be stable during the phase transition of 5CB to nematic phase.

When the addition amount of graphene is less than 0.15 wt.%, the coefficient of friction of the lubricant is relatively stable, this may be attributed to the absence of excess graphene on the friction surfaces and all graphene is adsorbed on the friction surfaces to fill surface pits or grooves to make the friction surfaces smooth [36,37]. When the addition amount of graphene exceeds 0.15 wt.%, the friction coefficient shows a clear fluctuation and increases with the increase of addition amount. Especially when the addition amount reaches 0.35 wt.%, the friction coefficient fluctuates violently with time, and the average friction coefficient is also large (μ = 0.041). This phenomenon indicates that the concentration of added graphene is too large and has affected the lubrication effect. This may be due to the fact that graphene tends to agglomerate into large bodies at higher concentrations, and it is not easy to form a continuous and uniform antifriction layer on the friction region.

Graphene, as a sheet-like nano material, is easy to enter the friction region [38]. In addition, graphene sheets with weak van der waals force are easy to slide between each other [39,40]. So we speculate that the addition of graphene reduces the friction coefficient.

Figure 3a presents the average wear scar diameter of the balls at various graphene concentrations. Clearly, all the graphene/5CB suspensions show smaller wear scar diameter, compared with pure 5CB (d = 235 μm). The lowest value of wear scar diameter (d = 138 μm, about 41.3% less than that of pure 5CB) is achieved when the graphene concentration is 0.15 wt.%.



Open in a separate window

Figure 3

(a) The average wear scar diameter at various graphene concentrations after friction tests. (b) The average wear scar diameter of 5CB and 5CB+0.15 wt.% G lubricants at different times during friction tests.

When addition amount of graphene is less than 0.15 wt.%, the average diameter of steel ball wear scar decreases with the increase of concentration. This phenomenon further proves that when the concentration is less than 0.15 wt.%, there is not enough graphene to form an antifriction and antiwear protective layer covering the wear surface [37]. The contact surfaces of the friction pairs cannot be completely separated, resulting in a larger friction coefficient and a larger wear scar diameter.

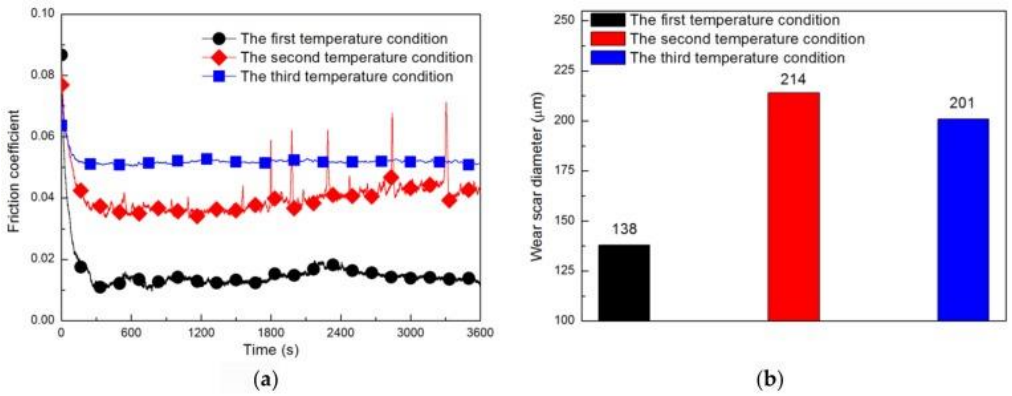
However, when the graphene concentration is higher than 0.15 wt.%, the average wear scar diameter starts to increase. This phenomenon further proves that graphene tends to agglomerate into large bodies at higher concentrations, and it is not easy to form a continuous and uniform antifriction layer on the friction region [41,42]. In addition, excessive graphene on the surface affects the formation of protective layer with low shear stress and self-repair [43].

Figure 3b shows a graph of steel balls wear scar diameter versus friction time. The antiwear mechanism of graphene can be inferred by analyzing the changes of wear scar diameter of balls with friction time under the lubrication conditions of 5CB and 5CB+0.15 wt.% G, respectively. As shown in Figure 3b, from the beginning of the friction tests, the wear scar diameter of the balls lubricated by 5CB+0.15 wt.% G suspension is smaller than that lubricated by 5CB in the same period of time. In addition, it can also be found that the wear scar diameter of balls increases steadily with

time under the lubrication of 5CB. While the wear scar diameter of balls increases relatively slowly with time under the lubrication of 5CB+0.15 wt.% G suspension, especially after 1200 s of test, the average wear scar diameter increases very slowly. It can be speculated that 5CB+0.15 wt.% G suspension formed a protective layer at the friction track during the friction tests, which effectively prevented the direct contact between the two contact surfaces [41,44]. Therefore, compared with 5CB lubrication, 5CB+0.15 wt.% G suspension exhibits more excellent antiwear properties.

3.2. Influence of Temperature on Lubrication Performance

The friction coefficient and wear scar diameter of the 5CB+0.15 wt.% G suspension were tested under the three temperature conditions set. The variation of the friction coefficient with the friction test time is shown in Figure 4a. As can be seen from Figure 4a, under the first temperature condition, the friction coefficient value is the lowest (μ = 0.015) and is relatively stable during the whole test process. This can be attributed to the good dispersion of graphene at the first temperature and the phase state of 5CB returning to nematic phase. Under the second temperature condition, the friction coefficient increased to 0.041 and there were many fluctuations during the tests, which might be the result of uneven graphene dispersion (under the second temperature condition, the friction coefficient of pure 5CB is 0.057). Under the third temperature condition, the coefficient of friction is the highest (μ = 0.052), which can be attributed to the change of phase of 5CB under this temperature condition, which damages its lubrication performance as a liquid crystal [45,46] (under the third temperature condition, the friction coefficient of pure 5CB is 0.071).



Open in a separate window

Figure 4

Friction coefficient curves (a) and the average wear scar diameters (b) of 5CB+0.15 wt.% G suspension under three temperature conditions.

Figure 4b shows the average wear scar diameter of balls under the three temperature conditions after the friction tests. At the first temperature, the average wear scar diameter of the balls is the smallest (d = 138 μm), which may be because the well dispersed graphene forms a complete protective layer on the friction surfaces, preventing the friction surfaces from directly contacting, thus reducing wear. Under the second temperature condition, the average wear scar diameter of the ball is the largest (d = 214 μm), which may be because the uneven graphene on the friction surface not only cannot form a complete protective layer but also acts as abrasive particles to

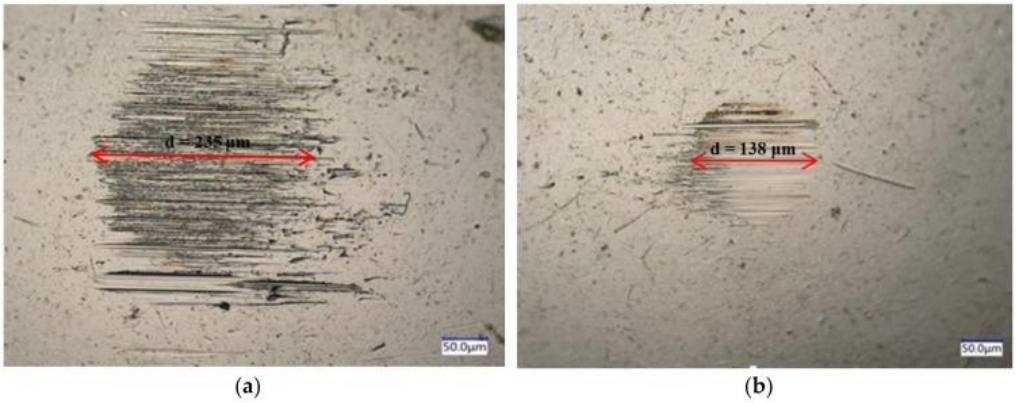
destroy the lubricating film. Therefore, the wear of steel balls cannot be effectively reduced (under the second temperature condition, the average wear scar diameter of ball lubricated by pure 5CB was 203 μm). Under the third temperature condition, the average wear scar diameter of the ball is also very large (d = 201 μm), which may be because the 5CB no longer has the lubricating properties of liquid crystal [45,46], thus increasing the average wear scar diameter of the balls (under the third temperature condition, the average wear scar diameter of steel ball lubricated by pure 5CB was 271 μm). The analysis of the average wear scar diameter of the steel balls shown in Figure 4b supports the previous assumptions about the friction and antiwear mechanism of graphene.

3.3. Analysis and Discussion on Lubrication Mechanism

The lubrication mechanism of 5CB+0.15 wt.% G suspension were emphatically analyzed with 5CB as the benchmark. All the test data and images analyzed were obtained under the first temperature condition.

3.3.1. Wear Surface Morphology of Steel Balls under Optical Microscope

To determine how graphene influences lubrication performance, the topography of wear surfaces after tests were investigated. As shown in Figure 5, the wear scar diameter of the ball lubricated with 5CB+0.15 wt.% G was much smaller than that of the ball lubricated with 5CB. The wear scar diameter of the ball for 5CB was very large, and the wear surface was very rough with irregular and deep grooves, as shown in Figure 5a. On the contrary, the wear scar diameter of the ball under 5CB+0.15 wt.% G lubrication was very small, and the worn surface was neat with even distribution of relatively shallow furrows, as shown in Figure 5b. This may be related to graphene adsorbing on and passivating the friction surfaces, because some literatures believe that graphene can reduce friction and wear in steel by making the surface inert [21,22]. By analyzing the wear scar morphology, it can be found that the addition of graphene reduces the wear scar diameter and roughness.



(a) (b)

Open in a separate window

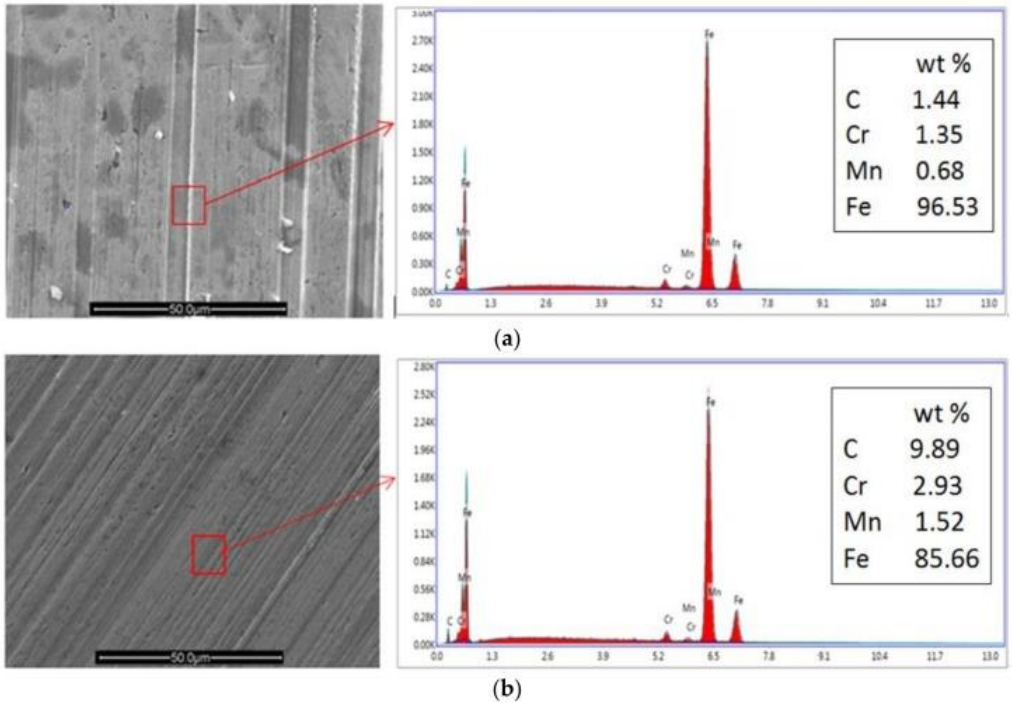
Figure 5

Optical micrographs of wear scars of the steel balls lubricated with (a) 5CB and (b) 5CB+0.15 wt.% G.

3.3.2. SEM and EDS Analysis

In order to prove that graphene exists on the friction contact surfaces and plays an important role

in the friction tests process, the wear surfaces of the balls lubricated by 5CB and 5CB+0.15 wt.% G suspension were analyzed by SEM and EDS, respectively. The test results are shown in Figure 6.



Open in a separate window

Figure 6

SEM micrographs of the friction surfaces of the ball and the corresponding energy dispersive spectroscopy analysis: (a) Lubricated with 5CB; (b) lubricated with 5CB+0.15 wt.% G suspension.

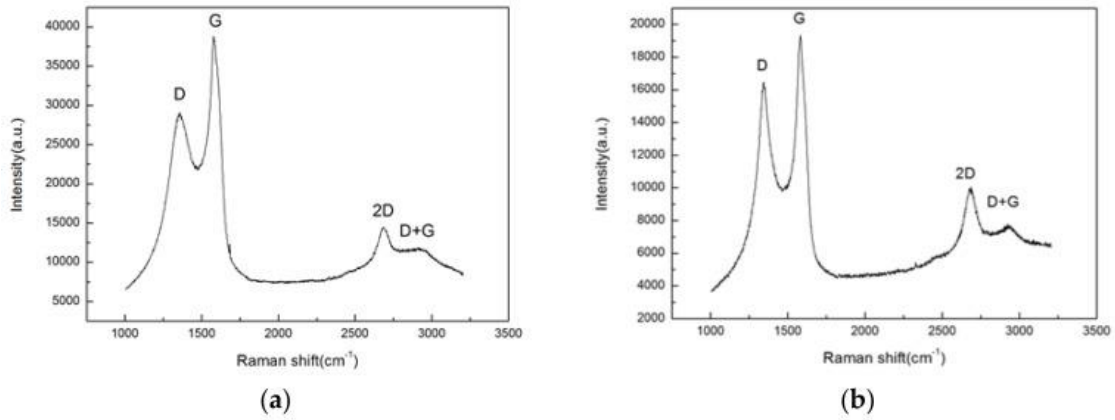
Obviously, the friction surface of the ball for 5CB had irregular and deep furrows, and the severe scratch was attributed to the relatively poor antiwear property of 5CB. The corresponding EDS analysis showed that the content of C element on the worn surface was only 1.44 wt.%, which may be due to the basal component of the steel ball and carbonizations of the 5CB, as shown in Figure 6a.

By contrast, some very regular and shallow furrows appeared on the wear surface of the ball for 5CB+0.15 wt.% G suspension. Many literatures show that friction coefficient is closely related to surface morphology [47,48]. In addition, the corresponding EDS analysis showed that the C element content on the worn surface was up to 9.89 wt.%, as shown in Figure 6b. Since graphene is composed of carbon, we can infer that graphene exists on the worn surface.

3.3.3. Raman Spectroscopy Analysis

Because Raman spectroscopy is a most suitable characterization technique for graphene materials [13], the Raman spectroscopy was used to further confirm that the better lubrication performance of 5CB+0.15 wt.% G is attributed to that the graphene enters the friction interface and forms a deposition layer on the friction surfaces. Figure 7a shows the Raman spectrum of the pristine graphene powders. Figure 7b shows the Raman spectrum of the wear surface of the steel plate lubricated with 5CB+0.15 wt.% G suspension. As shown in Figure 7b, the Raman spectrum of the

friction surfaces lubricated with 5CB+0.15 wt.% G suspension exhibits three characteristic peaks of the G peak (1580 cm−1), D peak (1350 cm−1) and 2D peak (2712 cm−1) which are the typical Raman signals of graphene [14]. This directly indicates that graphene exists on the worn surfaces.



Open in a separate window

Figure 7

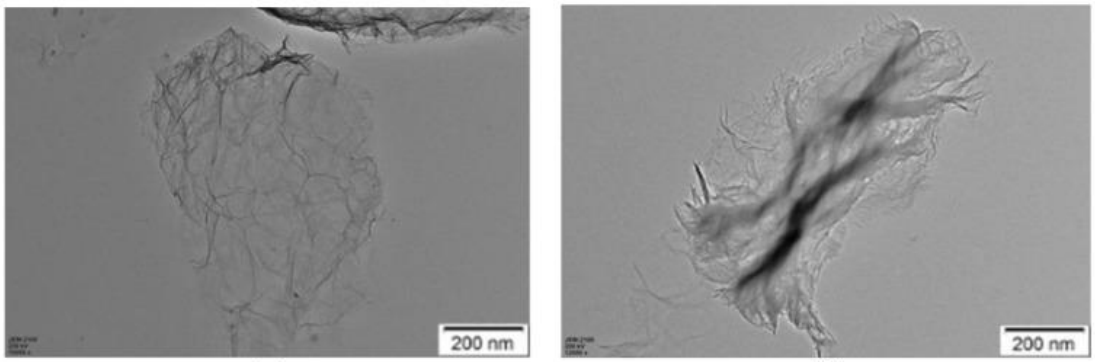
Raman results for (a) graphene before friction test, (b) the friction surfaces lubricated by the 5CB+0.15 wt.% G suspension.

Comparing Figure 7a with Figure 7b, it can be seen that the Raman spectrum for the graphene after friction tests has some different characteristics from that for the pristine graphene powder. The intensity ratio of the I2D/IG increased after the friction tests, which indicates that the thickness of the graphene is reduced [49,50,51]. In addition, the Raman spectrum of the graphene after the friction tests showed an increased ID/IG ratio to 0.89, as compared with 0.75 in the pristine graphene powder. This indicates that the defect density of graphene increases after friction tests [52,53]. This result supports our previous hypothesis that graphene exists at the friction interfaces and forms a protective layer with antifriction and antiwear effects together with 5CB on the friction surfaces.

3.3.4. TEM Analysis

Graphene protects the friction surfaces and reduces the friction coefficient by forming a protective layer on the friction surfaces during the friction process. Graphene has strong mechanical strength, so the protective layer can greatly protect the friction surfaces from abrasion and corrosion. In addition, graphene sheets with weak van der Waals force are easy to slide between each other, which helps to reduce shear resistance during friction [21,24]. In order to directly observe the changes in structure of graphene after the friction tests, TEM was used to study morphology of the graphene. The TEM morphologies of graphene before and after the friction tests were presented in Figure 8. Before the friction tests, the surface of graphene was very smooth, with a lateral size of about 0.2–2 μm as found in Figure 8a. However, after the friction tests, many folds were observed on the surface of graphene, as found in Figure 8b. This result shows that graphene bears frictional shear force in the friction tests, which changes the morphology of graphene and increases the surface defects of graphene. This result is in consistent with that of the Raman spectroscopy analysis. It further proves the lubrication mechanism that 5CB and graphene forms a protective layer on the

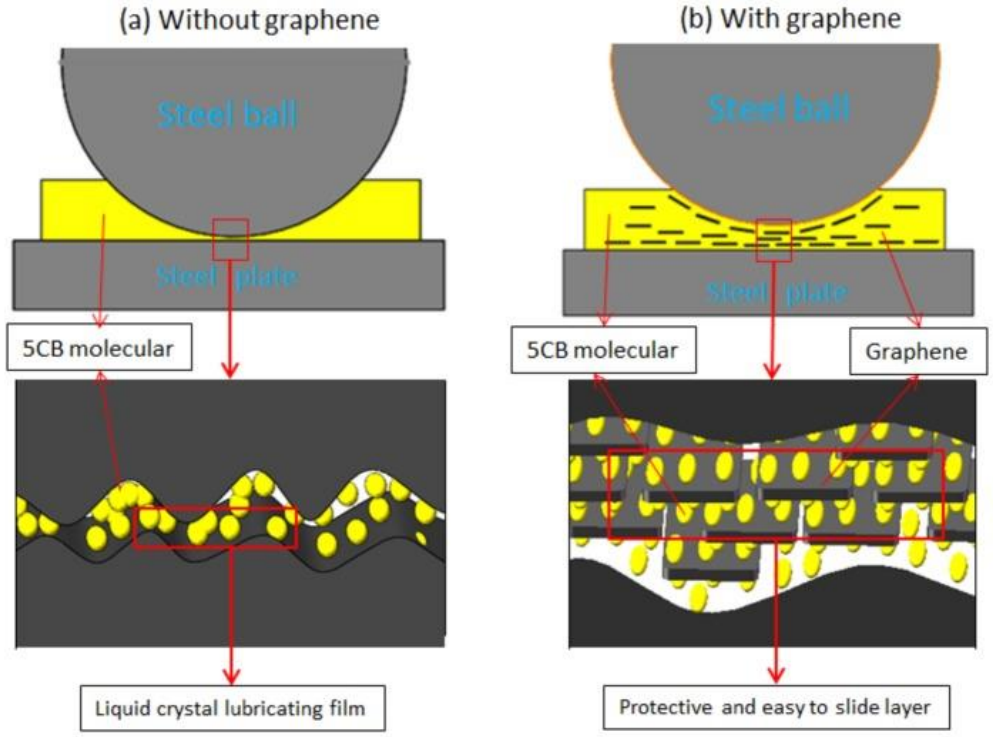
friction surfaces to reduce friction and wear. Scheme of the lubrication mechanism is illustrated in Figure 9.



Open in a separate window

Figure 8

Scanning electron microscopy images of graphene: (a) before and (b) after the friction tests.



Open in a separate window

Figure 9

Scheme of lubrication mechanism: (a) Lubricated with 5CB; (b) lubricated with 5CB+0.15 wt.% G suspension.

Go to:

4. Conclusions

In this work, the lubrication performances of graphene as additive of 5CB for steel/steel contacts

were studied by using a tribometer with a ball-on-plate configuration. Based on the analysis of the test results, the conclusions are as follows.

The concentration of graphene with the best antifriction and antiwear properties in the graphene/5CB suspension was 0.15 wt.%. Compared with pure 5CB, 5CB+0.15 wt.% G suspension reduced the friction coefficient and wear scar diameter by up to 70.6% and 41.3%, respectively. This outstanding lubricity is due to the low shear resistance and chemically stable protective layer formed by graphene and 5CB on the friction surfaces. Graphene with a sheet structure easily enters the friction interfaces and forms a protective layer on the friction surfaces, which makes the friction surfaces inert and prevents the two friction surfaces from direct contact, thereby reducing wear. In addition, graphene sheets are easy to slide, which is beneficial to reducing frictional resistance. Therefore, the addition of appropriate amount of graphene into 5CB can significantly reduce the friction and wear.

Graphene: a new emerging lubricant☆

Author links open overlay panelDianaBerman1AliErdemir2Anirudha V.Sumant1

Show more

https://doi.org/10.1016/j.mattod.2013.12.003Get rights and content

Under a Creative Commons license

open access

In recent years, reducing friction and wear-related mechanical failures in moving mechanical systems has gained increased attention due to friction's adverse impacts on efficiency, durability, and environmental compatibility. Accordingly, the search continues for novel materials, coatings, and lubricants (both liquid and solid) that can potentially reduce friction and wear. Despite intense R&D efforts on graphene for a myriad of existing and future applications, its tribological potential as a lubricant remains relatively unexplored. In this review, we provide an up-to-date survey of recent tribological studies based on graphene from the nano-scale to macro-scale, in particular, its use as a self-lubricating solid or as an additive for lubricating oils.

Previous article in issue

Next article in issue

Introduction

Increasing transportation and other industrial activities since the beginning of the last century have been consuming much of our non-renewable energy resources (like petroleum) day by day, and a significant portion of the energy produced is spent overcoming friction in moving mechanical systems. More important, much of the fuel used to generate energy turns into CO2, which contributes to climate change and could have dire consequences [1]. Accordingly, more effective control or reduction of friction in moving mechanical systems is very important for a sustainable future.

Frequently encountered in our daily activities, friction is a fact of life. Sliding, rolling, or rotating contact interfaces in every man-made, natural or biological system generate friction. If not reduced or controlled effectively, high friction often leads to higher wear losses and, hence, shorter life and

poor reliability. Consequently, friction has been one of the most active fields of study in the past. Many researchers are still working to understand the root causes of friction and new ways to nearly eliminate it to achieve much higher efficiency and longer durability in all types of moving mechanical systems [2].

One of the most effective ways to control friction is to use a lubricant in liquid and/or solid forms. Even certain gases may be used to lubricate rubbing surfaces. Liquid lubricants reduce friction by preventing sliding contact interfaces from severe or more frequent metal-to-metal contacts or by forming a low-shear, high-durability boundary film on rubbing surfaces. For example, depending on the sliding speed and other operating conditions, engine oils can effectively separate the contacting surfaces of rings and liners and, thereby, reduce the frequency of direct metal-to-metal contact and thus friction and wear. If and when there is metal-to-metal contact, the additives in these oils form a low-shear, highly protective boundary film to provide additional safety. In short, reducing friction means higher fuel savings; reducing wear means longer durability. Thanks to these solid and liquid lubricants, machine components of today's engines and other mechanical systems operate safely and smoothly for a long time.

Liquid lubricants are delivered to sliding interfaces through a pump or by other kinds of oil delivery mechanisms, while solid lubricants have to be applied as thin films using physical vapor deposition (PVD) and/or chemical vapor deposition (CVD) methods. Due to their finite thickness, solid lubricant films wear out eventually and lose their effectiveness. They are also very sensitive to the test environments; in fact, some of them, like MoS2, will not lubricate or last long if oxygen and/or water molecules are present; indeed, graphite and boric acid will not function without humidity in the surrounding air [3]. Therefore, the most desirable solid lubricant is environmentally insensitive, highly durable, and easy to deliver to the contact interfaces. In this review, we will make a case that graphene can provide extreme resistance to wear (as much as four orders of magnitude reduction in wear) regardless of test environments while not posing adverse environmental effects. Graphene, a two-dimensional carbon material, was stably isolated only in 2004 [4] but has already attracted significant attention in many different fields. Of these, tribological applications are still the least explored. With this review, we intend to highlight graphene's unusual properties to reduce wear and friction in nano-scale to macro-scale systems. Overall, we will show that graphene has much to offer as a high-performance solid lubricant or as an additive in liquid lubricants.

Why graphene?

Graphene being two-dimensional material, offers unique friction and wear properties that is not typically seen in conventional materials. Besides its well-established thermal, electrical, optical, and mechanical properties, graphene can serve as a solid or colloidal liquid lubricant. Its high chemical inertness, extreme strength, and easy shear capability on its densely packed and atomically smooth surface are the major favorable attributes for its impressive tribological behavior. Since it is ultrathin even with multilayers, it can be applied to nano-scale or micro-scale systems such as microelectromechanical systems (MEMS) and nanoelectromechnical systems (NEMS) with oscillating, rotating, and sliding contacts to reduce stiction, friction, and wear.

First of all, the extreme mechanical strength of graphene suppresses material wear. For example, Lee et al. [5] tested the mechanical properties of graphene and confirmed it to be one of the strongest materials ever measured. For their study, the authors used free-standing graphene membranes and analyzed them with a diamond atomic force microscopy (AFM) probe, which allowed measuring the breaking strength. The measured strength of defect-free graphene sheet corresponds to a Young's modulus of 1 TPa. The breaking force depends on the tip radius, not the diameter of the membrane. Moreover, it was shown recently that the grain boundaries do not affect the overall strength of graphene [6], even though the introduction of other kinds of defects (such as oxidation) largely contributes to the mechanical properties of graphene and decreases its strength and stiffness. From a tribological point of view, such extreme mechanical strength is highly desirable for wear protection.

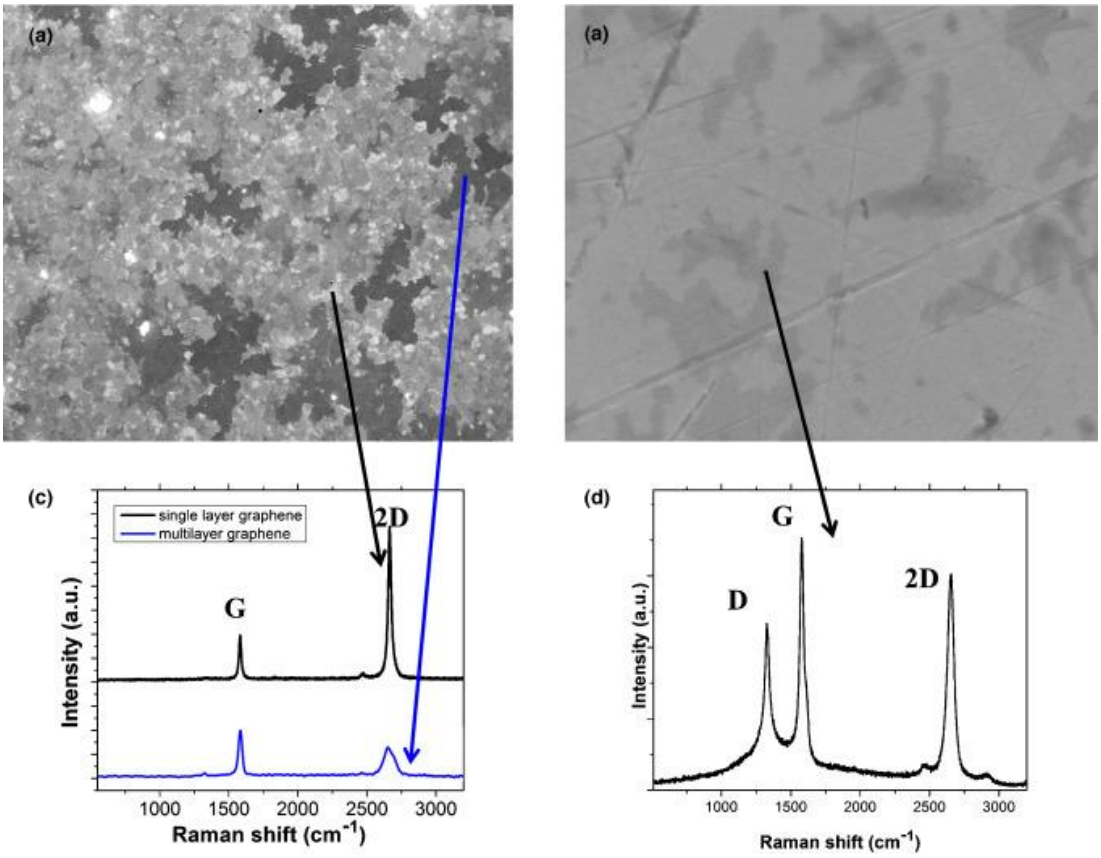
Secondly, graphene has been shown to be impermeable to liquids and gases [7], such as water or oxygen, thus slowing down the corrosive and oxidative processes that usually cause more damage to rubbing surfaces. Moreover, liquid water has been shown to minimize friction on graphene [8], thus presumably limiting the effect of capillary forces typical of humid environments. Singh et al. [8] demonstrated that the wetting angle is affected by the surface underneath the graphene layer; however, the effect of the substrate is modified by the number of layers and is negligible for multiple layers of graphene. Also, graphene is an atomically smooth two-dimensional material with low surface energy and is, therefore, able to replace the thin solid films usually used for reducing adhesion and friction of various surfaces.

All the properties mentioned above make graphene very attractive for demanding tribological applications to achieve low friction and low wear regimes.

Graphene synthesis

Different production methods are available for graphene. Depending on the type and the quality, the properties of the synthesized graphene may vary a great deal; in particular, the grain size, shape, thickness, and the density of defects change and thus affect the graphene's mechanical and tribological properties.

Initially, graphene was produced by the so-called ‘scotch-tape’ or mechanical exfoliation method [9], where commercially available adhesive tape is used to peel multiple layers from a highly ordered pyrolytic graphite (HOPG) and to transfer them by pressing the tape onto the desired substrate. Since then the number of methods for graphene production has significantly increased. Some of these include dry mechanical [4], [10] or chemical [11], [12] exfoliation; unrolling/unzipping of carbon nanotubes (CNTs) through a variety of ways such as electrochemical, chemical or physical methods [13]; CVD [14], [15] or epitaxial growth [16]; arc discharge; the reduction of graphene oxide [17], [18]; and many other organic synthetic methods. Widely used CVD methods are able to synthesize high-quality graphene on the catalytic surface, such as nickel or copper, in the presence of a carbon supply such as hydrocarbon gases [19]. In Fig. 1, Raman spectroscopy is used for analyzing the defects in the synthesized graphene, as well as the number of deposited graphene layers [20].



Download high-res image (1MB)

Download full-size image

Figure 1. Scanning electron microscopy images and corresponding Raman spectra for (a and c) CVD-grown multilayer graphene and (b and d) graphene deposited on steel from solution. Raman signatures indicate defect peak presence only for solution-processed graphene (d).

Graphene as a solid lubricant: from nano-scale to macro-scale

Unique physical, mechanical, and chemical properties of graphene make it an attractive candidate for many tribological applications where control of friction and wear is of paramount importance at different length scales. In the following sub-sections, we review the tribological performance of graphene from nano-scale to micro-scale and up to macro-scale.

Graphene tribology at nano-scale and micro-scale

The atomically thin nature of graphene and its ability to conformally coat micro-scale and nano-scale objects simply by dispensing graphene flakes via solution make it a potential low friction and wear resistance coating that would extend the lifetime of MEMS/NEMS devices and constitute the motivation behind current studies being carried out in this direction.

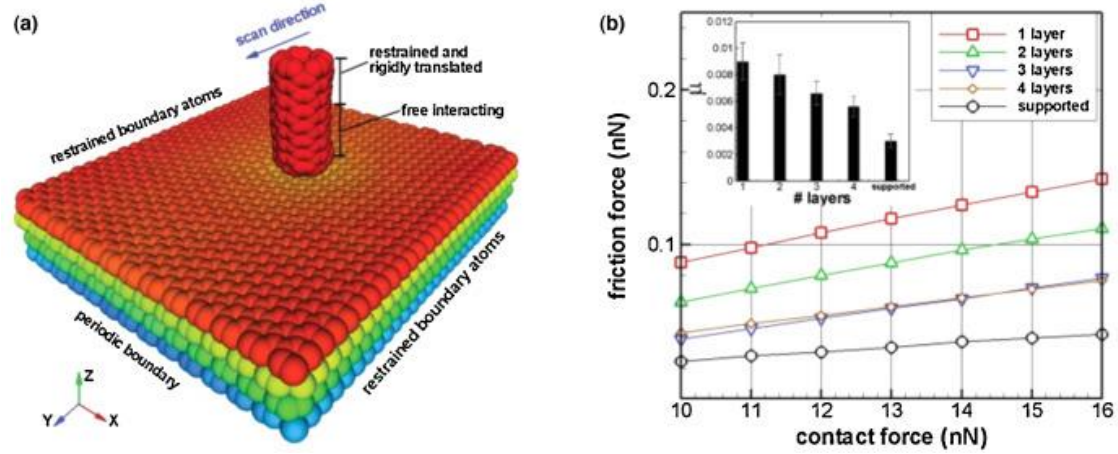
Nano-scale studies

Often, theoretical predictions drive future experiments and usage of novel materials. In the case of graphene, several studies predicted the nature of the graphene's friction mechanism based upon a variety of computational methods at scales varying from sub-nano up to meso [21], [22], [23], [24], [25], [26].

In most of the nano-scale computational and experimental studies on graphene, the tribological

behavior was shown to depend on stacking and other structural features, as well as the nature of the sliding surfaces. This observation is clearly seen for two different systems: (a) the friction of a nano-scale AFM tip sliding on a surface of graphene layers (which simulates AFM lateral force measurements) and (b) the friction between the graphene layers themselves. In case (a), it was shown that the friction decreases with increase of the number of layers [23], [25], while in case (b) the friction was found to behave in the opposite way, achieving higher friction or stick-slip behavior once the number of layers increased to more than three [21], [22].

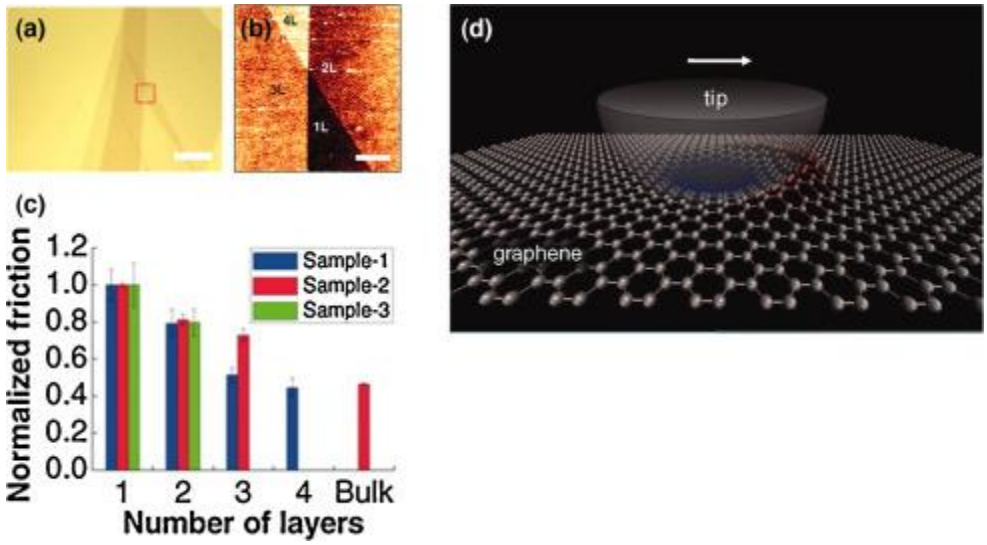
As shown in Fig. 2 [25], the modeling of the AFM tip-graphene interactions, where the lateral force was calculated as the sum of y-components of all van der Waals forces acting between the atoms of the CNT tip and those of graphene layers, demonstrated that the friction force decreases as the number of layers increases; that conclusion was also supported by the experimental AFM measurements [27]. That friction is dominated by the contribution from out-of-plane deformation, the so-called mechanism of 'puckering' in front of the scanning tip (Fig. 3d), which increases the contact area and, therefore, the amount of friction. Once the number of graphene layers increases, the interlayer interactions minimize the puckering effect and thereby reduce the friction. Moreover, in Ref. [23], Liu and Zhang stated that not only the increased number of layers, but also the increased tip-surface distance decreases the coefficient of friction for the sliding tip-surface interactions.



Download high-res image (527KB)

Download full-size image

Figure 2. (a) Four-layer suspended graphene assembly. The color of each atom is determined by its Z-position. (b) Contact force vs. friction force and the corresponding friction coefficients as function of number of layers. The results are obtained from Brownian dynamics simulations that model AFM lateral force measurements between the single-wall capped carbon nanotube tip (height and diameter were 2.3 and 1.2 nm, respectively) and suspended few-layer graphene (5.5 nm × 6.2 nm). The contact force was kept at the level of 10–16 nN. The simulations were thermostated at 300 K. Inset shows coefficient of friction versus number of layers. Reprinted figure with permission. Copyright (2012) by the American Physical Society [25].



Download high-res image (427KB)

Download full-size image

Figure 3. (a) Bright-field optical microscope image of graphene sample. The red dotted square represents the subsequent AFM scan area. Scale bars, 10 μm. (b) Topographic and friction (forward scan) images measured simultaneously by AFM from the indicated areas. 1 L, 2 L, 3 L, etc. indicate sheets with thicknesses of one, two, three, etc., atomic layers. Scale bars, 1 μm. (c) Friction on areas with different layer thicknesses. For each sample, friction is normalized to the value obtained for the thinnest layer. Error bars represent the standard deviation of the friction signals of each area. In the chart, the same color represents data from the same sample. (d) A schematic showing the proposed puckering effect, where adhesion to the sliding AFM tip creates out-of-plane deformation of a graphene sheet, leading to increased contact area and friction; the color scale of the atoms indicates their out-of-plane positions. Reprinted with permission from AAAS [5].

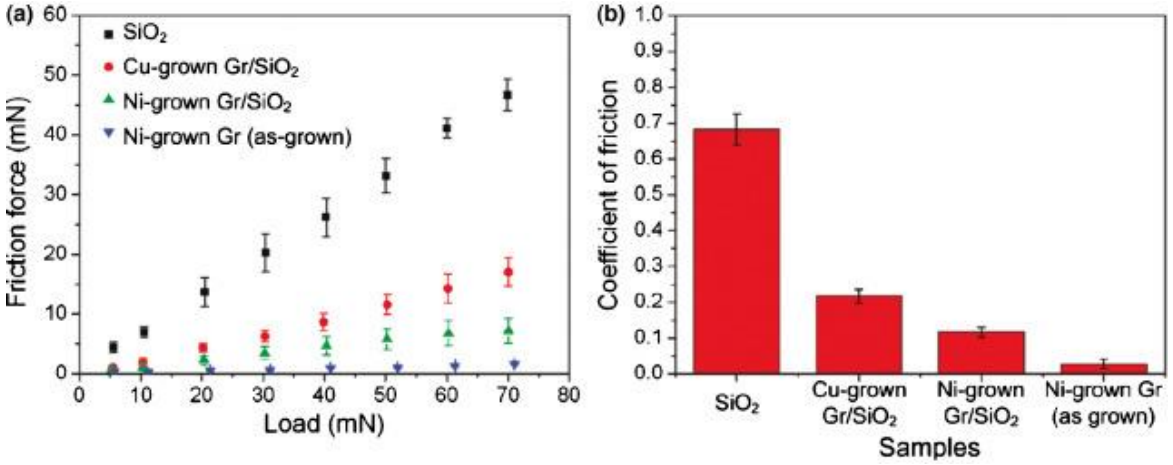
The great majority of experimental studies of graphene tribology at the nano-scale have used lateral force AFM or friction force microscopy (FFM) [28], [29], [30], [31], [32], [33].

The AFM lateral force measurements demonstrated the friction dependence on the number of graphene layers [27], [29], [31], in agreement with the predicted behavior in the simulation work reviewed above. Li et al. [5], [27] performed FFM studies in ambient conditions using silicon probes. Both free-standing graphene and graphene mechanically transferred on SiO2 showed a decrease in friction with number of layers (Fig. 3) perhaps due to 'puckering' effect. However, if the graphene layer is strongly bonded to the substrate (as was seen in the case of mica substrate [27]), the strong dependence of friction on the number of graphene layers is not observed. Such friction dependence on the number of layers occurs not only in graphene but in all atomically thin lamellar materials. [5], [29]

Micro-scale studies

Even though the transition between the nano-scale and micro-scale is not perfectly evident, we review below the tribological studies of graphene properties performed at small scales by techniques other than AFM.

Kim et al. [34] investigated the adhesion and friction properties of graphene at the micro-scale using a micro-tribometer. Graphene deposited on Ni and Cu substrates by CVD was transferred onto SiO2 substrates, and tribotests were performed in an ambient environment at room temperature using fused silica and polydimethylsiloxane (PDMS) lenses as counterparts. The contact loads ranged from 5 to 70 mN. The results demonstrated that both adhesion and friction force are reduced once the SiO2 surface is covered with graphene (Fig. 4). The variation in the properties of graphene grown on different metals is attributed to the weaker adhesion between Cu-grown graphene and the SiO2 surface, resulting in easily worn graphene, even at 5 mN loads.



Download high-res image (287KB)

Download full-size image

Figure 4. (a) Friction force as a function of load and (b) coefficient of friction for graphene samples. Only the fused-silica lens was used as a counterpart material in the friction tests. The coefficient of friction was calculated by dividing the friction force by the load. The error bars in both graphs indicate standard deviation. Gr, graphene. Reprinted with permission. Copyright (2011) American Chemical Society [34].

Shin et al. [35] conducted micro-scale scratch tests as another way for measuring the coefficient of friction of exfoliated and epitaxial graphene at the micro-scale. Results showed that at this scale the coefficient of friction stayed at ~0.03 irrespective of the number of layers. On the basis of both micro and nano studies, the authors attribute the difference in friction dependence on the thickness of the graphene films to the environment and the probe size. Moreover, introduction of defects (provided by oxygen plasma) increased the graphene friction. Therefore, differences can also arise from a defective or non-perfect top layer on the graphene film. Conversely, if the oxidation level of graphene oxide is decreased, as it was shown by Ou et al. [36] for chemically reduced graphene oxide nanosheets on the silicon substrate, the adhesive force is also reduced and this resulted in lowering of the friction.

Modified graphene studies

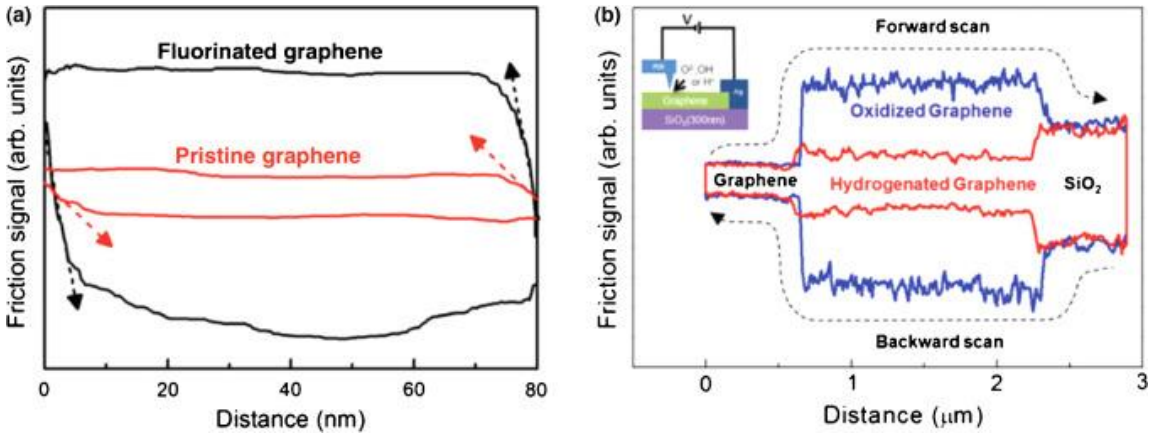
The change in the tribological performance of graphene as a function of surface chemistry was of obvious interest. Therefore, the tribological properties of chemically modified graphene (fluorinated, hydrogenated, or oxidized) were investigated experimentally as well as theoretically by density

functional theory (DFT) calculations [37], [38].

For oxidized graphene [37] the friction between two sliding graphene layers increases with the introduction of epoxide and hydroxyl groups, and is dominated by electrostatic and non-stable hydrogen bond interactions. The oxide system should overcome a much larger energy barrier due to hydrogen bond formation, thus resulting in high energy dissipation.

By contrast, for the single-side hydrogenated graphene sheets, the friction decreases greatly in comparison with pure graphene [38]. The DFT calculations for normal loads varying from 1 to 9 nN predicted the coefficient of friction to be in the range of 0.01–0.05 when hydrogen bonds are introduced. The lower friction is explained by electrons accumulated between the carbon atom and the attached hydrogen atom, resulting in the repulsion of two interacting sheets and thus in decreased energy of interaction.

For the interactions of two sliding surfaces, because no out-of-plane mechanical stresses are applied, the frictional changes are limited to the ones due to in-plane stresses. In the case of the tip interaction with the graphene surface, the out-of-plane stresses play an important role. Friction force microscopy measurements using a conductive AFM tip [39], [40] demonstrated that the nano-scale friction increased in comparison to pristine graphene by two, six, and seven times for hydrogenated, fluorinated, and oxidized graphene, respectively (Fig. 5).



Download high-res image (360KB)

Download full-size image

Figure 5. (a) Friction profiles measured on pristine and fluorinated graphene (applied load of 70 nN). (b) Friction profiles obtained from forward and backward scans across SiO2 and single-layer graphenes, including pristine, oxidized, and hydrogenated areas. The inset shows the experimental scheme of the oxidation and hydrogenation of graphenes. Copyright (2013) from Springer [39].

Despite the friction increase for modified graphene, the adhesive properties were shown to decrease for fluorinated graphene or remain almost unchanged for hydrogenated and oxidized graphene with chemical changes due to reduction of the van der Waal's contact area. This finding demonstrates that other factors than adhesion can play an important role in the tribological behavior of the interfaces. Ko et al. [39] suggest that mechanical properties dramatically change with sp3-hybridization arising from chemical modifications of graphene, and this fact plays the major role in the nano-scale friction increase. In addition to in-plane stiffness and adhesion energy

reduction, the chemical modification reduces the out-of-plane flexibility of graphene, which is associated with the increase of normal and bending stiffness of the modified graphene. For fluorinated, hydrogenated, and oxidized graphene, the out-of-plane flexibility drives the overall increase in friction.

Macro-scale tribology

Macro-scale friction studies are of direct interest to various industries where material losses due to wear as well as energy wasted due to friction are of great concern. Different bulk solid lubricants and their thin coatings have been used for friction and wear control in the past. Table 1 modified from [3], [41] provides quick overview of other known solid lubricant materials widely used by various industries worldwide with the new potential solid lubricant based on graphene.

Table 1. Overview of macroscale tribological properties of widely used solid lubricants.

Solid lubricant coating	Deposition methods	Coating thickness (μm)	Typical friction coefficient	Wear/friction mechanism
Graphite	Evaporation, pyrolysis	0.2–5	Dry: 0.5–0.6; Humid: 0.1–0.2	Interlayer shear and water intercalation
Diamond like carbon (near frictionless carbon)	Sputtering (rf and dc), ion-beam, PECVD	1–3	Dry: 0.001–0.05; Humid: 0.2–0.3	High chemical inertness and repulsive forces due to hydrogen termination
Tetrahedral amorphous carbon	Ion beam, cathodic arc, pulsed laser	0.01–1	Dry: 0.7; Humid: 0.1	Tribochemically induced surface reaction and termination of top carbon atoms
Ultrananocrystalline diamond	MPCVD, HFCVD	0.5–1.5	Dry: 0.05–0.13; Humid: 0.007–0.1	Tribochemically induced reaction with H, O, or OH
MoS2 and WS2	Sputtering (rf and dc), thermal evaporation CVD, ALD	0.2–2	Dry: 0.02–0.06; Humid: 0.15–0.25 initial and increasing	Interlayer shear and transfer film formation
Graphene/graphene oxide	CVD, chemical and mechanical exfoliation	0.001–0.002	Dry: 0.15–0.2; Humid: 0.15–0.2	Interlayer shear and prevention of tribocorrosion

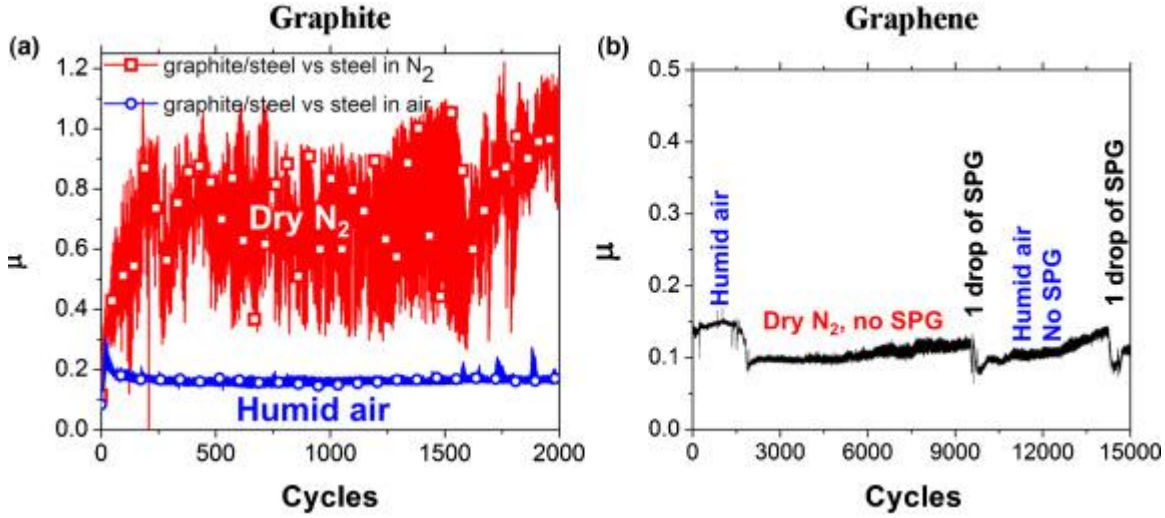
Surprisingly, less research has been conducted on the tribological properties of graphene at the macro-scale as compared to the nano-scale and micro-scale. We summarize in the following sections the macro-scale lubrication properties of carbon materials, such as graphene, graphene oxide, and graphite, when they are not intentionaly bonded to the surface of interest.

Graphite vs. graphene: how different is graphene?

Most tribological studies on graphene have been carried out at the nano-scale and micro-scale, building the case for graphene to be used as a solid lubricant. Recent meso-scale and macro-scale tribological investigations confirm previous predictions and open up new opportunities for graphene use as a solid lubricant in macro-scale systems too. Here, we look at graphite in order to better understand how graphene behaves differently tribologically at the macro-scale compared with bulk graphite.

Graphite as a macro-scale solid lubricant has been widely studied and has been used in industry for more than 40 years [42], [43]. It is well known that bulk graphite (a source of graphene) works the best in humid environments but fails to provide low friction and wear in inert, dry, or vacuum environments [44]. The reason for this behavior is the intercalation of water molecules between the graphite sheets, which allows easy shearing of graphite and provides low friction. Additionally, previous tribological studies using graphite flakes have indicated formation of graphite scrolls at the tribological interface [45]. These scrolls are favorable for decreasing the surface energy [46], [47] and reducing friction in the sliding interfaces.

For the purpose of comparison, in our recent work the graphite powder was mixed in ethanol (5 wt%, which is much larger than the concentration of graphene in ethanol) to reproduce the identical deposition procedure as the one mentioned in 'Graphene as a solid lubricant' section below. The tribological tests were performed in humid air and dry nitrogen under the same test conditions that were used for the graphene studies. As expected, graphite powder did not work well in dry nitrogen, showing high friction and high wear losses (Fig. 6a).



Download high-res image (428KB)

Download full-size image

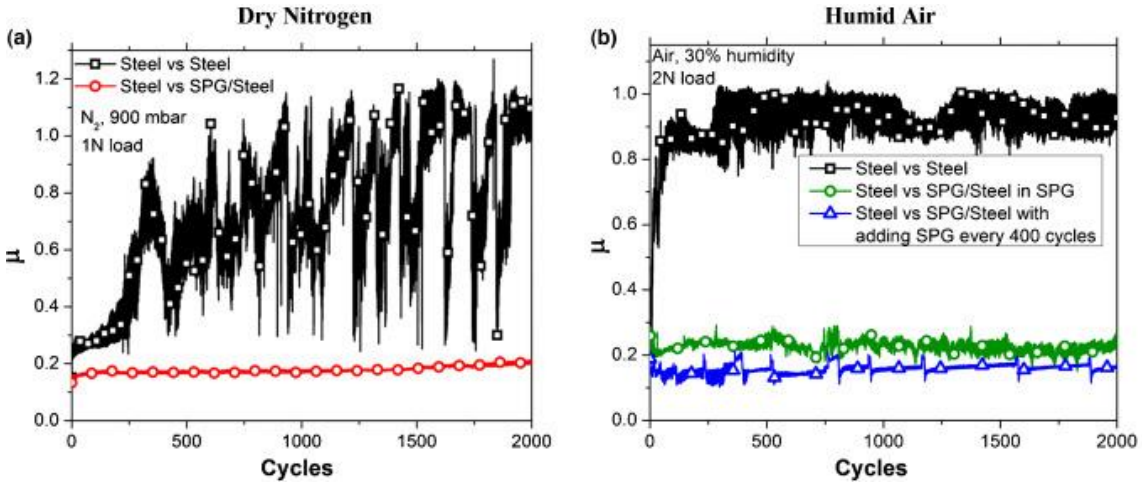
Figure 6. (a) Coefficient of friction for graphite deposited on steel from ethanol solution for tests performed in humid air and dry nitrogen. (b) Interchangeable behavior of graphene protection in dry and humid environments. The applied load is 1 N.

One of the major objectives of this study was to ascertain whether graphene behaves similarly to bulk graphite under dry and inert test conditions. For this graphene study, in addition to a dramatic reduction of friction when graphene is present at the sliding interfaces, the wear is reduced

significantly irrespective of the environment. These results (Fig. 6b) demonstrate the unique properties of graphene as a solid lubricant regardless of dry and humid test environments. This quality is unique to graphene and not possible with polycrystalline graphite or HOPG. To demonstrate the stable behavior of the coefficient of friction when graphene is applied on the steel surface, we performed the various tests: that is, changing the relative humidity by filling the test chamber with dry nitrogen to achieve ultra-dry test conditions and opening the test chamber to achieve humid air conditions. In every case, we repeatedly found unique behavior of graphene, showing low friction and wear in humid and dry environments. The macro-scale lubricative properties of graphene are discussed in more detail below.

Graphene as a solid lubricant

Previous studies [48], [49] demonstrated the unusual friction and wear properties of a few graphene layers on the steel surfaces. Specifically, a small amount of solution-processed graphene (SPG) was deposited from low concentration ethanol solution (1 mg/L) with only partial coverage of the steel surface (~25% of the total surface area), which was sufficient to reduce both friction and wear in the dry nitrogen and humid air environments (Fig. 7). In the dry nitrogen and humid air, the few layers of graphene demonstrated stable low friction (coefficient of friction equal to 0.15 in comparison to ~1 for bare steel) and four orders of magnitude reduction in wear in comparison to bare steel. Even in dry nitrogen, the coefficient of friction of the graphene layer derived from ethanol solution is comparable to that of HOPG in humid environments [42], [44]. Tests performed in the humid air required replenishing the graphene layer in the wear track for stable low friction and low wear regime. The results clearly demonstrated the wear protection qualities of graphene layers, especially when SPG is periodically fed to the sliding interfaces.



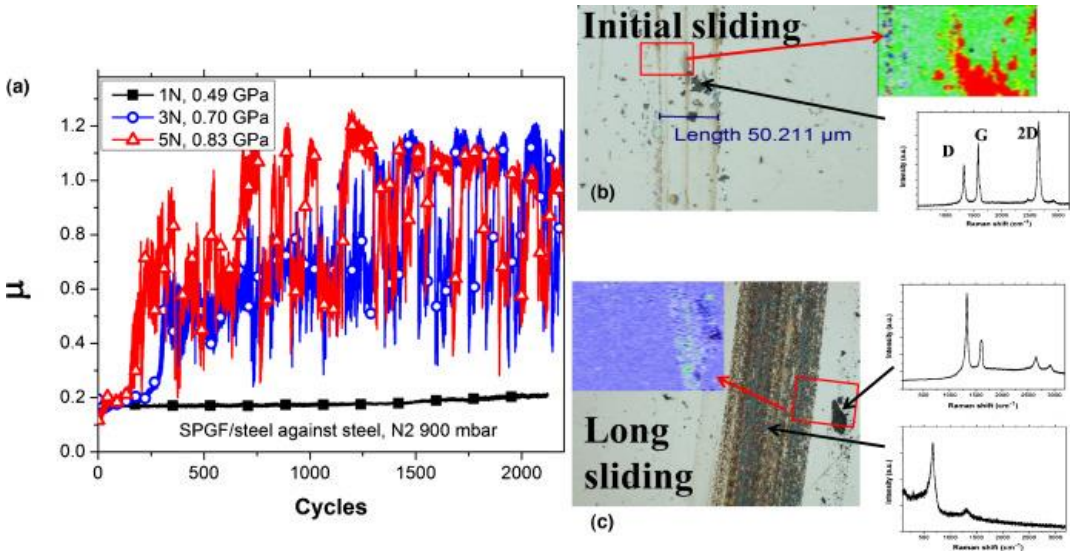
Download high-res image (499KB)

Download full-size image

Figure 7. Coefficient of friction (μ) for (a) SPG/steel and bare steel sliding interfaces in nitrogen and (b) self-mated steel test pair in humid air without SPG or ethanol, in ethanol solution with SPG, and in ethanol solution with intermittent supply of SPG. Reprinted from Carbon 54, Berman et al. Copyright (2013) [48].

The tribotests as a function of increasing load showed that the lifetime of the graphene protective

layer is shorter under higher loads, as illustrated in Fig. 8a. As is clear, the lifetime in dry nitrogen decreases to a few hundred cycles for 5 N load (or 0.56 GPa), while under low load condition (i.e., 1 N) the graphene protection is more durable. The graphene protective layer at 1 N load (Hertz contact pressure of 0.33 GPa) was shown to last without replenishment as long as 6000 cycles before the flakes of graphene started to be pushed outside of the wear track, with complete removal of the graphene layer at around 14,000 cycles.



Download high-res image (1014KB)

Download full-size image

Figure 8. (a) Coefficient of friction for steel with SPG under different loads for 2000 cycles in dry nitrogen. Raman signatures for (b) initial cycling with graphene protecting the wear track and (c) long cycling with graphene removed from the wear track. Reprinted from Carbon 59, Berman et al. Copyright (2013) [49].

To understand the mechanism behind the friction and wear reduction of the graphene lubricant, the wear tracks of the initial sliding low-friction regime and the follow-up high-friction stage were analyzed with Raman spectroscopy using a 633 nm red laser. The results demonstrated that at the initial stage, where the coefficient of friction is low and stable, graphene forms a uniform coating within the wear track area (Fig. 8b). The presence of a graphene layer everywhere at the wear track is confirmed with Raman mapping of the 2D peak (~2700 cm−1, red color corresponds to the highest intensity, blue to the lowest when no peak is present).

The Raman analysis of the wear track for the regime when the coefficient of friction is high and non-stable reveals that the majority of the graphene layers are worn out or removed from the wear track, thus indicating the presence of graphitic flakes near the track (Fig. 8c). In this case the 2D peak (at ~2700 cm−1) of graphene is weak while the defect peak D (at ~1350 cm−1) is much stronger, suggesting that graphene is converted to a disordered graphitic structure due to modifications during sliding. The presence of iron oxides (at ~1300 cm−1 and 1600 cm−1) and nitrides (at ~673 cm−1 and below) in the wear track itself is confirmed by Raman analysis, indicating severe damage and corrosion of the steel when the graphene layer is removed from the wear track.

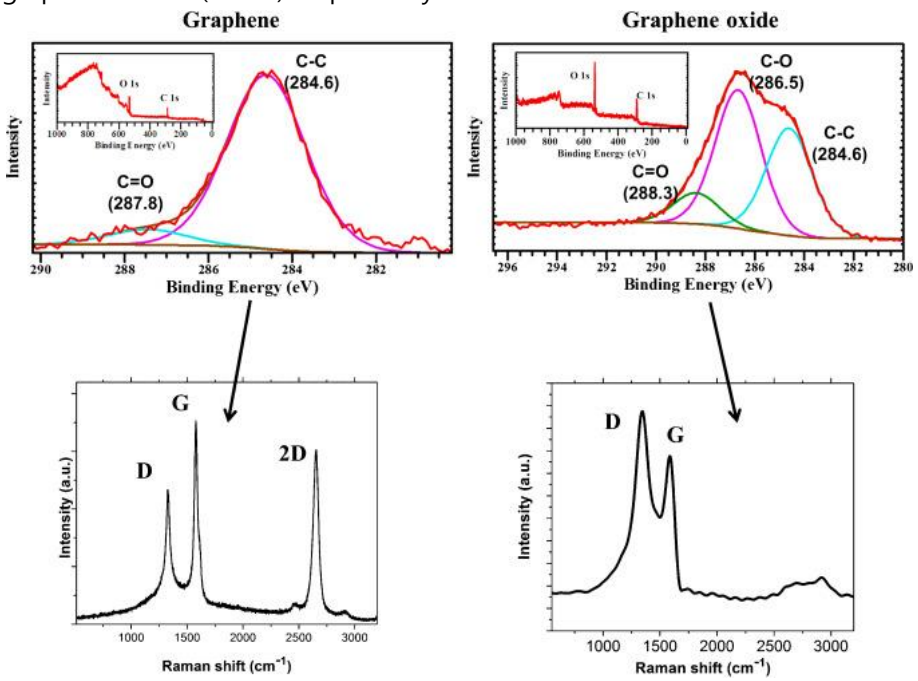
It is important to mention that for both dry nitrogen and humid air, as long as graphene is present at the sliding steel interfaces, the friction is reduced by 5–6 times and wear by four orders of magnitude for more than 15,000 wear cycles. Graphene as a two-dimensional material not only shears easily at the sliding contact interfaces but also provides protection against corrosion and oxidation, which can, in turn, help reduce friction and wear.

Graphene oxide vs. graphene

To complete the picture of the macro-scale properties of graphene, we also reviewed the role of chemically modified graphene, namely, graphene oxide. In a model experiment, solution-processed graphene oxide (SPGO) sheets in a highly concentrated water solution (5 g/L) were deposited onto highly polished steel surfaces. For the dry nitrogen environment tests, the water was evaporated to leave graphene oxide flakes on the steel surface. In the case of tests performed in a humid air environment, the sliding tests were performed in a water solution to ensure a sufficient supply of graphene oxide during the whole test procedure. Fig. 9 shows X-ray photon spectroscopy and Raman spectra for the SPGO and SPG layers. Both for graphene and graphene oxide the survey scan (shown in the inset) indicates the presence of oxygen on the surface of the protected steel surface (28 at% for graphene flakes and 43 at% for graphene oxide layers). However, the higher-resolution C1s spectra confirm that most of oxygen is chemically bonded to the carbon in the case

of SPGO (C O and C O peaks), and very small amount of oxygen is bonded to carbon for

SPG (only small C O peak is detected, possibly due to the oxygen bonded at the defect sites), consistent with previous XPS studies on graphene and graphene oxide mentioned in the literature [50]. Raman spectrum in Fig. 9c and d shows typical Raman signature of graphene (SPG) and graphene oxide (SPGO) respectively.

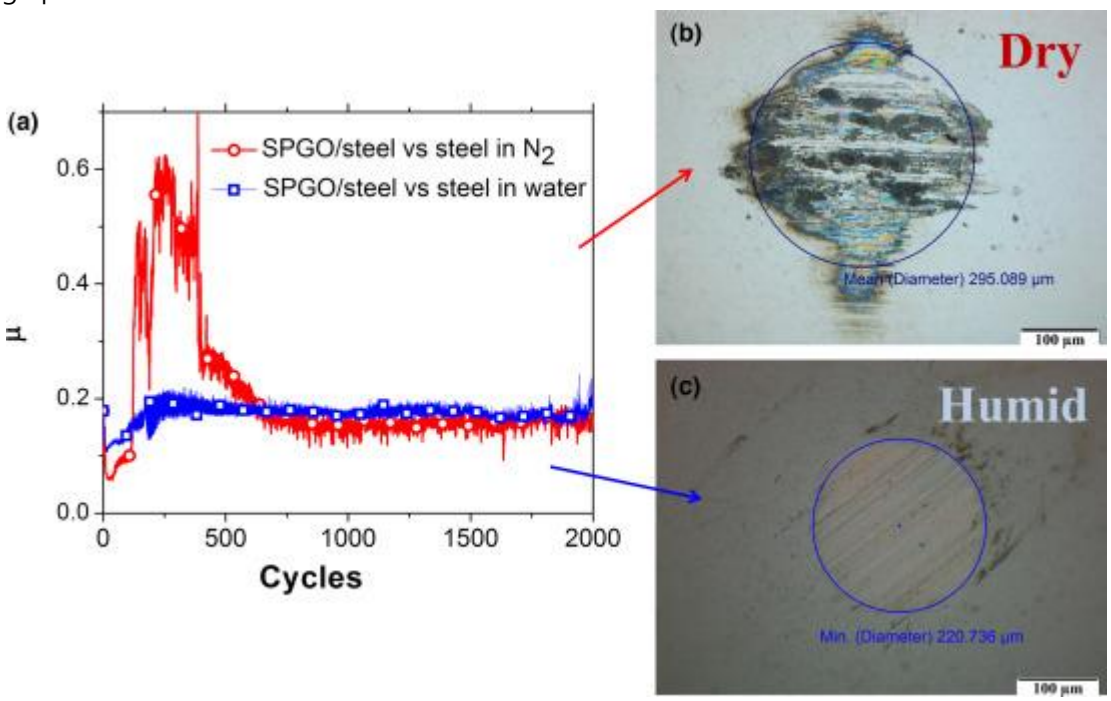


Download high-res image (630KB)

Download full-size image

Figure 9. X-ray photon spectroscopy (a and c) and corresponding Raman signatures (b and d) for solution processed graphene and graphene oxide.

The tribological behavior of graphene oxide layers at macro-scale is found to be not much different from that of the graphene layers, which is in contrast to the nano-scale and micro-scale studies on graphite oxide indicating different mechanism at play and needs further investigations to understand the exact mechanism. Fig. 10 shows the coefficient of friction and optical image of the wear track for the tests carried out using SPGO in dry and humid environments. The results confirm that graphene oxide may also be used to lubricate steel at macroscale by providing the COF below 0.2. However, the wear rate stays at higher level than the ones for unmodified graphene. The further wear rate comparison is presented in the following 'Comparison of wear for graphite, graphene, and graphene oxide' section.



Download high-res image (772KB)

Download full-size image

Figure 10. (a) Coefficient of friction and optical images of the wear track on the steel ball for the tests with SPGO showing (b) wear of in dry and in (c) humid (water solution) environment. The normal load was kept at 1 N, and the sliding speed was 60 rpm (or 9.4 cm/s) at the wear track of 15 mm radius.

Comparison of wear for graphite, graphene, and graphene oxide

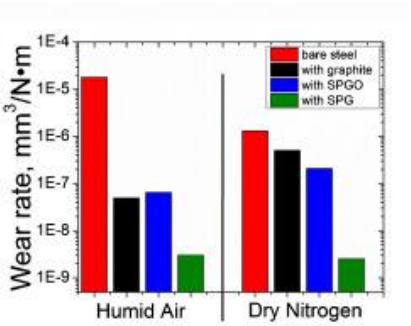
Fig. 11 summarizes the coefficient of friction and wear for uncoated steel and steel coated with graphite, graphene, and graphene oxide (1 N load, 2000 sliding cycles). For all three coatings, the amount of solution was 2–3 drops or 0.1–0.15 mL of solution per 1 cm2 steel; however, the concentration varied from 1 mg/L for graphene, to 10 g/L for graphene oxide, to 50 g/L for graphite.

Download high-res image (506KB)

Download full-size image

Figure 11. Wear rate for bare steel, graphite/steel, graphene oxide/steel, and graphene on steel in

Tribo pair	Test conditions	Calculated Wear Volume	Wear rate (Wear/(load·distance))	Coefficient of Friction
Steel/Steel	Air	6.8×10^{-3} mm^3	1.80×10^{-5} mm^3/N·m	1
	Nitrogen	4.9×10^{-4} mm^3	1.31×10^{-6} mm^3/N·m	0.9
With SPG	Adding drops/Air	11.4×10^{-7} mm^3	3.01×10^{-9} mm^3/N·m	0.15
	Nitrogen	9.6×10^{-7} mm^3	2.54×10^{-9} mm^3/N·m	0.15
With Graphite	Air	1.9×10^{-5} mm^3	4.94×10^{-8} mm^3/N·m	0.17
	Nitrogen	1.9×10^{-4} mm^3	5.07×10^{-7} mm^3/N·m	0.8
With SPGO	Water/air	2.5×10^{-5} mm^3	6.51×10^{-8} mm^3/N·m	0.17
	Nitrogen	7.8×10^{-5} mm^3	2.08×10^{-7} mm^3/N·m	0.16



humid and dry environments. From Refs. [48], [49].

Even though the coefficient of friction for graphene and graphene oxide in dry nitrogen and humid environments, as well as for graphite in humid air environment, stays at approximately the same level of 0.15–0.17 (Fig. 11), graphene layers provide the best wear protection, suppressing the wear by 3–4 orders of magnitude in comparison to bare steel sliding interfaces. This finding is especially impressive considering that, of the three coatings, the amount of graphene layers from ethanol solution used was the smallest to achieve good, stable lubrication lasting thousands of cycles.

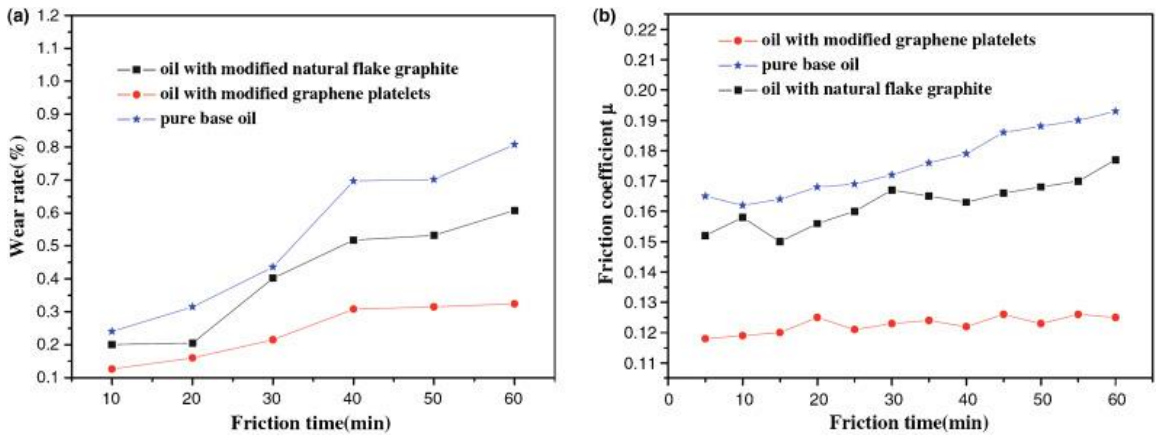
For graphene oxide the wear rate is 1–2 orders of magnitude larger than that for graphene layers. This difference is believed to arise because oxidized graphene does not have as good two-dimensional coverage as graphene, and the oxygen presence in graphene oxide may cause corrosion of steel, thus increasing the wear, while sliding between graphene oxide layers ensures low coefficient of friction. Therefore, the comparably low coefficient of friction for graphene oxide does not provide as good wear protection.

For the graphite powder, the low coefficient of friction in humid air can be attributed to the sliding occurring between graphite particles. However, graphite does not produce as good thin film coverage as graphene and does not protect the graphene surface from corrosion, which results in higher wear than that for sliding with graphene layers. Moreover, for graphite to establish a similarly low coefficient of friction requires a much larger amount of material.

Graphene as an additive in oils and composite materials

In addition to being used as a solid lubricant by itself, graphene can be used as an additive in conventional lubricants, such as oils, solvents, and other types of fluids. Results have indicated that even a minimal amount of graphene platelets added to oil [51], [52] is capable of noticeable reduction in friction and wear of steel. For chemically modified graphene platelets [51] that were dispersed in base oil by sonication and stirring with a magnet, tribological tests were performed on a four-ball machine with a 1200 rpm speed under constant load of 147 N at the elevated temperature of 75 °C. The optimal 0.075 wt% weight amount of modified graphene platelets was

able to provide a better load-carrying capacity than a base oil or oil with graphite flake additive. Both the coefficient of friction and wear reduced with the added graphene platelets (Fig. 12).



Download high-res image (392KB)

Download full-size image

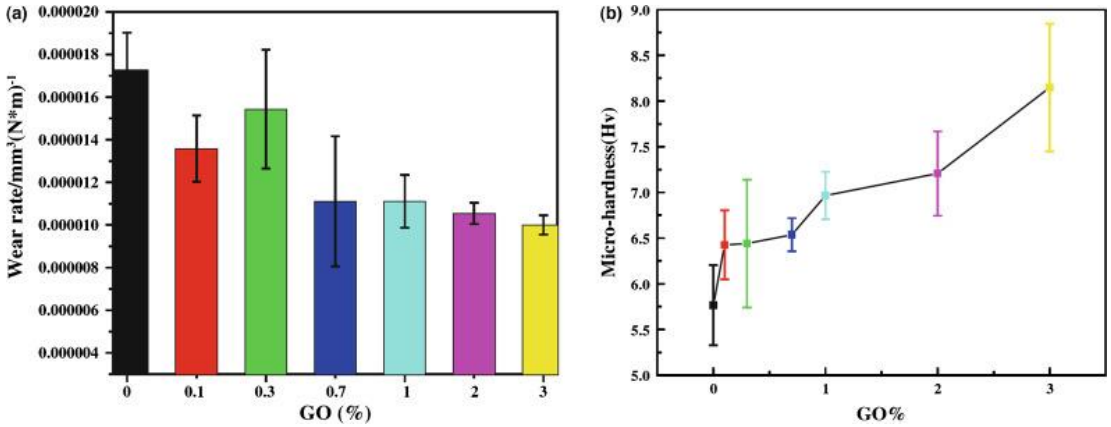
Figure 12. (a) Wear rate as a function of friction time (four-ball, 1200 rpm, 147 N, 60 min, 75 ± 2 °C). (b) Friction coefficient as a function of friction time (four-ball, 1200 rpm, 147 N, 60 min, 75 ± 2 °C). Copyright (2011) from Springer [51].

Adding 0.1 wt% graphene oxide nanosheets to oil was also [53] able to reduce friction and wear at high loads and different temperatures. For instance, the average coefficient of friction decreased by 20% in comparison to that of pure oil at the contact pressure of 1.17 GPa and temperature in the range 25–80 °C. The wear scar diameter was also reduced from 10% to up to 30% when graphene oxide nanosheets were introduced.

Graphene platelets are able to reduce the wear of other solid lubricants. Kandanur et al. [54] demonstrated that the wear rate of polytetrafluoroethylene (PTFE) was reduced by four orders of magnitude when 10 wt% of graphene platelets was incorporated as nano-fillers. In this study graphene platelets, consisting of 3–4 graphene sheets, were obtained by thermal exfoliation and reduction of graphite oxide. The authors showed that the wear rate reduces as platelets are introduced to 'Teflon'. Kandanur et al. [54] suggested that, initially, PFTE suffers high wear due to distribution of sub-surface cracks propagating parallel to the sliding interface and connecting eventually with the surface, while fillers are able to interfere with the formation of cracks, thus deflecting them and limiting the wear.

Dramatic reductions are attained on the wear rates of of ultrahigh molecular weight polyethylene (UHMWPE) composites by adding graphene oxide nanosheets at a range of concentration from 0.1 to 3 wt% as shown in Fig. 13. UHMWPE is used widely as a bearing material for hip and knee implants [55]. Even though the friction coefficient slightly increases, the wear is reduced by 40% when the content of graphene oxide in UHMWPE reaches 3 wt% (Fig. 13). This wear protective effect is attributed to increased tendency to form a protective transfer film and increased mechanical

strength and hardness, which limit microcrack initiation and growth and thus wear of UHMWPE during sliding.



Download high-res image (284KB)

Download full-size image

Figure 13. (a) Variation of wear rate of the GO/UHMWPE composites as a function of GO content after the wear tests. (b) The microhardness of GO/UHMWPE composites with the different GO contents. Copyright (2011) from Springer [55].

Organic solvent lubricants may also benefit from adding graphene. Choudhary et al. [56] prepared alkylated graphene with variable alkyl chain length by coupling of alkylamine with carboxylic groups of graphene oxide and then dispersed it in different organic solvents. They showed that during alkylation the size of the sp2 carbon domains increases, thus confirming reduction in oxidized graphene. The tribological tests using a four-ball machine confirmed friction and wear reduction of steel in hexadecane when 0.06 mg/mL of graphene nanosheets is introduced. In the tests performed under 392 N load at the speed of 1200 rpm at temperature 75 °C, the friction and wear were reduced by 26% and 9%, respectively. The enhancement in lubrication properties is attributed to the supply of graphene nanosheets between the rubbing surfaces, which prevent the direct contact of steel and provide low resistance to shearing.

Conclusions

This review highlights the recent developments regarding the use of graphene as a lubricant for nano-scale to macro-scales. In particular, research showing graphene's superior tribological properties compared with graphite and graphene oxide is covered. Further, recent studies dealing with graphene as an additive for lubricating oils and for the fabrication of self-lubricating nano-composite materials are presented. These dedicated studies have confirmed the following key findings.

•

Theoretical simulations predicted that the low friction of graphene is highly dependent on the sliding interfaces (whether the tip is sliding on the graphene surface or two graphene surfaces are sliding against each other) and on the number of graphene layers.

- AFM studies confirmed the theoretical prediction of decreasing friction when the number of layers is increased. Moreover it was shown that friction can reach the ultra-low friction regime at specific loads when the sliding occurs without stick-slip.
- Micro-scale tribological studies showed that introduction of defects in graphene increases friction. Also, chemical modifications of graphene by hydrogenation, fluorination, or oxidation result in 2, 6, and 7 times increase in friction, respectively.
- Macro-scale tribological studies clearly demonstrated how graphene is different from graphite in reducing friction and wear irrespective of atmospheric conditions (humid or dry) and also acting as a perfect passivation layer inhibiting the corrosion induced wear (tribo-corrosion) in case of steel contacts.
- Macro-scale studies demonstrated that graphene layers largely suppress the friction and wear of the sliding steel interfaces. Thus, the friction of steel drops from 0.9 to 1 for bare steel down to 0.15–0.16 for graphene coated steel in dry nitrogen and humid air environments. The wear volumes and rates are reduced by 3–4 orders of magnitude when graphene is present at the sliding interfaces.
- Overall in this review, graphene was shown to be very effective for friction and wear reduction not only as a lubricant but also as an additive to oils, composite materials and solvents.

Acknowledgments

Use of the Center for Nanoscale Materials was supported by the U. S. Department of Energy, Office of Science, Office of Basic Energy Sciences, under Contract No. DE-AC02-06CH11357.

Appendix A. Instrument citation

Macro-scale tribological tests were performed in humid air (30% RH) and dry nitrogen (900 mbar) at room temperature using a CSM tribometer with a ball-on-disk contact geometry. Stainless steel flat samples (440C grade) with rms roughness Rq = 20 nm were initially cleaned by sonication in acetone and then in isopropanol alcohol. The counterpart was a stainless steel ball (440C grade) of 9.5 mm diameter with rms roughness measured by the 3D profilometer Rq = 15 nm. The normal load during the tribotests was varied from 1 N up to 5 N at a speed of 60 rpm (or 9 cm/s), and the radius of the wear track was 15 mm. The sliding test durations were 2000 cycles or 190 m.

Solution-processed graphene was prepared by chemical exfoliation of highly oriented pyrolytic graphite (HOPG) and was then suspended in ethanol, while solution-processed graphene oxide was suspended in water (Graphene Supermarket Inc.). Raman spectroscopy was performed with an Invia confocal Raman microscope using red laser light (λ = 633 nm). The imaging of the wear scars was performed with an Olympus UC30 microscope. The wear rates on the ball and the flat sides were determined with a 3D non-contact MicroXam profilometer.

Recommended articlesCiting articles (415)

Synergy between graphene and ionic liquid lubricant additives

Author links open overlay panelJoséSanesMaría-DoloresAvilésNoeliaSaurínTuliaEspinosaFrancisco-JoséCarriónMaría-DoloresBermúdez

Show more

https://doi.org/10.1016/j.triboint.2017.07.030Get rights and content

Highlights

Addition of 0.005 wt. % graphene reduces more than a 70% the friction coefficient of motor oil at 150 ºC.

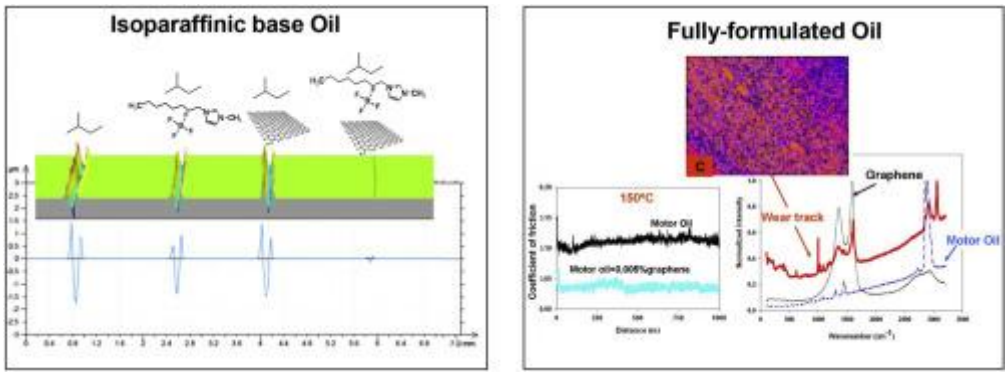
The formation of graphene surface layer reduces material loss from the steel surface.

For additive-free oil, graphene dispersed in ionic liquid achieves friction reduction and prevent wear at room temperature.

Abstract

Graphene (G) (0.005 wt%), the ionic liquid (IL) 1-octyl-3-methylimidazolium tetrafluoroborate (5 wt%) or a 5 wt% dispersion of 0.1 wt% graphene in IL (IL + G) have been evaluated as friction-reducing and antiwear additives of an additive-free isoparaffinic base oil (B), at room temperature, and a fully-formulated lubricant oil (FFO) at 150 °C. The best performances were found for [B+(IL + G)] and for (FFO + G), respectively. In the case of [B+(IL + G)], the presence of IL enhances the load-carrying and surface separating ability of graphene, leading to unmeasurable wear. In contrast, the lowest friction coefficient at 150 °C (0.03) is obtained for (FFO + G). Raman spectroscopy shows a carbon-rich graphene-containing layer on the wear track after lubrication with (FFO + G), which would be responsible for its outstanding tribological performance.

Graphical abstract



Download high-res image (292KB)

Download full-size image

Mild thermal reduction of graphene oxide as a lubrication additive for friction and wear reduction

Jun Zhao a, Yingru Lib, Yongfu Wangc, Junyuan Maoa, Yongyong He*a and Jianbin Luo*a

aState Key Laboratory of Tribology, Tsinghua University, Beijing, 100084, China. E-mail: heyy@mail.tsinghua.edu.cn; luojb@tsinghua.edu.cn

bInstitute of Materials, China Academy of Engineering Physics, Sichuan 621908, China

cState Key Laboratory of Solid Lubrication, Lanzhou Institute of Chemical Physics, Chinese Academy of Sciences, Lanzhou 730000, China

Received 8th November 2016 , Accepted 12th December 2016

First published on 9th January 2017

Recently, studies on graphene-based lubrication additives have been widely researched, but few refer to their preparation by thermal reduction which shows potential in not only significantly lowering the mass-production cost, but also the simple, nonchemical process. In this study, mild thermal reduction of graphene oxide (MRGO) has been achieved by high temperature (700 °C) treatment and the product used as a lubrication additive. It shows a relatively ordered lamellar structure and a certain level of oxygen by transmission electron microscopy (TEM) and X-ray photoelectron spectroscopy (XPS) analysis, and exhibits excellent tribological properties as a lubrication additive. The friction coefficient can be reduced by as much as 30% and the rubbing surfaces display few scratches at a lower additive concentration (0.5 wt%) compared with that of base oil (Poly Alpha Olefins Type 6: PAO 6) without MRGO additive under the same friction conditions. Based on the advantages of green, low-cost and simple synthesis operation, the MRGO offers significant potential application as a lubrication additive.

Retaining lower friction energy consumption and longer wear durability has been the development trend of the machine industry. In general, severe wear occurs in the start–stop state and low-speed operation of a machine, in which the rubbing surfaces are mainly under boundary regime.1 In that context, using lubrication additives has been an efficient way to improve tribological properties, for they can exhibit great anti-wear characteristics by forming a protective film on the friction interfaces and preventing the metal-to-metal contact.2–5 Nowadays, many additives containing polar components such as sulphur/phosphorus containing groups can lead to reducing wear, nevertheless, simultaneously are prone to make corrosion and pollution.1,6 Thus, to develop more efficient and environment-friendly lubrication additives is an urgent task for academia and industry. Graphene, is nowadays worthy to be used according to its high chemical inertia, extreme mechanical strength and easy to sliding between layers.7–10 However, the properties of graphene for applications varies with its production processes directly. The surface structure characteristics and elastic/plastic properties influencing the friction and wear properties, are strongly dependent on the synthesis methods such as mechanical exfoliation method, chemical vapor deposition (CVD) and reduction of graphene oxide, etc.11,12 Generally, mechanically exfoliated graphene exhibits better lubrication properties due to perfect graphitic structure and lower defects.12 Liquid phase and thermal

exfoliation of graphene oxide (GO) has been expected in the marketplace because of convenient and low-cost features13,14 compared with the mechanical method. Lately, our previous works have achieved the scale-up, low-cost and eco-friendly synthesis of GO techniques by an improved Hummers method15–17 which eliminates nitrogen oxygen impurities and simplifies the synthesis process. The above GO have been widely explored for many practical applications,15,17 but study about using it for synthesis of graphene additive in lubrication oil haven't been investigated. In addition, lots of studies have been published on preparation of graphene-based materials and their detailed lubrication properties,7,18–21 but there are few researches referring to the graphene additives from the reduced graphene oxide (RGO) by thermal reduction process which shows potential in not only significantly lowering the cost of mass-produced graphene but also the simple, nonchemical and thermal conversion of GO to RGO,22 while reduction by chemical process is much tedious and unsafe due to the residual hazardous reductants.23,24

Therefore, we investigated the tribological properties of the as-prepared graphene using the GO from above works by thermal reduction in this study. This mildly thermal reduction of graphene oxide (MRGO) displays several integrated layered structure and mild oxygen content, and exhibits excellent tribological properties. Moreover, the rubbing surface shows fewer scratches and smaller wear depth at a lower MRGO concentration (0.5 wt%). This work not only offers an efficient synthesis method of graphene additive for lubrication application due to the simple, low-cost and green operation, but conforms the further application value of the previous works of GO synthesis techniques.

The thermal temperature directly influences the structure and properties of reduced graphene. At a lower thermal temperature, the graphene can be weakly reduced which may result in lower C/O atomic ratio and higher wrinkled and folded structure.25 When reduction under much higher temperature even over 1000 °C, graphitic lattice or re-graphitization would occurs and the reduced sample approaches to bulk graphite.22,26 Therefore, for reaching not only relative high C/O ratio and integrated lamellar microstructure but also nano-thickness of graphene layers, the MRGO was prepared by the mildly thermal reduction of above GO at a temperature of 700 °C for 5 hours in a quartz tube, and then dry ball milling process was operated to make the additive size smaller and more uniform. The structure characteristic of MRGO was investigated by the combination use of scanning electron microscopy (SEM, FEI, Netherlands), transmission electron microscopy (TEM, JEM-2010, Japan), and X-ray photoelectron spectroscopy (XPS, Thermo Fisher Scientific, USA) operating with Al-Kα radiation and Raman spectroscopy (Raman, Horba JobinYvon, France) with 512 nm laser excitation. Friction experiments were carried out by a reciprocating sliding tester (UMT-3 CETR, USA) with a load of 2 N (the max initial Hertz contact pressure is approximate 1 Gpa). The reciprocating frequency and the sliding stroke are 0.4 Hz and 3 mm, respectively. The friction flat disk and the sliding ball (Ø4 mm) were made of bearing steel (GGr15), of which the surface roughness was about 20 nm measured by a white light interfering profilometer (MICROXAM-3D, America). The additives suspension in the PAO6 were mixed using a magnetic stirrer for 2 hours and then ultra-sonication for 0.5 hours to thorough dispersion.

The morphological characteristic of the MRGO is well revealed by SEM and TEM. By the ball milling process, the two dimension size of the MRGO is uniformly distributed within the range of about 1–2 μm (Fig. 1(a)). The surface of the MRGO (inset of Fig. 1(a)) has slightly wrinkled because of some defects, surface/edge dangling bonding and van der Waals interaction inevitably during thermal reduction.22,26 From the TEM image (Fig. 1(b)), the MRGO presents relatively integrated lamellar structure and the layer thickness is about 5 nm. In addition, the chemical structure of the graphene was analyzed by XPS. The C 1s (Fig. 1(c)) is presented into four Gaussian peaks with the binding energies of 284.77 eV (C–C/C=C), 286.22 eV (C–O), 287.37 eV (C=O) and 289.92 eV (O=C–OH), respectively. Although the oxygen-containing groups are relatively weak compared with that of GO (Fig. 1(c)), the observable content of oxygen (10.31%) remains in the MRGO, suggesting that the MRGO was mildly reduced. Raman spectroscopy is also an effective way to characterize graphene structure, which can reveal the degree of crystalline and order.27 The Raman spectra of the MRGO and GO are shown in Fig. 1(d). It displays prominent Raman peaks of D-band (at 1360 cm−1) and G-band (at 1595 cm−1). The integral intensity ratio (ID/IG) of the MRGO (2.26) is a little larger than that of GO (1.91), which means some local defects residues28 and the creation of numerous new graphite domains (Fig. 1(b))12,29 in the graphene by mild reduction. In a word, under mildly thermal reduction, the MRGO with integrated lamellar structure and mild oxygen content is well prepared.

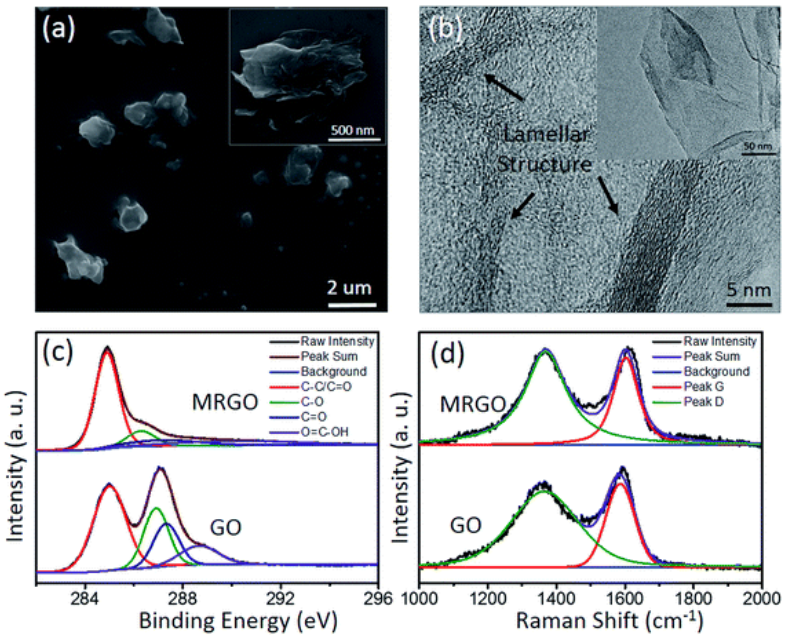


Fig. 1 Characteristic of the MRGO and GO. SEM and TEM images for the MRGO (a, b), XPS analysis (c) and Raman spectra (d) for the MRGO and GO, respectively.

The comparison of dispersion characteristic of GO with MRGO in oil have been tested after the same physical dispersion process above (Fig. 2). The MRGO lubricant showed stable dispersion state for 25 h, but sediment was apparent for the GO lubricant. After 50 h standing, the dispersion of GO displayed directly precipitated which could be due to rick oxygen-containing groups in GO resulting in interaction and agglomeration with each other while only slight agglomeration was observed for the MRGO dispersed oil, which means the MRGO is able to self-disperse in oil to some extent.20 Here, to identify the tribological properties of the MRGO, we also take the GO for comparison. The friction properties of the additives are shown in Fig. 3 after long friction time (5400 s). It can been seen that the MRGO presents excellent self-lubricating characteristic and the friction coefficient reaches a stable value of 0.1 and is decreased by 30% compared with that of the base oil which displays much higher and more tempestuously fluctuant in Fig. 3(a). The optimum concentration for MRGO is about 0.5 wt% for improving the lubrication property of the base oil (Fig. 3(b)). However, the GO lubricant only shows a little smaller friction coefficient than the based oil under the appropriate concentration range from 0.5 wt% to 1.0 wt%, of which the friction coefficient is much larger and more unstable than that of the MRGO lubricant after a short running-in stage, because there exists rick oxygen-containing groups in it, which impedes sliding motion between laminar layers as the result of previous study.12 After the long friction time, the rubbing surface lubricated by MRGO (Fig. 4(a)) only represents slender tracks while that lubricated by base oil or GO lubricant have wide wear tracks and deep furrows (Fig. 4(a) and (b)). According to the relationship between the wear depth and the MRGO or GO concentration (Fig. 4(d)), the wear depth of the rubbing surfaces lubricated by base oil is as large as 1161 nm, while the lowest wear depth for adding the MRGO is as low as 207 nm at the optimum concentration (0.5 wt%), which is decreased by almost 3 times than that of GO effect. However, the wear depths are higher under a larger concentration, which is corresponding to the variation of the friction coefficient, probably because of much higher concentration promoting the additive aggregation and impeding its permeating the rubbing interfaces. The wear behavior is also revealed by the SEM images of the rubbing surfaces in Fig. 5. It is clearly seen that the rubbing surfaces lubricated by the base oil suffer worse wear, because severe scratches and adhesion occurred on the friction disc and ball (Fig. 5(a) and (d)) under boundary lubrication. The rubbing disc and ball lubricated by GO (0.5 wt%) also exhibits severe scratches close to the contact regions (Fig. 5(b) and (e)). However, from the Fig. 5(c) and (f), there is few track on the worn surface lubricated by MRGO, and some slight wear tracks on the contact edge of the friction ball which is probably due to some graphene or wear debris stacking there and fretting the edge. Moreover, the worn diameter of the ball lubricated by MRGO is much smaller than that of both base oil and GO.

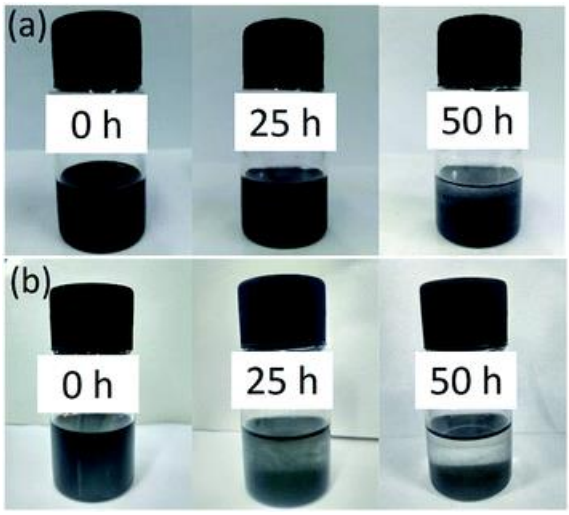


Fig. 2 Dispersion stability of the MRGO (a) and GO (b) dispersed lubricant (0.5 wt%).

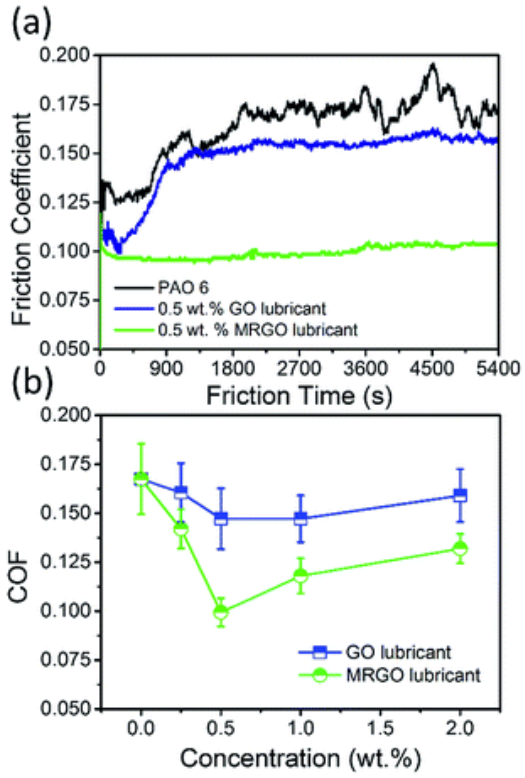


Fig. 3 Friction properties with the MRGO and GO dispersed lubricant. (a) Friction coefficient of MRGO and GO lubricant, compared with the base oil, (b) friction coefficient of MRGO and GO lubricant as a function of concentration.

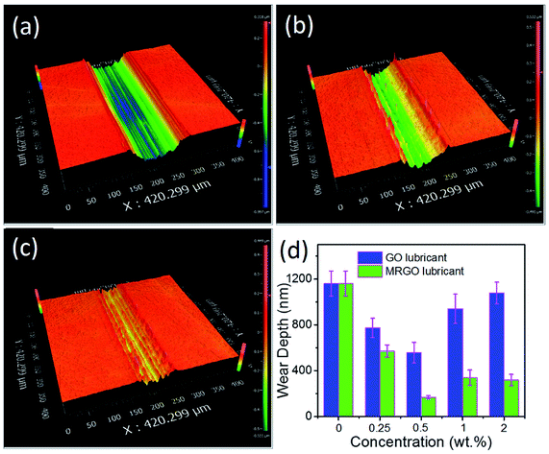


Fig. 4 Anti-wear capabilities with the MRGO and GO lubricant. (a), (b) and (c) the 3D morphologies of the rubbing discs respectively lubricated by base oil, the GO and MRGO lubricant (0.5 wt%), (c) wear depth of the rubbing discs under different MRGO and GO concentration. (d) Anti-wear capabilities of MRGO and GO lubricant as a function of concentration.

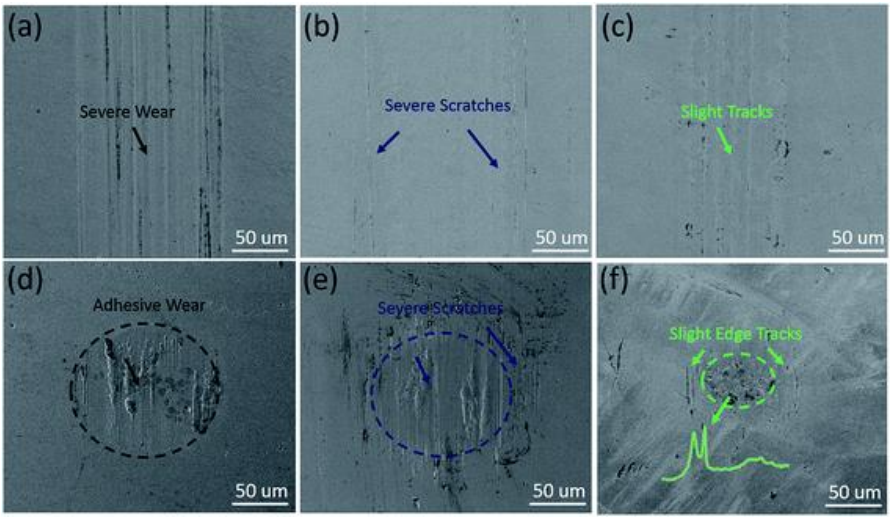


Fig. 5 SEM images and Raman spectra of the rubbing surfaces. (a), (b) and (c) the SEM images of the rubbing discs lubricated by base oil, GO and MRGO lubricant (0.5 wt%), respectively. (d), (e) and (f) the SEM images of the corresponding rubbing balls. The inset image (f) shows the Raman spectra after friction.

From above, the MRGO additive exhibits excellent lubrication and anti-wear ability. The uniform 2D-dimensional size of the as-prepared MRGO and the several nanometer thick of the layers (Fig. 1) promote the additive to permeate the friction interfaces and form a protective lubricating film more easily.30 According to the Raman spectra measured from the wear scar after 15 ultrasonic cleaning (inset of Fig. 5(f)), the characteristic peaks of MRGO (D-band at 1342 cm−1 and G-band at 1607 cm−1) are clearly observed, confirming that the MRGO stably adsorbed on the interfaces and a physical deposition film formed on the rubbing surfaces for prevent metal-to-metal contact.10,18 Moreover, the relatively integrated and ordered structure of the MRGO, composed of some laminated graphite planes by mildly reducing from the TEM image (Fig. 1(b)), may also improve the properties of anti-wear based on sliding between laminar layers after its adsorption on the friction interfaces. Additionally, slighter tracks on the contact edge lubricated by MRGO than that of GO in Fig. 5, may means the inferior self-dispersion of GO (Fig. 2) may be more likely to stack or aggregate there and scratch the surfaces. Therefore, the relative stable dispersion of MRGO improves the lubrication performance.20

In summary, MRGO was prepared and used as lubrication additive, which exhibits relatively integrated and ordered structure based on the uniform 2D-dimensional size (1–2 μm) and several laminar layers (5 nm). The friction coefficient can be decreased by as much as 30% and the scratches of the rubbing surfaces shows much slighter by adding the graphene of 0.5 wt%. Furthermore, this study about the thermal reduction of graphene oxide offers significant potential application as lubricant additive because of combination between the excellent lubrication ability and the advantages of green, low-cost and simple synthesis operation.

Acknowledgements

This work is supported by National Key Basic Research Program of China (973 Program) (No. 2014CB046404) and National Natural Science Foundation of China (51321092 and 51275263).



Energy efficient reduced graphene oxide additives: Mechanism of effective lubrication and antiwear properties

Scientific Reports volume 6, Article number: 18372 (2016) | Download Citation

Abstract

Optimized concentration of reduced graphene oxide (rGO) in the lube is one of the important factors for effective lubrication of solid body contacts. At sufficiently lower concentration, the lubrication is ineffective and friction/wear is dominated by base oil. In contrast, at sufficiently higher concentration, the rGO sheets aggregates in the oil and weak interlayer sliding characteristic of graphene sheets is no more active for providing lubrication. However, at optimized concentration, friction coefficient and wear is remarkably reduced to 70% and 50%, respectively, as compared to neat oil. Traditionally, such lubrication is described by graphene/graphite particle deposited in contact surfaces that provides lower shear strength of boundary tribofilm. In the present investigation, graphene/graphite tribofilm was absent and existing traditional lubrication mechanism for the reduction of friction and wear is ruled out. It is demonstrated that effective lubrication is possible, if rGO is chemically linked with PEG molecules through hydrogen bonding and PEG intercalated graphene sheets provide sufficiently lower shear strength of freely suspended composite tribofilm under the contact pressure. The work revealed that physical deposition and adsorption of the graphene sheets in the metallic contacts is not necessary for the lubrication.

Introduction

Reduction of friction in mechanical elements is one of the most important factors for improving energy efficiency of machine, enhancing the durability of the components and minimizing the emission of harmful gases in the environment. The automobile and transport industry faces challenges due to the emission of carbon monoxide and other chemically poisonous substances that substantially increase the global warming and risk level for living beings and equally it is hazardous for environment1. Layered materials such as graphene2,3,4 graphite5,6,7, hexagonal boron nitride (h-BN)4, and 2H molybdenum disulphide8,9 are proven as effective solid lubricants. The unique anisotropic crystal structure of layered materials signifies strong covalent intralayer and weak van der Waals interlayer interactions which are the main reasons for the effective solid state lubrication2,3. Bahareh Yazdani et al. reported enhanced tribological properties of graphene embedded with Al2O3 composite10. In other work, Hyo Jin Kim et al. reported synthesis of unoxidized graphene/alumina composite materials having enhanced toughness, strength, and wear-resistance11. Unfortunately, the solid phase lubrication of lamellar materials is restricted to the specific application and, therefore the use of these materials in liquid phase lubrication as additives becomes an important issue. Among the above mentioned layered materials, graphene is considered as unique material due to its high chemical inertness, extreme strength, and easy shear capability on its densely packed and atomically smooth surface2,4. It can exist stable in ultrathin state and dispersion in lubricant makes it a potential material for low friction and wear resistant additives12,13,14. For the effective lubrication, the covalent/non-covalent interaction of graphene

with lubricant is required15,16,17. However, such interactions of hydrophobic graphene are challenging in hydrophilic polar lubricant due to difference in cohesive energy. Graphene consists of sp2 carbon atoms with delocalized π electrons in 2D network, which is chemically inert and easily agglomerates due to the π-π stacking interaction18. This becomes one of the main problems dispersing it with polar lubricant. However, higher specific surface area of lamellar materials enhance the ability towards chemical functionalization and better dispersibility in lube medium. The π electrons become localized while creating the oxygen functionlization leading to 2D sheet chemically active19. There are several reports which showed functionalized graphene as a compatible lube additive for friction and wear reducing additives15,16,17,20. The functionalized graphene provides chemical grafting with lube facilitating weak shear forces acting between the lamellar sheets16,17,21,22,23. Large amount of graphene concentration in the dispersive medium poorly lubricate the sliding system, generating high friction and wear. Graphene agglomerates and precipitates if the concentration is higher which does not provide the well known mechanism of weak interlayer sliding resistance of graphene sheets. In addition, higher concentration is responsible for shear thickening and inter-sheet collision that may produce high friction and wear24. In contrast, at low graphene concentration, the effective lubrication becomes weak due to scarcity of graphene sheets and in this condition lubrication is mainly governed by the lube medium. Therefore, optimized graphene concentration as an additive in the lubricant becomes one of the puzzling issues for effective lubrication. Its mechanism for controlling friction and wear becomes even more puzzling topic. There are few reports which showed concentration dependent friction and wear behavior in graphene/graphene oxide additives in lube medium15,16,17,20,25. However, lubrication of graphene and concentration dependent lubricity mechanism in the literature is poorly understood. Schluter et al. showed that thermally reduced graphene oxide (TRGO) containing lubricant significantly enhanced the friction and wear properties26. It is predicted that the enhancement in above properties are attributed to the interaction of amphiphilic additive and functionalized TRGO filler particles on metal oxide surfaces.

In this novel and pristine work, friction and wear of steel-steel contact was proposed to investigate which is lubricated with various concentration of graphene dispersed PEG200 at various loads. The contact pressure was varied to find the generalized experimental proof for concentration dependent lubrication mechanism. Contact surface was analyzed by electron dispersive spectroscopy mapping and local area Raman mapping of wear tracks for describing chemical nature of tribofilm formation. Based on experimental results, the lubrication model in graphene lubricated contacts is proposed.

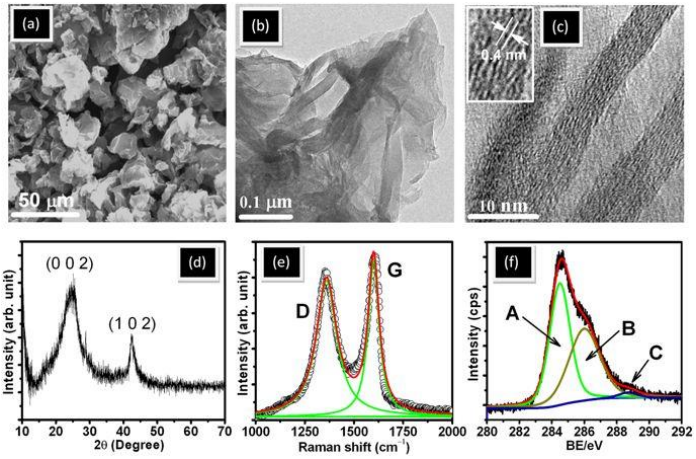
Results and Discussion

Morphology, microstructure and chemical characteristic of rGO

SEM image clearly shows curly flakes signifying graphene features (Fig. 1a). Further, low resolution TEM shows wrinkles, lateral corrugations and scrolled morphology of rGO, indicating presence of few layers of graphene sheets where strain is localized (Fig. 1b). The high resolution TEM image clearly reveals bunches of crystalline rGO nanosheets with thickness 5–6 nm and number of sheets ranging from 12–15 (Fig. 1c). The lateral dimension of the sheet is significantly larger than the

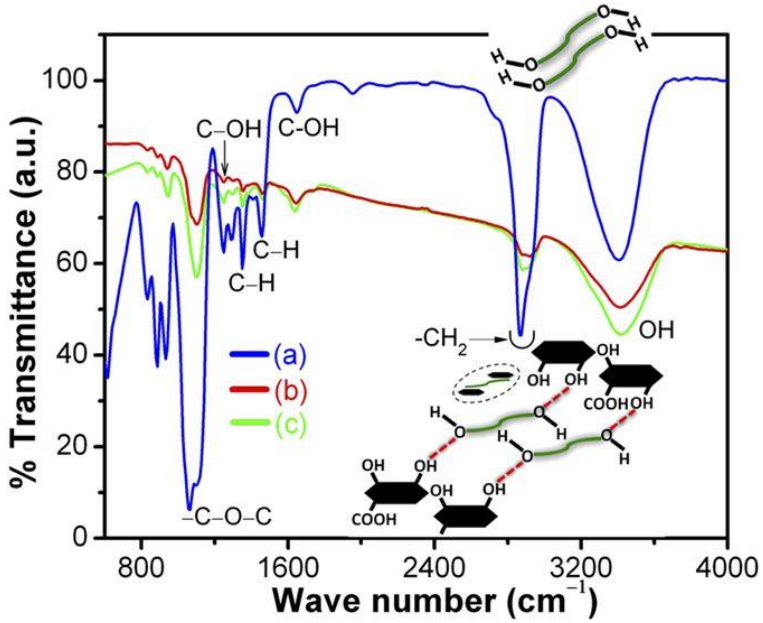
thickness of the sheet. The lattice fringes show interlayer distances of 0.4 nm which belongs to the (002) plane. This is supported by the XRD data showing a diffraction peak at 24.5° 2θ of (002) plane with lattice spacing 0.4 nm (Fig. 1d). The diffraction from (102) plane are observed at 42.45° 2θ and the FWHM of this plane is a measure of lateral dimension of the sheet which is approximately 68 nm. This is well in agreement with high resolution TEM result. In rGO, the D and G bands are observed at 1343 and 1593 cm−1, respectively (Fig. 1e). It is known that the D band originates from the edges and it is attributing to defects27,28. The G band corresponds to the first-order scattering of the E2g mode of sp2 domains present in graphite structure. The relative strength of D band as compared to G band depends strongly on the amount of disorder present in the graphite material. In this case, the intensity ratio I(D)/I(G) in rGO is 1.05 signifying defect and disorder in structure due to the oxygen functionalization. To investigate the chemical composition, the XPS of the rGO is carried out (Fig. 1f). The C 1s spectra is de-convoluted into three chemically shifted components designated as A, B and C at binding energies of 284.4, 286 and 288.6 eV, respectively. Component A is non-oxygenious carbon in C–C/C=C configuration, component B is assigned to carbon atoms bonded to the oxygen in hydroxyl (C–OH) or epoxide (C–O–C) and component C shows a small amount of carbonyl (>C=O) and carboxyl groups (COOH or HO–C=O)29,30,31. The sp2 fraction in rGO is approximately 70% and remaining carbon atoms is sp3 hybridized connected with hydroxyl, epoxy, carbonyl and carboxyl groups. FTIR characterization is unique method for understanding the functionlization of rGO and its interaction with PEG molecules. In PEG, strong band at 2868 and 2932 cm−1 corresponds to –CH2 (antisymmetric) and –CH2 (symmetric) stretching vibration in alkyl chains, respectively, and 1062 cm−1 is assigned to vibration of –C–O–C groups (Fig. 2a). Weak signal of alkyl chains are appeared in rGO-PEG dispersed sample, indicating formation of hydrogen bonding between rGO and PEG molecules (Fig. 2b,c). A strong band at 1651 cm−1 originates from vibration of C-OH group32. These peaks are observed in rGO-PEG dispersed sample and are attributed to coordination between PEG with functionalized rGO through hydrogen bonding. Strong band at 1342 and 1460 cm−1 are attributed to vibrations of C–H group and C–OH vibration at 1245 cm−1 occurs in PEG molecules. These two bands are also exhibited in rGO-PEG sample and could be a combination frequency of CH + OH group. An absorption band of –C–O–C–at 1062 cm−1 is observed in PEG while this peak is also appearing in rGO-PEG indicating cross-linking between PEG and rGO.33 Band at 3407 cm−1 is due to stretching O–H mode of C–OH group in PEG and these bands are also present in functionalized graphene samples. Therefore, shifting of the band and its widening clearly indicate the presence of hydrogen bonding between PEG and functionalized rGO sample33,34. The above results are the clear signature of dispersion of rGO in PEG through hydrogen bonding.

Figure 1: SEM image (a) low resolution TEM of the rGO (b) high resolution TEM of the rGO (c) XRD (d) Raman spectra (e) and C1s of XPS analysis (f).



Full size image

Figure 2: FTIR of (a) PEG200 (b) PEG-rGO, concentration 0.2 mg. mL−1 and (c) PEG-rGO, concentration 1.0 mg. mL−1.



Full size image

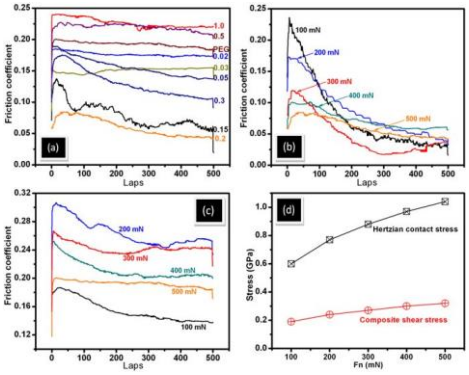
Lubrication properties of rGO additives in PEG

Friction coefficient of dry steel-steel contact is approximately 0.6 (Figure S1) and this value is reduced to 0.2 in neat PEG steel-steel lubricated condition at 500 mN load (Fig. 3a). This value decreased up to 7% using minute concentration 0.02 mg mL−1 of rGO in PEG. The reduction is significant where friction coefficient decreased to 0.06 i.e. 78% less at 0.2 mg mL−1 rGO concentration. The concentration dependent trend of friction values is shown in Figure S2. In addition, wear scar is reduced to almost 50% in 0.2 mg mL−1 rGO concentration as compared to neat PEG (Figure S3). Further, increase in concentration, the friction coefficient increases and becomes 0.22 at 1.0 mg mL −1 of rGO. Wear depth also increases in the same trend as friction coefficient (Figure S2, S3). It is worth to mention that optimized concentration of rGO is not a universal value. It largely depends on physical and chemical properties of the solid-body contact and contact stress. In early report, lowest value of friction coefficient was achieved in 0.03 mg. mL−1 concentration while sliding

between 100Cr6 steel ball and 316LN stainless steel disc15,17. However, concentration dependent trend of friction and wear is observed almost for any conventional additive in the oil or polymer matrix. It is usually determined by change in viscosity at low concentrations and degradation of lubricity at high ones. Here, generally, the viscosity (dynamic and kinematic) of rGO dispersed in PEG200 does not much change with the concentration of rGO additives (Figure S4). Neat PEG (shown by arrow in Figure S4) and PEG with rGO concentration 0.02 mg. mL−1 do not show any changes in viscosity. Further, with increase in concentration up to 0.3 mg. mL−1, the slight increase in viscosity is shown and this is related to good dispersibility of rGO additives (dispersion stability will be shown in later section). However, at higher concentration, the viscosity value is almost saturated, indicating no more chemical dispersion of rGO additives is further possible in PEG. Here, the result indicates that the role of viscosity in friction and wear is not a dominant factor. This is well corroborated by contact angle measurement which also does not change with concentration and slightly varies in the range 53° to 56° (Figure S5). This indicates that balance of rGO polarity is retained in the respect of PEG where concentration does not play a major role. Analogically, the tribologically effective concentration 0.2 mg mL−1 of rGO was selected to analyze load dependent friction stability (Fig. 3b). The trend of friction coefficient vs sliding cycles was more or less similar at all the loading condition while with increase in load, the initial value of friction coefficient decreases. This clearly describes decrease in standard deviation of friction coefficient with increasing load (Figure S6a). This is possibly an indication of (a) alignment of graphene in the contact region and (b) shear induced plastic deformation of surface asperities, leading to contact smoothening. In microscopic scale, a lamellar graphite-like structure is formed with in-plane sp2 bonding and weak interlayer coupling. Thus, the decrease in friction is a result of diminishing and ultimately vanishing interlayer bonds. In this condition, the selforganizing response to shear action and formation of highly ordered and lamellar structure are observed35. The virgin contact surfaces represent rougher asperities (values are given in the characterization section) that plastically deformed during the initial sliding cycles and in this regime, the friction energy is dominated by plastic deformation. At high loads, the rough asperities suppose to break down, suppressing the extent of plastic deformation, attributing to decrease in friction value (Fig. 3b). In the similar experiment, the value of friction coefficient is high in PEG lubricated condition but the trend is similar to the 0.2 mg mL−1 rGO lubricated condition (Fig. 3c). However, at 100 mN load, the friction of PEG lubricated system is lower. Here also, the standard deviation of friction coefficient becomes less at high loads (Figure S6b). It is shown that with increase in load, Hertzian and composite shear stress are increased that help to (a) align the graphene sheets and (b) suppress the plastic deformation of surface asperities (Fig. 3d). The possible reason of such alignment will be discussed below. Graphene sheets may lead to the formation of a boundary tribofilm in the contact and therefore, the lubrication of PEG effectively works. In addition, better alignment of the linear PEG molecules cannot be ignored at high pressure that provides low shear resistance of the sliding plane and therefore, load carrying capacity was improved with decreased wear depth (Figure S7). This is effective both in base oil and rGO dispersed PEG lubricated system which clearly indicates that this property is inherently present

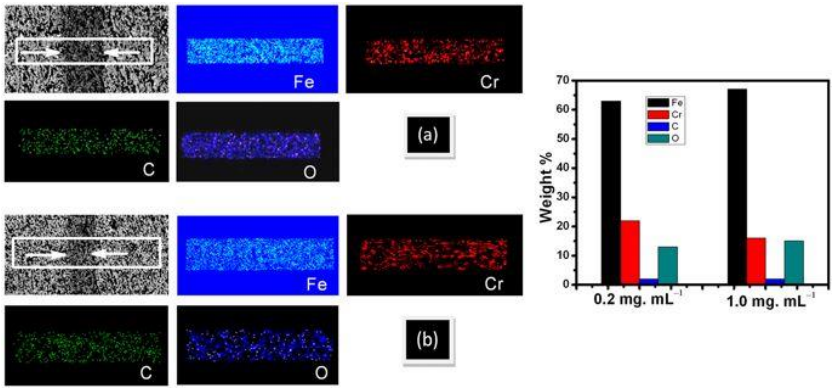
in PEG molecules. In order to explain friction and wear behavior, two wear tracks formed in 0.2 and 1.0 mg mL−1 concentration was used for analysis. For better understanding, these wear tracks will be designated as W1 and W2 respectively. Selection of these tracks is logical because 0.2 mg mL−1 rGO showed lowest value of friction coefficient (0.02) while 1.0 mg mL−1 rGO has shown highest friction value (0.22). In order to confirm the deposition on the wear track, the EDS analysis is performed across the W1 and W2 wear tracks. The motivation behind this analysis was to observe the distribution of carbon concentration in the wear track along with surface region of steel. It is shown that across the steel surface to wear track, there is no difference in carbon concentration (Fig. 4). The average elemental weight % of the mapped region in both the concentration shows negligible amount of C that mostly belong to residual amount of carbon present in T42 HSS steel disc. Signal of carbon is same in selected region, indicating absence of any carbon deposition in the track. The signal of other elements such as Fe, Cr and O is also having uniform distribution in the selected region. For quantitative chemical analysis, the extensive Raman mapping inside the wear track is carried out (Fig. 5). Selected frequency range was used to detect the possible phases like metal-oxide at (a) 600–700 cm−1 (red), D and G band of carbon (Fig. 5b) and (Fig. 5c) at 1300–1400 cm−1 (green) and 1500–1600 (blue), respectively. Superimposed mapping pattern of these phases are represented in (Fig. 5d) of both the figures. In both the wear tracks, D and G bands along with few very weak signal of metal oxide are observed. The individual spectra of the typical features mostly do not show above mentioned characteristic of phases (Figure S8a,b). Such a broad and weak signal of D and G band is signature of elemental carbon inherently present in steel sample. This indicates absence of any physisorbed/chemisorbed graphene/graphite substances in the wear track.

Figure 3: Friction coefficient vs rGO concentration in PEG (a) load dependent friction coefficient of 0.2 mg mL−1 of rGO concentration (b) load dependent friction coefficient of PEG200 (c) and load vs Hertzian contact and composite shear stress (d).



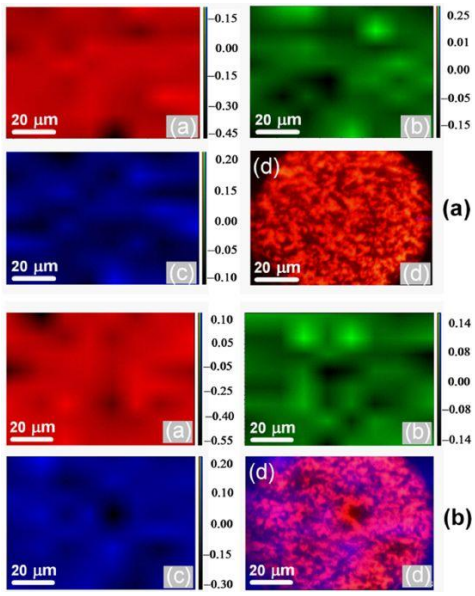
Full size image

Figure 4: EDS mapping across the wear track and weight % of elements at rGO concentration (a) 0.2 and (b) 1.0 mg mL−1, Tribology condition: Load: 500 mN, Linear speed: 0.5 cm/s, Ball: steel (dia. 2 mm).



Full size image

Figure 5: Raman mapping inside the wear track at rGO concentration (a) 0.2 and (b) 1.0 mg mL−1.



Sublevel both in figure (a) and (b) describes: (a) metal oxide (b) D band (c) G band and (d) superimposed mapping pattern of D and G band, the scale in image show intensity. Tribology condition: Load: 500 mN, Linear speed: 0.5 cm/s, Ball: steel (dia. 2 mm).

Full size image

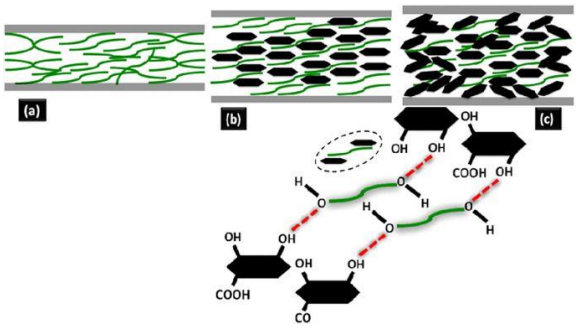
Lubrication mechanism

Several reports showed that the adsorbed graphene/graphite tribofilm formation in the contact plays the key role for the reduction in friction and wear15,16,21,25,36,37. Such reduction was realizable only at optimized concentration of graphene dispersed in the lube15,16,17,25. Also, adsorbed graphite tribofilm was observed at high concentration but it was not participated in the lubrication process17. It is argued that graphene is agglomerated when concentration is high and due to this the weak shear strength of the interlayer sliding plane disrupts. The question arises about the physical reason behind the deposition of graphene in the metallic contact. Primarily, it is useful to take a contact stress in account that possibly helps for deposition. It was shown that rGO dispersed in PEG was found to well deposited in the steel contact in microtribometric test15,17, but here it is unable to deposit in nanotribometric contact where contact stress is higher. It is worth to mention that ball diameter was 6 mm in microtribometric experiment15,17. In this case, the

calculated Hertz stress and shear stress is 0.65 and 0.2 GPa, respectively and these values are well below to stress observed in nanotribometric contact condition where diameter of the ball is 2 mm and applied force 500 mN (Fig. 3d). Therefore, the possibility to deposit the graphene film is higher in high contact stress condition i.e. nanotribometric contact. At high stress, shear ability of graphene sheets enhances due to repulsive Coulomb interaction. Interfacial repulsions can also originate from π orbital interaction between adjacent sheets in graphite, which has been reported to possess superlow friction at large contact stress38,39,40. In addition to contact pressure which is invalid, the deposition of graphene/graphite should be related to plastic deformation of the steel contact which is high in microtribometric test condition. This is shown in the work reported by Gupta et al.17. In this report, the 100Cr6 steel ball, diameter 6 mm and hardness 2.3 GPa was used against 316 LN steel. Plastic deformation releases the high energy and it is useful for the physisorption and chemisorptions of graphene/graphite dispersed PEG molecules. Based on the experimental fact, it is obvious that graphene/graphite deposition is mediated by plastic deformation of the metallic contact17. Mild deformation is observed where scratches, grooves and adhesive failure are insignificant in the wear track of nanotribometric contact (Figure S9). However, linear scratches and grooves are clearly visible in neat PEG contact and at higher concentration rGO-PEG contact. In neat PEG lubrication, boundary film squeezes and does not have sufficient ability to bear the load (Fig. 6(a)). Literature reports mostly argue that lubrication of dispersed graphene/graphite is effective if these substances are deposited in the contact region which easily shears under the action of contact stress15,16,21,25,36,37. However, in the present work, extensive analysis of wear track does not show deposited graphene/graphite substances. In this condition, lubrication can be defined by proposing other relevant model. It is clearly shown in FTIR studies, that rGO is linked with PEG molecules through hydrogen bonding (Fig. 2). Under the contact pressure, the graphene could be aligned along the linear direction of PEG molecules without disturbing the hydrogen bonding linkages which is schematically shown in Fig. 6b. In solid graphene, the lubrication is basically mediated by low shear strength which is acting between the graphene sheets. The structure and morphology of grapehene is stable and shear mechanism is active when rGO is well dispersed in the oil. Undispersed graphene made aggregated particles and shearability is disrupted. The dispersion stability is high in 0.2 mg.mL−1 rGO concentrations, where absorbance decreases marginally with time (Fig. 7a). Digital images were obtained after 240 minutes that clearly shows well dispersed rGO of concentration 0.2 mg.mL−1 in the oil. For a comparison, the shear rate vs shear stress relationship of neat PEG and PEG with 0.2 mg.mL−1 graphene concentration shows a characteristic of definite Newtonian liquid-like behavior (Figure S10). Comparatively, graphene dispersed PEG sample clearly shows less shear stress which could be related to less shear strength of graphene lamella interacting to the PEG molecules. Under the contact pressure, the alignment stability of graphene sheets is mostly controlled by PEG molecules and it may forms stable composite boundary tribofilm of PEG intercalated graphene sheets. Mainly at high contact pressure, the shear mobility of the graphene sheets in lube becomes effective, providing efficient lubrication and load bearing capacity. At higher rGO concentration, the lubrication is ineffective, increasing the

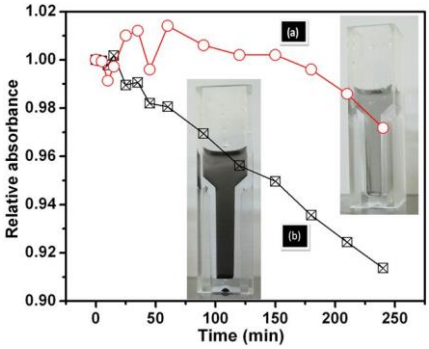
friction and wear adversely, as it is mechanistically presented in Fig. 6c. This could be explained by defining two possible reasons. Firstly, at high concentration, undispersed particles are agglomerated and then losing its alignment. The poor absorbance properties of 1.0 mg mL−1 rGO indicate time dependent agglomeration of the rGO in oil (Fig. 7b). This is a signature of weak dispersion stability and therefore, viscosity does not change much. The TEM analysis shows that at higher concentration of 1.0 mg.mL−1 graphene, the whole region is heavily loaded by graphene flakes and it becomes darker, indicating agglomeration (Fig. 8b). This may interrupt shear mobility between weak interlayer graphene sheets. In this condition, PEG molecules do not participate to form a composite boundary tribofilm lubricant. Secondly, the agglomerated randomly oriented graphene particles physically form the obstacles between the sliding surfaces while intercepting the interfacial sliding. It is worth to mention that composite boundary tribofilm is freely suspended in the contact and do not deposit in metallic contact. However, at concentration 0.2 mg.mL−1, the TEM results show transparent, wrinkled and curly feature which is typical morphology of graphene sheets. Only small region is heavily loaded by graphene as indicated by arrow Figure 8a. This clearly indicates that effective dispersion of graphene need optimized concentration in PEG based lube.

Figure 6: Lubrication mechanism in (a) PEG steel-steel contact (b) 0.2 mg mL−1 rGO-PEG lubricated contact and (c) 1.0 mg mL−1 rGO-PEG lubricated contact.



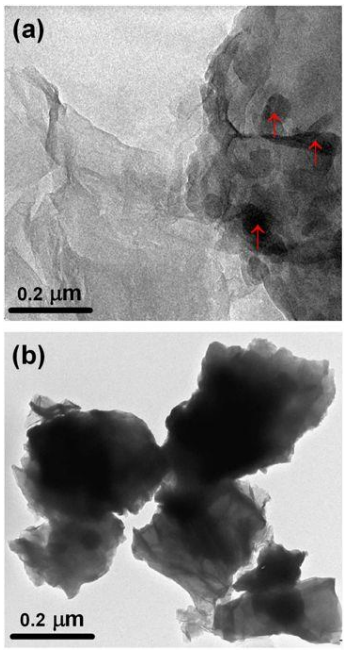
Full size image

Figure 7: Suspension stability of the lubricating oils with rGO concentration (a) 0.2 and (b) 1.0 mg.mL−1 as determined by ultraviolet–visible light (UV– VIS) spectrophotometry.



Full size image

Figure 8: Morphology and dispersion stability of the lubricating oils with rGO concentration (a) 0.2 and (b) 1.0 mg.mL−1 analyzed by TEM.



Full size image

Conclusions

Concentration of rGO additives in the lube is an important aspect for controlling the friction and wear of the lubricated solid contacts. At lower and higher concentration, the lubrication is ineffective, producing higher friction and wear. However, in optimized concentration 0.2 mg.mL−1 of rGO in lube medium showed extremely lower value of friction coefficient 0.06 and wear reduced up to 50% as compared to neat PEG lubricated steel-steel contact. Moreover, at high contact pressure, the energy efficiency of optimized rGO additives is improved. This is related to effective shearing of graphene dispersed in PEG through formation of low shear strength boundary film. It is shown that boundary film in the form of graphene/graphite was not deposited in the contact region. Therefore, an effective lubrication properties are described by freely suspended boundary tribofilm formation of PEG intercalated composite graphene sheets. The graphene sheets are linked with PEG molecules through hydrogen bonding and under the contact stress, low shear strength of interlayer sheets easily slides, providing effective lubrication. The graphene sheets along the PEG molecules become superior at high contact pressure, reducing the friction significantly and more importantly deformation of the wear tracks become negligible.

Method

Synthesis of rGO

Synthesis of GO is based on Hummer's methods followed by its reduction by hydrazine treatment. For the GO synthesis, 3.0 g of graphite powder dispersed in 150 ml of 1M H_2SO_4 at room temperature. Subsequently, 8.0 g of $KMnO_4$ was added in the reaction mixture under room temperature with constant stirring. After 2 hrs of stirring; 90 ml distilled water was slowly added in the reaction mixture followed by heating at 90 °C for 12 hrs. After 12 hrs of heating, 30% H_2O_2 was added in the reaction mixture and allowed for further 2 hrs of stirring. After completion of reaction solid, brownish black precipitated was filtered and washed with 100 ml of 30% HCL and 100 ml of

ethanol. Finally, precipitates were dried under vacuum at 60 °C of temperature. For reduction of GO to rGO, 100 mg of GO was mixed in 30 ml of water and treated with 3 ml hydrazine under efflux condition at 95 °C for 24 hrs. After completion of reaction, reaction mixture was filtered, washed and dried similar to that of GO mentioned above.

Characterizations and analysis

Morphology of rGO was analyzed by scanning electron microscope (SEM) whereas wear track elemental mapping was carried out by energy dispersive X-ray (EDX). High resolution morphology and microstructure of rGO was analyzed by transmission electron microscope (TEM) working in low resolution (LR) and high resolution (HR) mode. Crystallographic details and chemical composition were studied by X-ray diffraction (XRD) using Cu Kα radiation (λ = 0.15418 nm) and X-ray photoelectron spectroscopy (XPS- ULVAC-Phi ESCA1800) coupled monochromatic Mg Kα source (400 W, 1253.6 eV), respectively. Chemical structure of rGO and wear track was mapped locally by micro-Raman spectrometer (Horiba 800) operating in laser wavelength of 514.5 nm. FTIR spectrometer (Bruker Optics), operating in transmission mode with a spectral resolution 4 cm−1 was used for the analysis of functional groups in rGO. For this analysis, rGO was dispersed in PEG200 followed by ultrasonication and processed in dry form. The rGO dispersed PEG200 was used as synthetic lube base oil for tribology evaluation. Neat PEG itself is considered useful for lubricating additives41,42,43. Before the tribology test, the PEG functionalized rGO powder sample was thoroughly dispersed in the PEG medium by ultrasonication process for 1 hour and their dispersion stability was monitored for 4 hours. It was carried out at room temperature and ultrasonic frequency of 25 KHz. The viscosity measurement was carried out by Anton Paar rolling ball viscometer (Lovis 2000 M/ME). Rolling time of ball in the viscous liquid is estimated in accordance to Hoeppler's falling ball principle at room temperature. In each measurement, the 2 ml volume of sample was used. The test was repeated several times and average value is reported. Contact angle measurement was carried out by contact angle meter equipped with CCD camera (Holmarc, HO-IAD-CAM-01, and India). Volume of the water droplet used for contact angle measurement was ~l µL. The measurement was performed at ambient conditions and room temperature. Standard deviations in contact angle measurements were typically ± 1°. The images obtained were analyzed to measure the contact by using the Image J software. The supernatant fluid decanted at specified time intervals to evaluate absorbance using a UV–VIS spectrophotometer. Based on the Lambert–Beer law, the absorbance is proportional to concentration. Therefore, the dispersion stability of rGO in base oil was evaluated by assessing the absorbance. The tribo-evaluation of dispersed graphene was carried out by measuring friction and wear using a ball-on-disc nanotribometer (NTR2, CSM Instrument, Switzerland). A 100Cr6 spherical steel ball with diameter 2 mm and hardness 2.3 GPa was used as a sliding counterbody against the static lubricated high-speed steel (grade T42) disc. This is a wear resistance and high compressive strength material with hardness value 0.7 GPa. This material is useful for machine and industrial application. The chemical composition of 100Cr6 steel ball and T42 grade steel is given in the Table 1. The friction coefficient was determined by a linear variable differential transformer (LVDT) sensor, measuring the deflection in the cantilever spring. The

experiments were carried out with change in rGO concentration in PEG medium. The normal force was varied 50 mN to 500 mN, linear sliding speed 0.5 cm/s, wear track radius of curvature 1 mm. In each tribo-test, 5 ml ultrasonicated rGO was dispersed in PEG lubricant and it was thoroughly lubricated the sliding interfaces. Rheological measurements were carried out at 25 °C on MCR301 using a cone and plate geometry of gap 0.052 mm and diameter 25 mm.

Tribological properties of graphene oxide as a lubricating additive in water and lubricating oils

Hiroshi KINOSHITA, Hideki ONO, Aidil Azli ALIAS, Yuta NISHINA, Masahiro FUJII

Abstract

High-performance lubricating additives are desired in order to improve the properties of lubricating fluids. Recently, carbon nanomaterials such as fullerenes, carbon nanotubes, and carbon onions have been studied as lubricating additives for water and lubricating oils. However, the costs of these carbon nanomaterials are too high for practical use. On the other hand, graphene oxide (GO) is a carbon nanomaterial that consists of single atom thick sheets that possess a large number of oxygen functional groups. Since GO is synthesized from graphite using a chemical liquid process, the cost of GO is significantly lower than other carbon nanomaterials. In this study, the application and tribological properties of GO monolayer sheets as additives in water and poly-alpha olefin (PAO) were investigated. The dependence of the friction coefficient of GO-water dispersions on GO concentration (0.01-1.0 mass %) was investigated. In particular, GO-water dispersions with a concentration of less than 0.1 mass % demonstrated low friction coefficients. In this study, GO was simply dispersed in PAO using surfactant and intermediary solvents without the need for drying treatments. We found that the use of anionic surfactants in the GO-PAO dispersions was better than cationic surfactants in terms of the degree of wear observed. Specifically, GO-PAO dispersions that used an anionic surfactant with a GO concentration of 4 mass % had the smallest wear in this study. Moreover, friction coefficients were not decreased by the addition of GO in PAO. Finally, we found that intermediary solvents did not affect lubrication.

According to many researches, nano based graphene was proven to be the best material used in lubricating fluids as they have better thermal conductivity, friction reducing capability, anti-wear performance and viscosity stability



SOLUTIONS UNLIMITED

Appl. Chem. Eng., Vol. 29, No. 5, October 2018, 533-540
https://doi.org/10.14478/ace.2018.1038

Article

액체 윤활제 첨가제용 알킬 기능화된 산화 그래핀의 합성/분산 및 트라이볼로지적 특성

최진영 · 김용재 · 이창섭†

계명대학교 자연대 화학과

(2018년 4월 3일 접수, 2018년 4월 23일 심사, 2018년 5월 26일 채택)

Synthesis, Dispersion, and Tribological Characteristics of Alkyl Functionalized Graphene Oxide Nanosheets for Oil-based Lubricant Additives

Jin-Yeong Choe, Yong-Jae Kim, and Chang-Seop Lee†

Department of Chemistry, Keimyung University, Daegu 42601, Korea
(Received April 3, 2018; Revised April 23, 2018; Accepted May 26, 2018)

한국공업화학회
THE KOREAN SOCIETY OF INDUSTRIAL AND ENGINEERING CHEMISTRY

SOLUTIONS UNLIMITED

Appl. Chem. Eng., Vol. 29, No. 5, October 2018, 533-540
https://doi.org/10.14478/ace.2018.1038

Article

액체 윤활제 첨가제용 알킬 기능화된 산화 그래핀의 합성/분산 및 트라이볼로지적 특성

최진영 · 김용재 · 이창섭†

계명대학교 자연대 화학과

(2018년 4월 3일 접수, 2018년 4월 23일 심사, 2018년 5월 26일 채택)

Synthesis, Dispersion, and Tribological Characteristics of Alkyl Functionalized Graphene Oxide Nanosheets for Oil-based Lubricant Additives

Jin-Yeong Choe, Yong-Jae Kim, and Chang-Seop Lee†

Department of Chemistry, Keimyung University, Daegu 42601, Korea
(Received April 3, 2018; Revised April 23, 2018; Accepted May 26, 2018)

초 록

그래핀은 표면 에너지가 낮고 원자단위의 얇은 물질로서 다양한 소재의 표면에 코팅시키거나 윤활제에 분산시켜 접착력과 마찰을 줄여주는 우수한 윤활유 첨가제로 보고되고 있다. 본 연구에서는 산화 그래핀 나노시트를 세 가지 종류의 염화알킬(butyl chloride, octyl chloride 및 tetradecyl chloride)을 이용하여 액체 윤활제 첨가제용 기능화 산화 그래핀(alkyl functionalized GO, FGO)을 제조하였다. 제조한 기능화 산화 그래핀의 화학적 및 구조적 특성은 Fourier transform infrared (FT-IR), X-ray photoelectron spectroscopy (XPS), X-ray diffraction (XRD), Raman spectroscopy, scanning electron microscope (SEM), and transmission electron microscope (TEM)으로 분석하였다. 제조한 기능화 산화 그래핀은 PAO-0W40 오일에 0.02 wt%의 농도로 분산시켰으며, 트라이볼로지적 특성을 high frequency friction/wear tester로 분석한 결과, FGO-14이 첨가된 PAO-0W40 오일은 ball-on-disk의 직선왕복운동 하에서 기유에 비해 ~5.88%의 마찰계수와 ~3.8%의 마모 트랙 폭을 감소시킴으로써 내마모성이 향상됨을 확인하였다. 본 연구에서는 산화 그래핀의 성공적인 기능화와 더불어 다양한 탄화수소사슬 길이에 따른 분산 안정성 및 트라이볼로지적 특성의 향상을 입증하였다.

Abstract

Graphene has been reported to be an excellent lubricant additive that reduces friction and wear when coated on the surface of various materials or when dispersed in lubricants as an atomic thin material with the low surface energy. In this study, alkyl functionalized graphene oxide (FGO) nanosheets for oil-based lubricant additives were prepared by using three types of alkyl chloride chemicals (butyl chloride, octyl chloride, and tetradecyl chloride). The chemical and structural properties of the synthesized FGOs were analyzed by Fourier transform infrared (FT-IR), X-ray photoelectron spectroscopy (XPS), X-ray diffraction (XRD), Raman spectroscopy, scanning electron microscope (SEM), and transmission electron microscope (TEM). The synthesized FGOs were dispersed at 0.02 wt% in PAO-0W40 oil and its tribological characteristics were investigated using a high frequency friction/wear tester. The friction coefficient and the wear track width of poly alpha olefin (PAO) oil added with FGO-14 were tested by a ball-on-disk method, and the measured results were reduced by ~5.88 and ~3.8%, respectively compared with those of the conventional PAO oil. Thus, it was found that the wear resistance of PAO oil was improved. In this study, we demonstrated the successful functionalization of GO as well as the improvement of dispersion stability and tribological characteristics of FGOs based on various alkyl chain lengths.

Keywords: *Graphene oxide, Functionalization, Lubrication, Tribology, Additive*

1. Introduction

Friction and wear are very common in daily life and cause energy waste, material loss, and shorter life span of machines. The most effective way to reduce friction and wear is to apply an appropriate lubricant in the contact surfaces. Lubrication effectively controls production facility systems and greatly affects the efficiency of products, the life extension of the machinery, and the stability of the facility system. Therefore, the development of new lubricants has been attracting considerable attention in an attempt to minimize friction coefficients and amount of wear of machinery. Such development is very

† Corresponding Author: Keimyung University,
Department of Chemistry, Daegu 42601, Korea
Tel: +82-53-580-5192 e-mail: surfkm@kmu.ac.kr

pISSN: 1225-0112 eISSN: 2288-4505 @ 2018 The Korean Society of Industrial and Engineering Chemistry. All rights reserved.

SOLUTIONS UNLIMITED

important for the sustainable future of machinery[1-3].

Materials such as graphite, molybdenum disulfide (MoS_2), tungsten disulfide (WS_2), and hexagonal-boron nitride (h-BN) have a layered structure and have shown tremendous potential as solid lubricants. However, they have limitations caused by poor dispersibility as liquid lubricant additives[4-6]. Since graphene with a single layer was discovered in 2004, thin two-dimensional (2D) materials have been developed[7]. In comparison with bulk materials, very thin materials have many beneficial characteristics and potential applications in various fields. These materials have attracted considerable attention in tribological research[8]. Graphene, which is a carbon nanosheet with a sp^2 hybrid structure, exhibits strong mechanical strength and has high thermal conductivity and thermal properties which are notable in the lubrication industry[9]. In addition, it is a very thin material with the carbon-carbon bond length of 0.142 nm and plane spacing of 0.335 nm. It also has excellent friction characteristics and wear resistance when mixed with a liquid lubricant.

In general, multi-layer graphene is known to have lower friction than single-layer graphene. The tribological characteristics of multi-layer graphene are attributed to anisotropic bonding. The atoms of the basal plane have strong covalent bonds, but have weak van der Waals bonds between basal layers. Due to these weak van der Waals bonds, they are easily separated from each other even at low shear forces, resulting in tribological effects[10].

Graphene can be prepared by mechanical method, chemical method, epitaxial growth method, and chemical vapor deposition. Among these methods, chemical method using graphene oxide (GO) as a precursor is effective for the mass production of graphene, and is advantageous for the graphene preparation process using organic solvents[11]. GO has large numbers of oxygen functional groups on graphene sheets. Large numbers of epoxide groups and hydroxyl groups are mainly distributed on the basal plane of GO. Carbonyl and carboxyl groups are attached to the edge of GO[12]. On the other hand, various methods have been proposed to enhance the physical properties of GO by its reduction, because it is difficult to apply GO to hydrophobic organic solvents due to the large numbers of oxygen functional groups and the remarkably poor physical properties. To solve this problem, many attempts have been made to transform graphene into covalent bonds or noncovalent bonds[13]. Zhang et al. showed that the friction coefficient and wear were reduced by 17% and 14%, respectively, when oleic acid modified graphene was used as a lubricant additive[14]. Mungse et al. improved the dispersion stability of lube oil and effectively reduced the friction coefficient and wear through functionalization of octadecylamine (ODA) on the basal plane of GO. They demonstrated that long-term dispersion stability caused by van der Waals interactions between the alkyl chain of alkylamine and the alkyl chain of the lube oil is very important for the efficient performance of tribological characteristics[15].

In this study, we have functionalized GO nanosheets with hydrocarbon chains using the various alkyl chlorides and investigated the structure, dispersion stability, and tribological characteristics of the graphene nanosheets depending on the various alkyl chain lengths via the various spectroscopic and ball-on-disk techniques.

2. Experimental

2.1. Preparation of NH_2-GO

0.25 g of GO (Angstron Materials: N002-PS, 0.25 wt%) was mixed with 100 mL of ethanol to prepare a dispersion solution. After 3 mL of ethylenediamine (0.044 mol) was added to the GO dispersion, NH_2-GO was obtained by performing a reflux reaction at 75 ℃ for 16 h. And NH_2-GO was then sufficiently filtered and washed with enough amount of ethanol, and then dried at 60 ℃ for 24 h.

2.2. Preparation of Alkyl functionalized GO

The dispersion was prepared by mixing 0.25 g of NH_2-GO with 100 mL of distilled water. Another dispersion was prepared by mixing 0.5 mL of butyl chloride (0.5 wt%) with 100 mL of ethanol. After the butyl chloride dispersion was slowly added to the NH_2-GO dispersion, the reflux reaction was carried out at 80 ℃ for 24 h. Butyl functionalized GO (FGO-4) was then sufficiently filtered and washed with enough amount of ethanol, and then dried at 60 ℃ for 24 h. FGO-8 and FGO-14 were also prepared using octyl chloride and tetradecyl chloride according to the above method.

2.3. Chemical and structural analysis

Fourier transform-infrared (FT-IR, Vertex-80/Hyperion-3000) spectroscopy was used to investigate the functional groups present in the samples. The binding energies of the atoms in each sample were measured and compared using X-ray photoelectron spectroscopy (XPS, Thermo Fisher Scientific, Multilab-2000). The crystal structures of the samples were analyzed using X-ray diffraction (XRD, Ultima IV) and Raman spectroscopy (Horiba Jobin-Yvon, LabRam HR). The morphology and structure of the samples were examined using scanning electron microscope (SEM, Hitachi, S-4800) and transmission electron microscope (TEM, JEM-2100F).

2.4. Tribological Characteristics

In this study, the tribological characteristics of the friction coefficient and wear of the prepared samples were examined using a high frequency friction/wear tester (TE 77 AUTO). The reciprocating ball-on-disk method was used for the test. Bearing steel SUJ2 (Ø = 10 and HRC: 60~63) was used as the material for the ball and disk. Figure 1 shows a schematic diagram of ball-on-disk testing in which the steel disk is pressed by a steel ball with the reciprocating motion under rubbing condition. PAO-0W40 engine oil (poly alpha olefin, GS Caltex Corporation) was used as a base lubricant. The FGO was dispersed into PAO-0W40 oil through ultrasonication treatment for 1,800 s. The concentration of the dispersion in which the FGO was added in PAO-0W40 oil was 0.02 wt%. The ball and disk were ultrasonically cleaned with acetone before testing their friction characteristics. Then, 10 mL of lubricant was poured into a bath placed between the ball and disk. The tribological tester was run at a reciprocation frequency of 10 Hz and a load of 50 N for 360 s. During the test, the disk was fixed

SOLUTIONS UNLIMITED

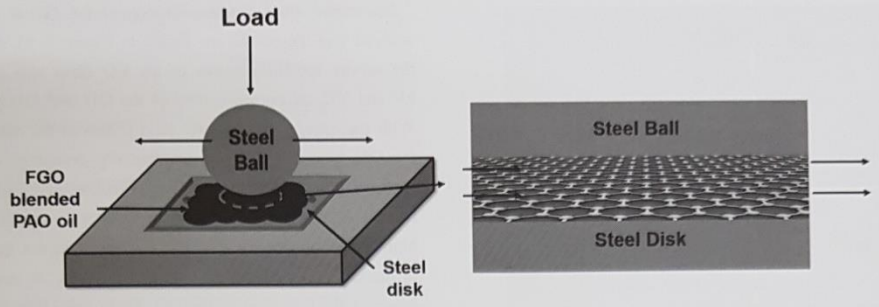


Figure 1. Schematic diagram of ball-on-disk testing under rubbing condition.

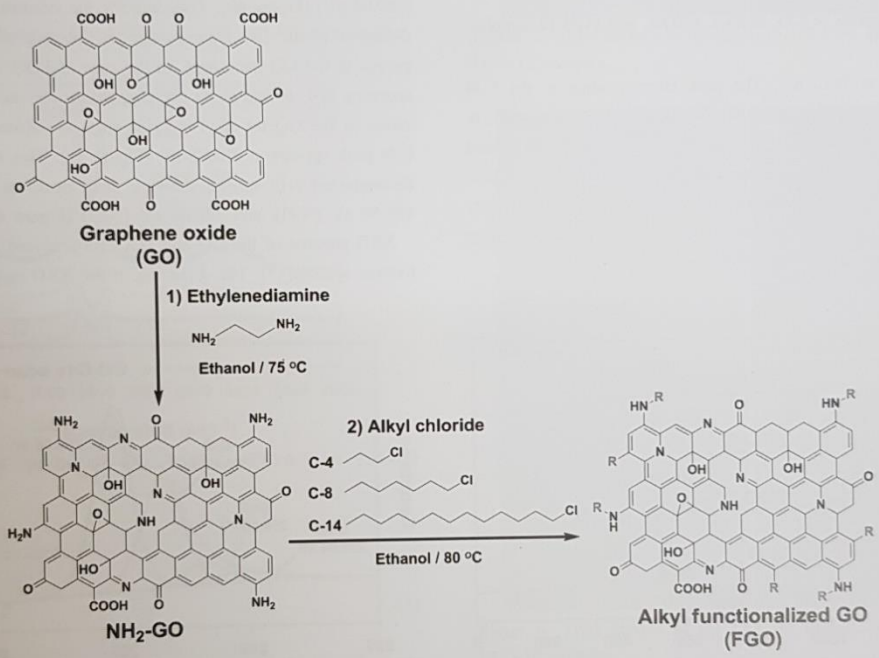


Figure 2. Synthesis process of alkyl functionalized GO (FGO).

to the bottom of the measuring device and the disk was pressed by the ball through the reciprocating motion. A new ball and disk were used for each test. After the test, the disk was ultrasonically cleaned with acetone in order to observe the surface condition. Morphological characteristics of wear track were observed using an optical microscope (Nikon Eclipse Ni-U).

3. Results and Discussion

In this study, alkyl functionalized GO synthesis was carried out in a two-step reaction. In the first step, an amide bond was formed between the carboxyl groups distributed on the edge of GO and the -NH_2 groups of ethylenediamine. In the second step, Cl acted as a good leaving group between NH_2-GO prepared in the first step and alkyl chloride, followed by the formation of N-R bond. This alkyl functionalized GO reaction consists of the strong two-step nucleophilic substitution reaction. Figure 2 shows a schematic diagram of the synthesis and preparation steps of the GO nanosheets in which alkyl chloride is introduced.

FT-IR spectra analysis of the synthesized samples provides direct evidence of the functionalization of GO because it presents information on the functional groups present in the sample[16]. The FT-IR spectra of the GO and FGOs are shown in Figure 3. As shown in Figure 3, the spectrum of the GO exhibits a wide range of typical peaks related to the hydroxyl groups at 3,244~3,777 cm^{-1}, 1,725 cm^{-1} corresponds to the carboxyl groups and 1,588 cm^{-1} corresponds to the aromatic ring, C = C. 1,042 cm^{-1} and 1,113 cm^{-1} correspond to the epoxide groups. Therefore, the FT-IR spectra confirm that the oxygen functional groups are present in GO. For the FGO samples in which the surface of the GO nanosheets is functionalized with alkyl chloride, the

SOLUTIONS UNLIMITED

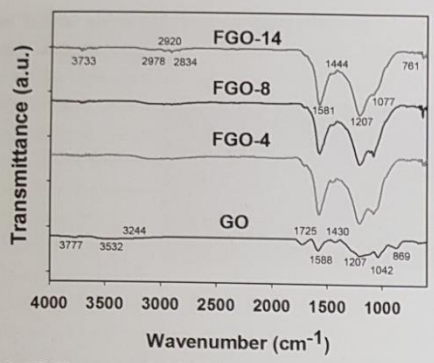


Figure 3. FT-IR spectra of GO, FGO-4, FGO-8, and FGO-14 samples.

peak is observed at 761 cm^{-1}. The peak corresponding to the C-H stretching vibration of alkyl chain is observed at 2,834-2,978 cm^{-1}. In the FGO samples, the peak at 1,581 cm^{-1} corresponds to the N-H band and represents the successful amination of the GO. After functionalization of the GO, the bands corresponding to the carboxyl and epoxide at 1,725 cm^{-1} and 1,042 cm^{-1} are attenuated. A new peak representing the formation of the N-H band appears at 1,581 cm^{-1}.

Successful alkyl functionalization of the GO is confirmed by XPS analysis and the results are shown in Figure 4. As shown in Figure 4a, the survey spectrum results of the GO show two strong peaks at 287 eV and 532 eV corresponding to the C1s and O1s peaks, respectively. With the introduction of long alkyl chains in the nanosheets of the GO, the O1s peak (532 eV) is substantially decreased, while the intensity of the C1s peak (280 eV) is significantly increased. In addition, successful functionalization shows a new peak of N1s at 399 eV. The high-resolution spectra of C1s, O1s, and N1s are measured. C1s scans of the GO and FGO-14 are shown in Figures. 4b and 4c. The deconvolution of the C1s scan of the GO shows four main peaks corresponding to C-C (284.64 eV), C-O (284.48 eV), C=O (288.08 eV), and COO (289.04 eV) (Figure 4b). They indicate the substantially high degree of oxidation of the GO representing the presence of oxygen functional groups in the GO nanosheet. In the case of FGO-14, the peaks corresponding to C-O and COO decrease drastically due to the functionalization of the GO by alkyl chloride such as tetradecyl chloride, and a C-N peak appears at 285.88 eV (Figure 4c). This is confirmed by the deconvoluted N1s spectra showing three peaks at 399.49 eV (C-N), 400.50 eV (N-H), and 398.68 eV (N-O) (Figure 4d).

XRD patterns of the GO and FGO are analyzed to calculate the interlayer spacing[15]. The d-spacing of the XRD patterns can be calcu-

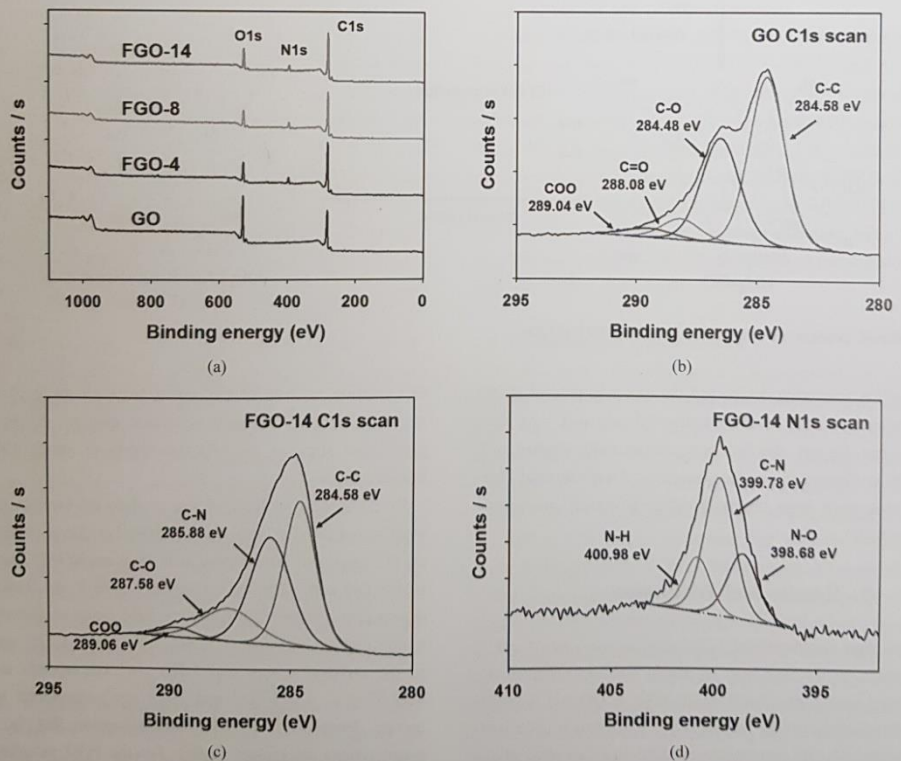


Figure 4. XPS spectra of (a) survey scan, (b) GO C1s scan, (c) FGO-14 C1s, and (d) FGO-14 N1s scan.

SOLUTIONS UNLIMITED

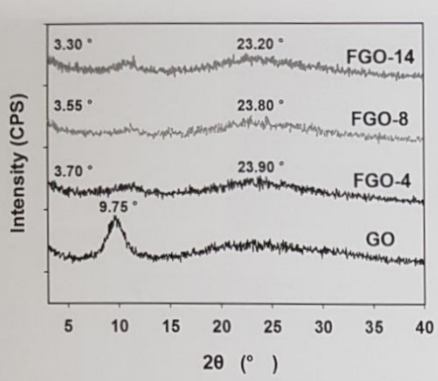
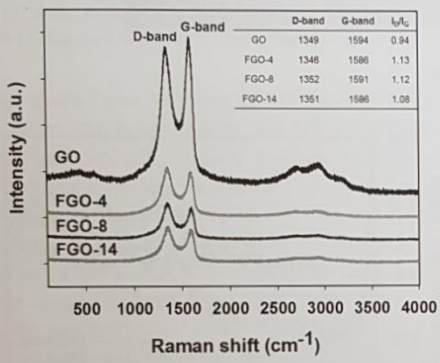


Figure 5. XRD patterns of GO, FGO-4, FGO-8, and FGO-14 samples.



	D-band	G-band	I_D/I_G
GO	1349	1594	0.94
FGO-4	1346	1586	1.13
FGO-8	1352	1591	1.12
FGO-14	1351	1586	1.08

Figure 6. Raman spectra of GO, FGO-4, FGO-8, and FGO-14 samples.

lated by Bragg's equation (1).

$$n\lambda = 2d \sin \theta \quad (1)$$

where λ is the wavelength of the characteristic x-rays, θ is the x-ray incidence angle, and d is the lattice interplanar spacing of the crystal. As shown in Figure 5, the GO shows the diffraction peak at $2\theta = 9.75°$ and the corresponding d-spacing is 0.91 nm[17]. Graphite has only one diffraction peak near $2\theta = 26.4°$ and its d-spacing is about 0.334 nm[16]. The interlayer distance of the GO is higher than that of graphite, because oxygen functional groups exist in the basal plane and edge. The introduction of long alkyl chains to the graphene interlayer reduces the degree of graphite crystallinity, lowering the main diffraction peak. FGO-4, FGO-8, and FGO-14 exhibited broad peaks at $2\theta = 3.70°$, 3.50°, and 3.30°, respectively. The d-spacing between the FGO-4, FGO-8, and FGO-14 nanosheets was 2.39 nm, 2.49 nm, and 2.67 nm, respectively. This was higher than 0.91 nm of GO d-spacing due to the successful functionalization of alkyl chloride. At the same time, the XRD pattern of the FGO shows a new peak at 2θ = 23-24°, which approaches closer to the diffraction peak of graphite ($2\theta = 26°$). This is caused by the formation of disordered graphene nanosheets which are rearranged due to the reduction of the oxygen

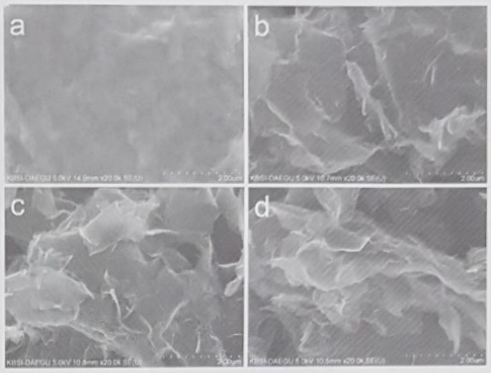


Figure 7. SEM images of (a) GO, (b) FGO-4, (c) FGO-8, and (d) FGO-14 samples.

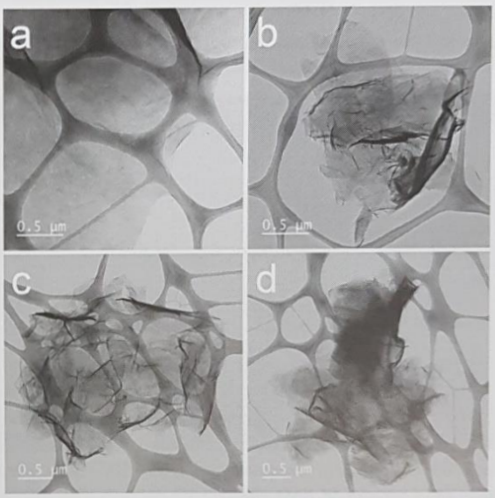


Figure 8. TEM images of (a) GO, (b) FGO-4, (c) FGO-8, and (d) FGO-14 samples.

functional groups on the GO nanosheets[18].

Most of carbon-based materials have various nanostructures such as diamond, graphite, carbon nanotube (CNT), and graphene depending on the carbon allotropes. Carbon nanostructures are composed of C-C bonds with different orientations. Raman spectrum is a powerful means of characterizing the degree of graphite of these carbon-based materials [19]. The Raman spectra of the GO and FGOs are shown in Figure 6. The D-band at 1,349 cm^{-1} in the GO nanosheets corresponds to sp^3-hybridized carbon or a structural defect, and G-band at 1,349 cm^{-1} corresponds to planar sp^2-hybridized carbon. The relative intensity ratio (ID/IG) of the D and G bands has been known to depend on the structural characteristics of carbon[20]. The G-band of the functionalized FGOs is red-shifted due to the reduction of the oxygen functional groups on the GO nanosheets in comparison with the conventional GO[21]. FGOs approach closer to the G-band (1,579 cm^{-1}) of typical graphite than the GO, which implies the restoration of the sp^2 network.

SOLUTIONS UNLIMITED

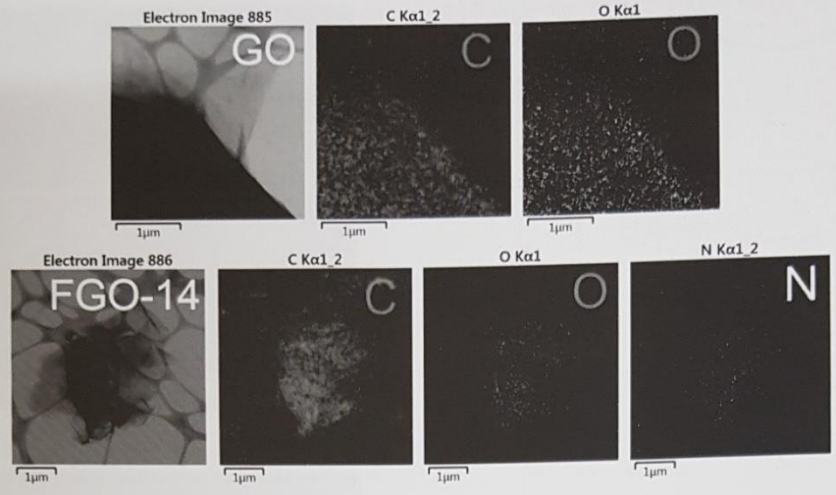


Figure 9. Elemental mapping results of TEM images for GO and FGO-14 sample.

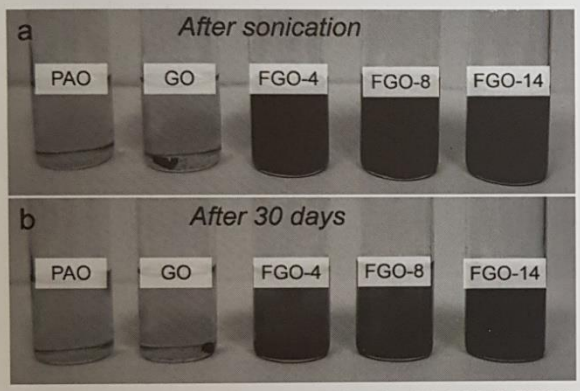


Figure 10. Test results of dispersion stability for GO, FGO-4, FGO-8, and FGO-14 samples in PAO oil.

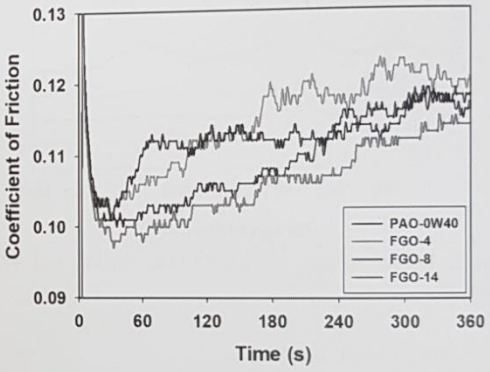


Figure 11. Friction coefficients of PAO oil and FGO-4, FGO-8, and FGO-14 samples dispersed in PAO oil.

The intensity ratio (I_D/I_G) of the GO and FGO-4, FGO-8, and FGO-14 are 0.94, 1.13, 1.12, and 1.08, respectively. This indicates that the I_D/I_G is slightly increased after the functionalization of GO. These changes demonstrate that amorphous carbon is formed with reduced regularity as long alkyl chains increase the spacing of the nanosheets[22].

In tribological applications, nanostructured materials must be completely dispersed in lubricants to ensure efficient lubrication. In this context, the surface characteristics of the nanomaterials are important parameters that control their dispersibility when applied to lubricants [23]. Figure 7 and Figure 8 show SEM and TEM images, respectively, of the surface morphology and characteristics of the GO and FGOs. As shown in Figure 7 and Figure 8, the conventional GO (Figure 7a and Figure 8a) has a similar morphology to a flat sheet with a smooth surface in comparison with the FGOs (Figures 7b-7d and Figures 8b-8d). However, after the introduction of long alkyl chains to the GO, the FGOs show crumpled sheets with wrinkles and some folded areas in random orientations resembling crumpled paper. This indicates that long alkyl chloride chains have been successfully introduced to the GO surface indicated by the thick area which becomes more crumpled and rougher with the longer alkyl chloride chains.

Figure 9 shows the elemental mapping results of TEM images for the GO and FGO-14. The results of elemental mapping for the GO show abundant oxygen and carbon. This indicates the oxygen functional groups present on the GO nanosheets. On the other hand, the results of elemental mapping for the FGO-14 functionalized with long alkyl chains show that nitrogen appears due to the reduction of oxygen functional groups on the existing GO nanosheets and successful amination. Thus, as a result of the elemental mapping, it has been confirmed that the two-step synthetic reaction was successfully performed in this study.

GO is not mixed with PAO oil, but the FGOs nanosheets are mixed with PAO oil and are then ultrasonically treated. These samples are carefully observed for 1 month. As analyzed by FTIR and XPS, the FGOs could be dispersed in the PAO lubricant due to the presence of

SOLUTIONS UNLIMITED

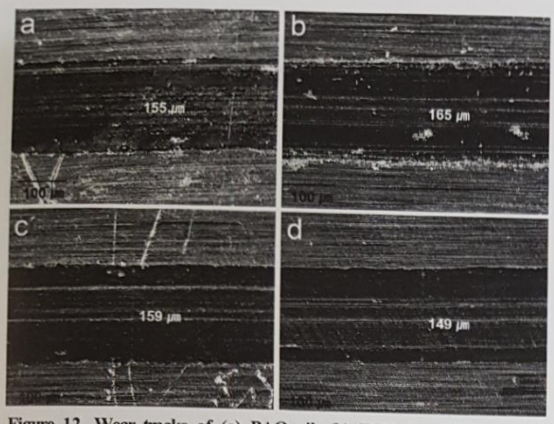


Figure 12. Wear tracks of (a) PAO oil, (b) FGO-4, (c) FGO-8, and (d) FGO-14 dispersed in PAO oil, after tested by ball-on-disk method.

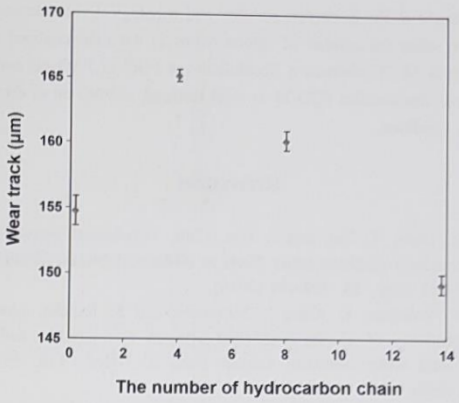


Figure 13. Distributions of wear tracks of PAO oil and FGOs with the various numbers of hydrocarbon chain.

long alkyl chains. Figure 10 shows the test results of the dispersion stability of the GO, FGO-4, FGO-8, and FGO-14 in PAO oil. As shown in Figure 10b, after ultrasonic treatment, the FGO-4, FGO-8, and FGO-14 are successfully dispersed in PAO oil, but only FGO-14 shows a very stable dispersion status after 30 days. The long-term dispersion stability of the FGO-14 is caused by the introduction of hydrophobicity to the GO as well as the high specific surface area of the FGOs like crumpled paper[24]. Thus, as the van der Waals interactions between the tetradecyl chains of the FGO-14 and the alkyl chain of PAO oil increased, these nanosheets are fully dispersed and long-term dispersion stability is provided.

The tribological characteristics of the FGOs mixed with lubricant additives are analyzed under ball-on-disk rubbing for 360 s at a reciprocation frequency of 10 Hz and a load of 50 N. Figure 11 shows the changes of the friction coefficient of the FGOs depending on the length of various alkyl chains and conventional base lubricant. In comparison with PAO-0W40 oil, the friction coefficient of the FGO-4 and FGO-8 is increased by ~34.48% and ~9.70%, respectively, but the friction coefficient of the FGO-14 is decreased by ~5.88%. In the case of FGO-4 and FGO-8, the increases in the friction coefficient are caused by their poor dispersion stability. In the case of FGO-14, the tribological characteristics and wear resistance are improved. GO is a type of nanosheet material similar to a smooth plate and tends to aggregate due to strong van der Waals interactions between the layers. However, the FGOs functionalized with long alkyl chains is a type of nanosheet material similar to crumpled paper and maintains excellent mechanical strength of the existing graphene while reducing the aggregation between layers due to high specific surface area. Thus, the mechanism of a reinforced nano bearing could improve the tribological characteristics[25].

Figure 12 shows images of the wear track of the steel disk lubricated with base lubricant and the FGOs blended lubricants acquired by the optical microscope. As shown in Figure 12, the width of the wear track of the lubricants added with the PAO oil and FGOs are ~155 μm and ~165 μm, ~159 μm and ~149 μm, respectively. As mentioned above, the FGO-4 and FGO-8 have poor dispersion stability which decreases their tribological characteristics, resulting in increases in the width of the wear track in comparison with that of base lubricants. On the other hand, the width of the wear track of FGO-14 is decreased by ~3.8%. The decrease in the which of the wear track could be caused by the improvement in the wear resistance of the steel disk due to the morphology of the FGO-14, like crumpled paper, which reduces the friction. Figure 13 shows the distributions of wear tracks of PAO and FGOs with the various numbers of hydrocarbon chain.

4. Conclusions

FGOs are functionalized on the surface of the GO by introducing alkyl chloride with various alkyl chain lengths. From the results of the FT-IR and XPS analyses, the introduction of long alkyl chains and appearance of C-N bonds are found together with the decreases in the oxygen functional groups of the GO. The results of XRD and Raman spectra analyses show that the structure of the FGO is characterized by wider interlayer spacing and the formation of amorphous carbon of disordered SP^2. In addition, SEM and TEM images show that the FGOs have a morphology like crumpled paper after functionalization. The results of the friction test show that the FGO-14 has a reduced friction coefficient of ~5.88% and a width of wear track of ~3.8% under the rubbing action of the ball-on-disk in comparison with those of the existing PAO oil, even when the concentration is as low as 0.02 wt%. Thus, the wear resistance of the PAO oil has been found to be improved. The van der Waals interactions between the tetradecyl chain of FGO-14 and the alkyl chain of the lubricant have provided long-term stable dispersion in the lubricant, which has been proved to be very important for the efficient friction wear performance. In this study, we confirm the successful functionalization of GO and the dispersion stability and tribological characteristics depending on various alkyl chain lengths. In particular, it has been proved that the most im-

SOLUTIONS UNLIMITED

provement in the dispersion stability and tribological characteristics is shown when the number of carbon atoms in the functionalized alkyl chains is 14. It enhances a lipophilicity of FGO in PAO oil and enables to functionalize FGO-14 as solid lubricant in PAO oil to the optimum condition.

References

1. Z. Chen, Y. Liu, and J. Luo, Chin. Tribological properties of few-layer graphene oxide sheets as oil-based lubricant additives, *J. Mech. Eng.*, **29**, 439-444 (2016).
2. T. Yokohata, K. Kato, T. Miyamoto, and R. Kaneko, Load-dependency of friction coefficient between silicon-oxides and diamond under ultra-low contact load, *J. Tribol.*, **120**, 503-509 (1998).
3. K. Holmberg, P. Andersson, and A. Erdemir, Global energy consumption due to friction in passenger cars, *Tribol. Int.*, **47**, 221-234 (2012).
4. O. Tevet, P. Von-Huth, R. Popovitz-Biro, R. Rosentsveig, H. D. Wagner, and R. Tenne, Friction mechanism of individual multilayered nanoparticles, *Proc. Natl. Acad. Sci. U.S.A.*, **108**, 19901-19906 (2011).
5. Y. Tian, Z. Li, W. Gao, K. Cai, F. Wang, D. Zhang, and S. Fatikow, Mechanical properties investigation of monolayer h-BN sheet under in-plane shear displacement using molecular dynamics simulations, *J. Appl. Phys.*, **115**, 14308-14330 (2014).
6. M. Chhowalla and G. A. Amaratunga, Thin films of fullerene-like MoS_2 nanoparticles with ultra-low friction and wear, *Nature*, **407**, 164-167 (2000).
7. A. K. Geim and K. S. Novoselov, The rise of grapheme, *Nature Mater.*, **6**, 183-191 (2007).
8. D. Berman, A. Erdemir, and A. V. Surmant, Graphene: A new emerging lubricant, *Mater. Today*, **17**, 31-42 (2014).
9. K. S. Kim, H. J. Lee, C. Lee, S. K. Lee, H. Jang, J. H. Ahn, J. H. Kim, and H. J. Lee, Chemical vapor deposition-grown graphene: the thinnest solid lubricant, *ACS Nano*, **5**, 5107-5114 (2011).
10. S. B. Rho, H. Lee, and K. H. Son, Studies on solid inflammable lubricants for refractory slates, *J. Korea Acad. Ind. Coop. Soc.*, **16**, 2308-2313 (2015).
11. H. Chen, L. Xiao, Y. Xu, X. Zeng, and Z. B. Ye, A novel nano-drag reducer for low permeability reservoir water flooding: Long-chain alkylamines modified graphene oxide, *J. Nanomater.*, **2016**, 8716257-8716265 (2016).
12. W. S. Ma, J. Li, B. J. Deng, and X. S. Zhao, Preparation and characterization of long-chain alkyl silane-functionalized graphene film, *J. Mater. Sci.*, **48**, 156-161 (2013).
13. S. H. Lee, J. M. Yun, J. Kwon, and S. O. Kim, Tailored assembly of graphene from solvent dispersion, *Polym. Sci. Technol.*, **22**, 130-136 (2011).
14. W. Zhang, M. Zhou, H. Zhu, Y. Tian, K. Wang, J. Wei, and D. Wu, Tribological properties of oleic acid-modified graphene as lubricant oil additives, *J. Phys. D*, **44**, 205303-205306 (2011).
15. H. P. Mungse, N. Kumar, and O. P. Khatri, Synthesis, dispersion and lubrication potential of basal plane functionalized alkylated graphene nanosheets, *RSC Adv.*, **5**, 25565-25571 (2015).
16. N. A. Daud, B. W. Chieng, N. A. Ibrahim, and Z. A. Talib, Synthesis and characterisation of functionalised-graphene oxide by gamma-ray irradiation, *J. Eng. Sci.*, **13**, 1-17 (2017).
17. S. Arunvisut, S. Phummanee, and A. Somwangthanaroj, Effect of clay on mechanical and gas barrier properties of blown film LDPE/clay nanocomposites, *J. Appl. Polym. Sci.*, **106**, 2210-2217 (2007).
18. J. Jang, V. H. Pham, B. Rajagopalan, S. H. Hur, and J. S. Chung, Effects of the alkylamine functionalization of graphene oxide on the properties of polystyrene nanocomposites, *J. Colloid Interface Sci.*, **424**, 62-66 (2014).
19. S. H. Ryu and A. M. Shanmugharaj, Influence of long-chain alkylamine-modified graphene oxide on the crystallization, mechanical and electrical properties of isotactic polypropylene nanocomposites, *Chem. Eng. J.*, **244**, 552-560 (2014).
20. W. Sun, R. Hu, M. Zhang, J. Liu, and M. Zhu, Binding of carbon coated nano-silicon in graphene sheets by wet ballmilling and pyrolysis as high performance anodes for lithium-ion batteries, *J. Power Sources.*, **318**, 113-120 (2016).
21. S. Stankovich, D. A. Dikin, R. D. Piner, K. A. Kohlhaas, A. Kleinhammes, Y. Jia, and R. S. Ruoff, Synthesis of graphene-based nanosheets via chemical reduction of exfoliated graphite oxide, *Carbon*, **45**, 1558-1565 (2007).
22. A. C. Ferrari and J. Robertson, Interpretation of Raman spectra of disordered and amorphous carbon, *Phys. Rev. B*, **61**, 14095-14107 (2000).
23. R. Gusain and O. P. Khatri, Ultrasound assisted shape regulation of CuO nanorods in ionic liquids and their use as energy efficient lubricant additives, *J. Mater. Chem. A*, **1**, 5612-5619 (2013).
24. J. Luo, H. D. Jang, T. Sun, L. Xiao, Z. He, A. P. Katsoulidis, and J. Huang, Compression and aggregation-resistant particles of crumpled soft sheets, *ACS Nano*, **5**, 8943-8949 (2011).
25. X. Dou, A. R. Koltonow, X. He, H. D. Jang, Q. Wang, Y. W. Chung, and J. Huang, Self-dispersed crumpled graphene balls in oil for friction and wear reduction, *Proc. Natl. Acad. Sci. U.S.A.*, **113**, 1528-1533 (2016).

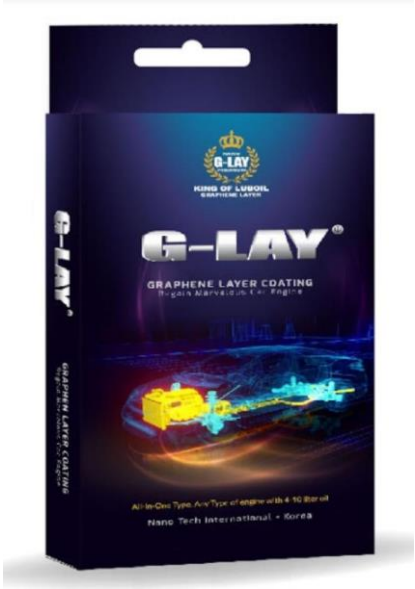
Contact our Nationwide Distributor in Accra, Ghana International

Tel: +233245820888

email:Sales@strategicfocusafrica.com




G-LAY
ALL-IN-ONE TYPE
30


KING OF LUBOIL
G-LAY
GRAPHENE LAYER COATING
Nano Tech International • Korea


G-LAY UNICO
G-LAY
GRAPHENE LAYER COATING
ENGINE OIL ADDITIVE
All-in-one Type
Any Type a Engines with 4-10 Liter Oil


More Powerful, Smoother Drive
Much Comfortable, Silent Drive
Great Engine Performance
Graphene Layer Coating
Ball Bearing Function
G-LAY


EINSTAR
G-LAY


KING OF LUBOIL
G-LAY
GRAPHENE LAYER COATING
GRAPHENE LAYER COATING


Nanotec Ventures
Ghana Introduces
G-LAY
Graphene Engine
Oil Additive
G-LAY
GRAPHENE LAYER
KING OF LUBOIL
NANO TECH
I'm proud to use G-LAY
Increase Pick-Up
Reduces Pollution
Increases Milage
Increases Hours of Usage
Diesel & Petrol Engine Compatible
Compatible With All Type of Engine Oil
VISIT OUR OFFICE
Okpongle Bus Stop Opposite
Legon University Gate, East Legom
Tel: 0202-051 792 / 0241-440 120


Nanotec Ventures
Ghana Introduces
G-LAY


Nanotec Ventures
Ghana Introduces
G-LAY
Graphene Engine
Oil Additive
NANO
G-LAY
PREMIUM
KING OF LUBOIL
GRAPHENE LAYER
GRAPHENE LAYER COATING
EASY ENGINE RESTORING & PROTECTION
Increase Pick-Up
Reduces Pollution
Increases Milage
Increases Hours of Usage
Diesel & Petrol Engine Compatible
Compatible With All Type of Engine Oil
Emission Reduce
MAX 77%
Power Increased
28%~33%
Fuel Saving 7%~12%
How to Use:
G-LAY: AIO (all-in-one) Types
For any type of engine available: petrol, diesel &CNG
Add one 30ml pouch AIO into engine oil tank for 4-10 liter oil capacity
Application Method
Warm up engine & shake G-LAY enough before injection.
Open oil filter cap and inject G-LAY into engine oil.
Close oil cap. Available to be injected in any types of engine oil.
MOBILE:
0202-051 792
0241-440 120
VISIT OUR OFFICE
Okpongle Bus Stop Opposite
Legon University Gate, East Legom


G-LAY®
All-in-One Type. Any Type of engine with 4-10 liter oil
G-LAY
All-in-One Type
of engines with 4-10 liter oil

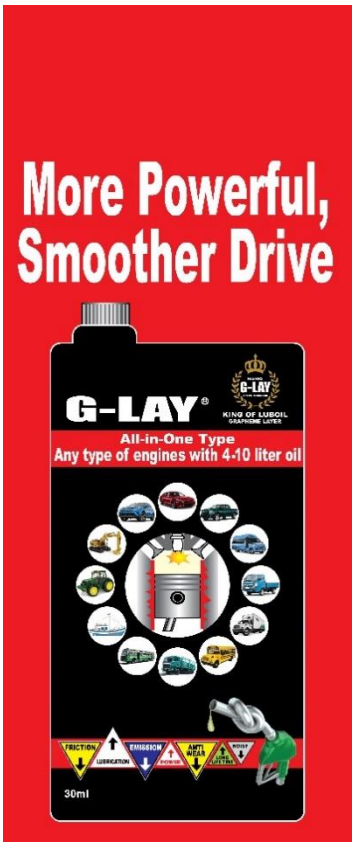

G-LAY UNICO
World Unique Car Nano Graphene Layer Coating
Emission Reduce MAX 77%
Power Increased 28%~33%
Noise Reduce 35%~56%
Fuel Saving 7%~12%
G-LAY GRAPHENE LAYER
KING OF LUBOIL
NANO TECH
Make New Engine
Easy, Simple, Lower Cost
Power
Noise
Emission
Fuel
+91 9818 127 037
www.glayunico.com
A4-201, Ganga Satellite Wanowrie,
Pune-411040, Maharashtra.

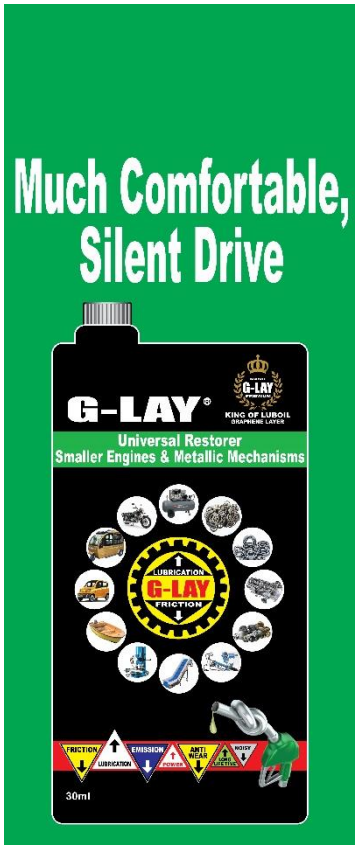

NEW
G-LAY
All-in-One Type
Any type of engines with 4-10 liter oil
30ml
MADE IN KOREA
Great Engine Performance
Emission Reduce MAX 77%
Power Increased 28%~33%
Noise Reduce 35%~56%
Fuel Saving 7%~12%

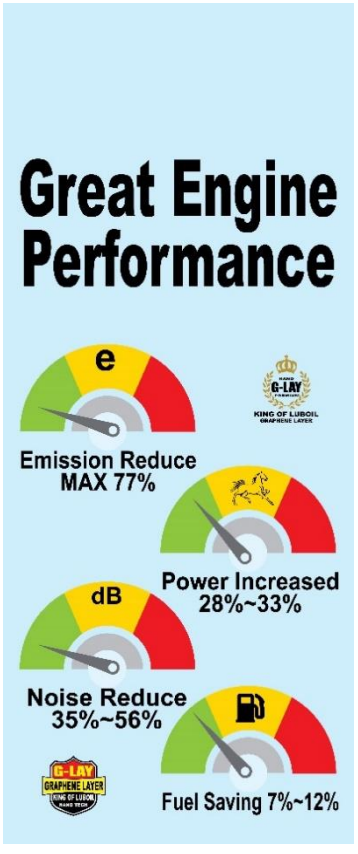

UNICO
G-LAY
Easy Engine Restore & Protect
More Power
Better Fuel Economy
Less Smoke & Noise
Long Engine Life Time
Nano Graphene
Dream & Wonder Material
Miracle Effect
Change the World
Make King of Lube Oil
KING OF LUBOIL
ENGINE GRAPHENE LAYER

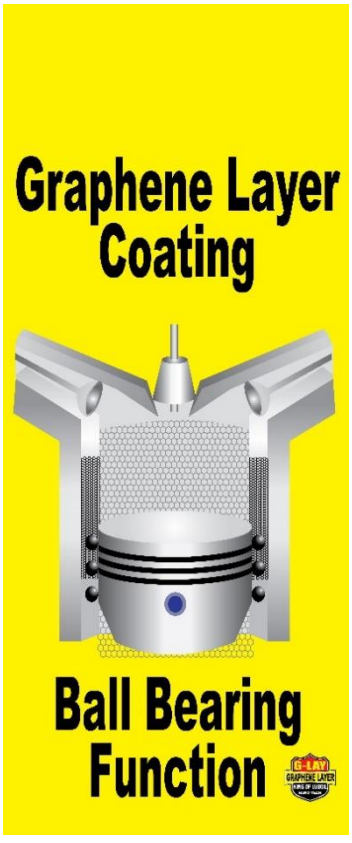

NANO
G-LAY
PREMIUM
KING OF LUBOIL
GRAPHENE LAYER
FRICTION
LUBRICATION
EMISSION
POWER
ANTI WEAR
NOISY
G-LAY
GRAPHENE LAYER COATING
EASY ENGINE RESTORE & PROTECT
GRAPHENE LAYER COATING


NANO
G-LAY
PREMIUM
KING OF LUBOIL
GRAPHENE LAYER
FRICTION
LUBRICATION
EMISSION
POWER
ANTI WEAR
NOISY
G-LAY
GRAPHENE LAYER COATING
EASY ENGINE RESTORE & PROTECT
GRAPHENE LAYER COATING

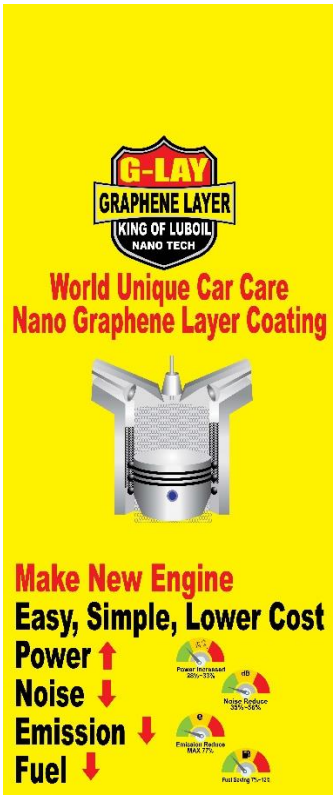

More Powerful,
Smoother Drive
G-LAY
All-in-One Type
Any type of engines with 4-10 liter oil
30ml


Much Comfortable,
Silent Drive
G-LAY
KING OF LUBOIL
Universal Restorer
Smaller Engines & Metallic Mechanisms
LUBRICATION
G-LAY
FRICTION
30ml


Great Engine
Performance
e
Emission Reduce
MAX 77%
Power Increased
28%~33%
dB
Noise Reduce
35%~56%
Fuel Saving 7%~12%


Graphene Layer
Coating
Ball Bearing
Function


GRAPHENE LAYER
G-LAY
NANO COAT
PREMIUM
Easy Engine
Restore & Protect
More Power
Better Fuel Economy
Less Smoke & Noise
Long Engine Life Time
Nano Graphene
Dream & Wonder Material
Miracle Effect
Change the World
Make King of Lube Oil
NANO
G-LAY
PREMIUM
KING OF LUBOIL
GRAPHENE LAYER
ENGINE GRAPHENE LAYER


G-LAY
GRAPHENE LAYER
KING OF LUBOIL
NANO TECH
World Unique Car Care
Nano Graphene Layer Coating
Make New Engine
Easy, Simple, Lower Cost
Power
Noise
Emission
Fuel


World Unique Car Care
Nano Graphene Layer Coating
G-LAY
GRAPHENE LAYER
KING OF LUBOIL
NANO TECH
Make New Engine
Easy, Simple, Lower Cost
Power
Noise
Emission
Fuel
NANO
G-LAY
PREMIUM
KING OF LUBOIL
GRAPHENE LAYER
www.nanozr.com


NANO
G-LAY
PREMIUM
KING OF LUBOIL
GRAPHENE LAYER
FRICTION
LUBRICATION
EMISSION
POWER
ANTI WEAR
NOISY
G-LAY
GRAPHENE LAYER COATING
EASY ENGINE RESTORE & PROTECT
GRAPHENE LAYER COATING
World Unique Car Care
Nano Graphene Layer Coating
G-LAY
GRAPHENE LAYER
KING OF LUBOIL
NANO TECH
Make New Engine
Easy, Simple, Lower Cost
Power
Noise
Emission
Fuel
KING OF LUBOIL
GRAPHENE LAYER
www.nanozr.com


Great Engine Performance
Emission Reduce MAX 77%
Power Increased 28%~33%
Noise Reduce 35%~56%
Fuel Saving 7%~12%
NANO G-LAY PREMIUM
KING OF LUBOIL GRAPHENE LAYER
FRICTION LUBRICATION EMISSION POWER ANTI WEAR NOISY LONG LIFE TIME
G-LAY
GRAPHENE LAYER COATING
EASY ENGINE RESTORE & PROTECT
GRAPHENE LAYER COATING
GRAPHENE LAYER G-LAY NANO COAT PREMIUM
Easy Engine Restore & Protect
More Power
Better Fuel Economy
Less Smoke & Noise
Long Engine Life Time
Nano Graphene
Dream & Wonder Material
Miracle Effect
Change the World
Make King of Lube Oil
KING OF LUBOIL GRAPHENE LAYER
ENGINE GRAPHENE LAYER


More Powerful, Smoother Drive
G-LAY
All-in-One Type
Any type of engines with 4-10 liter oil
30ml
G-LAY GRAPHENE LAYER KING OF LUBOIL NANO TECH
NANO G-LAY PREMIUM
KING OF LUBOIL GRAPHENE LAYER
GRAPHENE LAYER G-LAY NANO COAT PREMIUM
GRAPHENE LAYER COATING
Much Comfortable, Silent Drive
G-LAY
Universal Restorer
Smaller Engines & Metallic Mechanisms
LUBRICATION G-LAY FRICTION
30ml







BETTER ENGINE PERFORMANCE STARTS WITH G-LAY NANO COAT

Contact us today to make your engine perform well.

Email: sales@solutionsunltd.com
Call / WhatsApp: +233.24.5820.888
Landline number: 233.30.222.0871
Address: GV-003-0404 #20 Sunyani Avenue, Kanda. Accra. Ghana
www.solutionsunltd.com



SOLUTIONS UNLIMITED LTD.